Indigo derivatives and their colour

Zepeng Cao

A Thesis Presented for the degree of Master of Science by research

Supervised by Prof. Andrew Beeby

Department of Chemistry,

University of Durham

England

August 2021

Abstract

This thesis focuses upon the spectroscopic properties of indigo and its derivatives.

The first chapter introduces the background of indigo and derivatives that are found in nature and used in industry. The historical literature and works were reviewed to understand the reason for indigo's blue colour from both a spectroscopic and computational perspective.

Using Suzuki and Sonogashira coupling methods, this research prepared a range of indigo derivatives appended with aromatic and arylethynyl substituents. Also dibromoindirubin, and *N,N'*-diBoc-indigo were prepared. UV-Visible spectroscopy was used to characterise the indigo derivatives prepared herein, and DTF-based molecular modelling (Gaussian-16) calculations were done on the di(p-tolyl)-indigos (B3LYP/6-31+G(d)).to investigate the effects of substituent position. The synthetic methods and results are reported.

This research has found that the absorption spectra of indigo derivatives with aryl or arylethynyl substituents around the benzene ring of the indole unit (positions 4-7) are dominated by the indigo core and have an absorption maximum of around 600 nm.

However, although indigo itself is very stable towards light and oxygen, it has been noticed that a few of the indigo derivatives prepared here rapidly degrade and lose their intense blue colour. This is particularly noticeable when they are dissolved, a degradation would occur with a colour change from a deep blue to a colourless/yellow solution as a result of oxidation to the isatins.

Glossary of abbreviations, terms, and symbols:

ASAP	Atmospheric solids analysis probe
Boc	*Tert*-butyloxy-carbonyl (-COO-^{t}Bu) group or Boc's *N,N'*-substituted indigo
CF_3Ph	p-trifluoromethyl-phenyl group or substituted chemical
CNPh	p-cyano-phenyl or substituted chemical
CSD	Cambridge Structural Database
DCB	*Ortho*-dichlorobenzene
DCE	1,2-dichloroethane
DCM	dichloromethane
DMAP	4-(dimethylamino)pyridine
DMSO	Dimethyl sulfoxide
DME	1,2-dimethoxyethane
EDG	Electron donating group
ESP	Electrostatic potential surface
EWG	Electron withdrawing group
H-chromophore	The two symmetrical merocyanine linkages that joints between the two indoles within an indigo
HOMO	Highest Occupied Molecular Orbital
IDB	Indirubin
IDL	Indole
IDG	Indigo
LCAO	Linear combination of atomic orbitals
LUMO	Lowest Unoccupied Molecular Orbital
Merocyanine	A polymethine chain of "– NH – C = C – C (= O) –"
MLCT	Metal-to-ligand charge transfer
^{m}OMePh	m-methoxyphenyl group or substituted chemical
^{n}BuPh≡	p-n-butyl-phenylethynyl group or substituted chemical
NMP	*N*-methyl-2-pyrrolidone
NMR	Nuclear magnetic resonance
$Pd(PPh_3)_4$	Tetrakis(triphenylphosphine)palladium(0)
^{t}Bu≡	p-*tert*-butyl-ethynyl group or substituted chemical
^{t}BuPh≡	p-*tert*-butyl-phenylethynyl group or substituted chemical
TCE	1,1,2,2-tetrachloroethane
ThioIDG	thioindigo
Tol	p-Tolyl substituted chemical
TriMePh	2,4,6-trimethylphenyl group or substituted chemical
Tyrian purple	6,6'-dibromoindigo
UV-Vis	Ultraviolet-visible spectroscopy

Contents

1. Introduction

1.0 Terminology

To clarify, there are a few different commonly used terms to describe compounds of this type: indigo, indigo, indigoid, and indole.

Indigotin is the name of the organic compound (**1**, $C_{16}H_{10}N_2O_2$), which has a blue colour and it is also the critical component for the indigo dye. However, the reality is that most scientists prefer to use "indigo" as the name of the dye rather than "indigotin" as the name of the compound. The word, "indigotin", is not used further within this thesis.

Indigo is the name of the dye and one of the plants from which the dye is made, and it may also refer to the plant where indigo comes from in certain circumstances. In most of the cases in this thesis, the word, "indigo", refers to the compound indigo (where some theories may apply to other indigoids). The word, "Indigos", refers to several indigoids that have indigo as their core or parent skeleton.

Indigoid is the family of compounds to which indigo belongs, and they are molecules that may have atoms that substitute the nitrogen on indigo, e.g. sulphur-substituted indigo is thioindigo.

Indole (**3**, C8H6N) is the heterocycle that comprises the basic unit of indigo.

1.1 History of indigo and its derivatives.

1.1.1 History of indigo

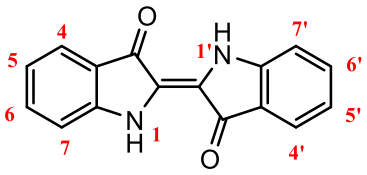

1, Indigo

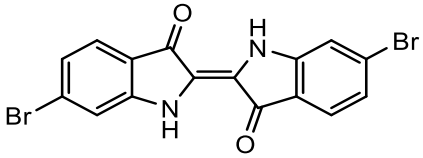

2, Tyrian Purple

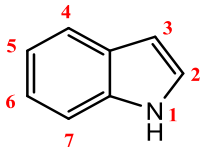

3, Indole

Indigo blue is a non-toxic dye with a characteristic blue colour that has been known since antiquity. It is still widely used as a pigment, for example, it is used for dyeing jeans. The word "indigo" came from Latin, which was because for many centuries India was the major exporter of the dye to Europe.

The usage of dye has a history of more than 6000 years in different parts of the world and was originally made from the fresh leaf of plants. In Europe, the species is called *Isatis tinctoria* (woad), and this plant grew widely in England, France, and Germany where some people still cultivate and trade this material. This species was the primary source of indigo in Europe until the 16th century. Then, it was gradually replaced by another species of plant, *Indigofera tinctoria, a plant* that

originates in Asia and one that can have a higher yield of indigo.

In both cases, the indigo plants were collected and dried in the air and the stems were removed. The leaves were piled in a wet room to be decomposed by microorganisms, where fermentation would occur after a few days.

Figure 1 – Indigo dye

Figure 2 - *Indigofera tinctoria (Left) and Isatis tinctoria (Right)*

Within the leaf of the indigo plants, there is a chemical called indican, a derivative of 3-hydroxyindole, which is a colourless precursor for indigo production. An endogenous enzyme, β-glucosidase, can be found in the chloroplast of the leaf. During the fermentation, in the presence of wood ash (acting as alkali) or limestone, the indican is hydrolysed by β-glucosidase, removing the attached β-glucose and forming another colourless compound, 3-hydroxyindole or indoxyl, which spontaneously oxidises in the air to form indigo (Scheme 1).[1]

Because of its sophisticated and beautiful chemistry, the ancient Greeks and Romans considered indigo a rare and luxurious commodity.

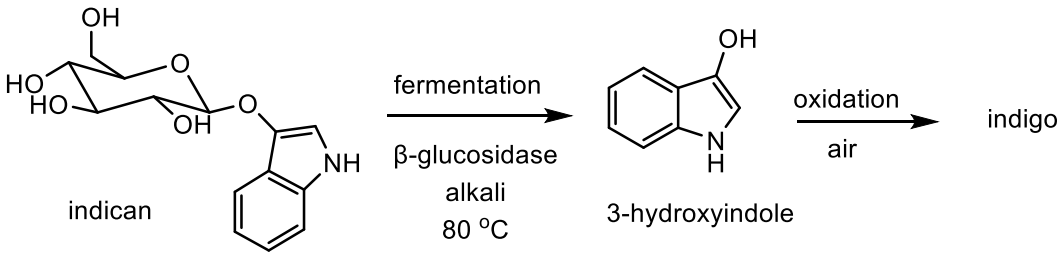

Scheme 1 - natural indigo production method

Practically, indigo is hardly soluble in any common solvent, i.e. water, acetone, ethanol, etc. The advantage of this chemical property makes it effectively a pigment and allows it to last longer and maintain the original colour when used in the paints and or clothing without being blurred or washed off. However, this is also its disadvantage because it is also hard to directly apply this blue dye which the colour will just stay on the very top layer of the textile.

1.1.2 History of Tyrian purple

6,6'-dibromoindigo (**2**, $C_{16}H_{10}N_2O_2$) is known as Tyrian purple and was named after the port city, Tyre, where it was produced in antiquity. Tyrian purple is an indigoid pigment that was prepared by the ancient people in the Mediterranean and was also known as the Imperial Purple or the Royal Purple. Due to the laborious preparation methods needed for this material it was significantly more valuable than indigo. Tyrian purple was obtained by the fermentation of the mucus of the hypo-branchial gland of several species of Murex snails that are 1-3 inches long each. The most commonly used species is *Bolinus brandaris* (originally called *Murex brandaris*): to collect 1 cm^3 of

Figure 3 - *Bolinus brandaris*

Tyrian purple would require nearly 10,000 of these snails. Also due to the difficulties to access and treat the body fluid from those snails, Tyrian purple became the most expensive pigment and highly prized for thousands of years. Its high value pushed the manufacturers to keep the details of production a secret, restricting its production and limiting access to the material. Because of this, Tyrian purple was reserved exclusively for the Roman Emperor and it was forbidden for others to possess this valued dye used by the emperors and high priests. Evidence for this was even mentioned several times in the Exodus of the Old Testament of the Bible. By the 4th century, only the Roman emperor was permitted to wear Tyrian purple and any violation of this law would mean execution for the perpetrators. As a result, purple became a symbol of supremacy, and there is almost no country that has purple on national flags because of the tremendous cost to make those flags in the past.

As an indigo derivative, Tyrian purple has very similar physical and chemical properties to indigo, with the exception that it is a rich deep purple colour rather than indigo blue.

1.1.3 History of Indirubin

When natural indigo was extracted and generated from the indigo plant, there are isomers of indigo that can also be found as impurities. Among these impurities, the most common is indirubin, **4**. The colour of indirubin is red rather than the vivid blue colour of indigo.

Because of the red colour, the presence of indirubin within raw indigo affects the perceived colour of the indigo, detracting from the bulk indigo's pure bluish colour. As a consequence for most places in the world, indirubin was considered a wasted by-product of textile dye.

However, in ancient China, indirubin was also used in medicine it is believed to inhibit tumour growth and as an active anti-leukaemia ingredient. It was found in traditional Chinese medicine, Danggui Longgui Wan. The recipe for this medicine requires Qingdai, which is a herb that contains indirubin.

This has re-invigorated clinical and biological research into this material and related compounds in recent years. [2]

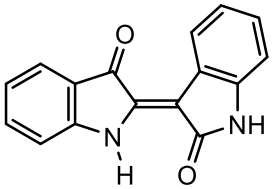

4, Indirubin

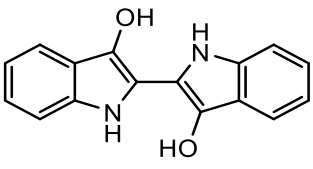

5, Leuco indigo

1.1.4 History of industry and leuco indigo

Because of the poor solubility of indigo, the industrial usage of indigo as a dyestuff required a complex vat process. Firstly, the indigo is reduced to yield the water-soluble derivative leuco indigo, **5**, in which the carbonyl group is reduced to an -OH. Leuco indigo is also known as "white indigo". This reduction can be carried out with a mixture of NaOH and sodium dithionite

($Na_2S_2O_4$), generating leuco indigo. The leuco form of indigo has a non-planar structure, decreasing its tendency to aggregate, and in basic solution it forms the dianion making it soluble in water, creating a light-yellow solution.

When the yarn of fabric is immersed into this solution the liquor and the dissolved leuco-indigo penetrate deeply into the fibres. When the fibres are taken from the reducing environment of the dye solution the leuco indigo is exposed to the air and spontaneously oxides back to the insoluble and planar, deep blue indigo. Any material that has penetrated the fabric structure is now and trapped so the colouring process can be completed. [3] Pigment located on the surface of the fabric is not bound so strongly and is readily removed by washing.

1.2 Historical development of synthetic indigo.

In the nineteenth century a German chemist, Adolf von Baeyer, spent over two decades trying to determine indigo's structure and create a synthetic route to the material. He described his attempts to make indigo from isatin and also tried to start from cinnamic acid although both of them failed to give indigo in any useful yield.

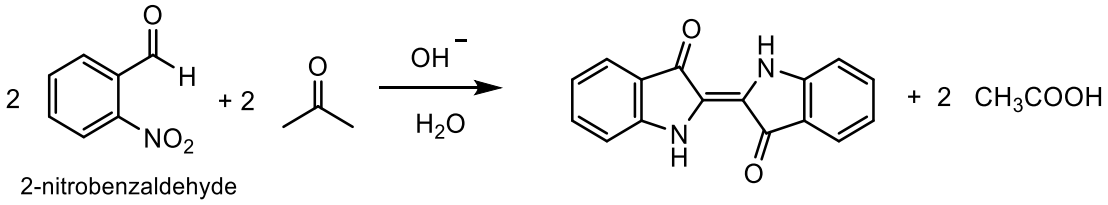

Scheme 2 – Overall reaction of Baeyer–Drewson indigo synthesis as the first synthetic indigo method[4]

The third trial with his colleague Viggo Drewsen was reported in 1882, is considered the first synthetic route to indigo. [4] This was achieved by aldol condensation of 2-nitrobenzaldehyde and acetone (Scheme 2). Because of these achievements, Baeyer was awarded the Nobel Prize in Chemistry in 1905 as a milestone in the production of synthetic indigo. However, Baeyer's synthetic process was not economically viable on an industrial scale.

Following this work a Swiss-German scientist, Karl Heumann, suggested two commercially viable routes to indigo in 1890 known as the first and second Heumann indigo syntheses as shown in Scheme 3. The first one attempted to make indigo from *N*-phenyl-glycine, but the overall yield of this intermediate was so low that the industry showed little interest in developing this method of production. Hermann's second route solved the previous problem but used a more expensive reactant, anthranilic acid. This modified route was scaled up to an industrial level in 1897 and made a considerable amount of indigo.

In 1901, Heumann's first synthetic route was further improved by Heumann's colleague, Johannes Pfleger. The addition of sodamide ($NaNH_2$) significantly increased the efficiency of the synthesis and reached the point where the synthetic indigo was cheaper than the imported plant-derived product. This scheme is still used as the current manufacturing method and is known as Pfleger's indigo synthesis plan.[5,6]

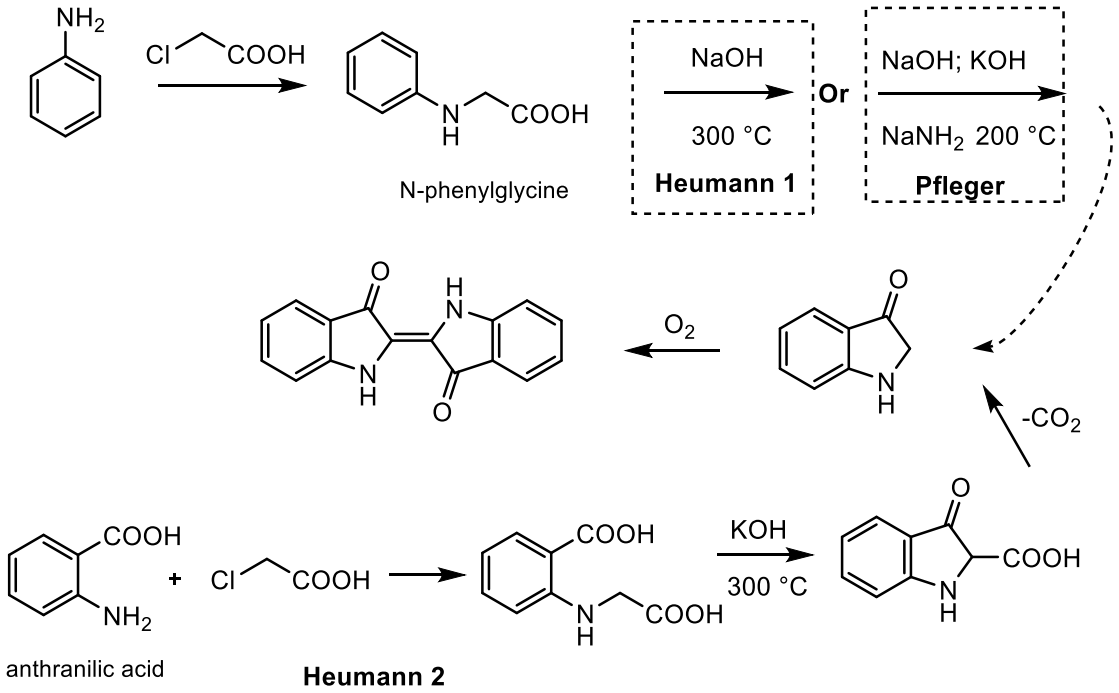

Scheme 3 – commercial indigo synthesis plans of Heumann's route and the improved version by Pfleger.[5,6]

In 1925, the synthesis of the intermediate product of the Pfleger's route, *N*-phenyl-glycine, has also further improved with a lower cost method by a chemical company, Badische Anilin und Soda Fabrik (BASF) (Scheme 4)[7]. This further reduced the cost of synthetic indigo and made blue an affordable colour for ordinary people in a larger quantity.

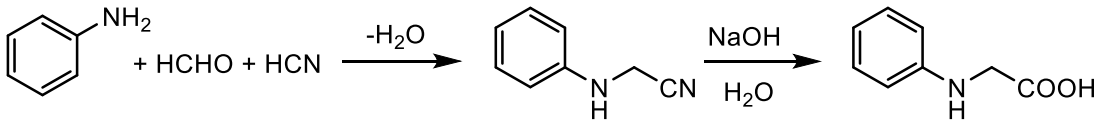

Scheme 4 – BASF's *N*-phenyl-glycine synthesis[7]

Currently, there are several research groups investigating biosynthetic indigo routes to indigo. For example, Kwon-Young Choi and his team are working on a method that starts from glucose and *E. coli* cells. The *E.* coli converts the glucose to indole via the *shikimate pathway*, and this indole is further reacted on the microorganism to form 3-hydroxyindole.[8]

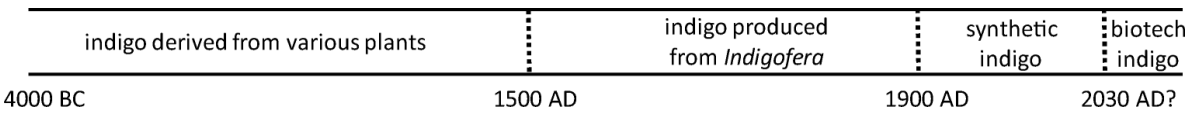

Figure 4 – Indigo production method timeline[9]

The breakthroughs in creating facile routes to synthetic indigo have greatly lowered the cost of production of Tyrian purple as well, the traditional "snail-slaughtering" route has been abandoned and companies have cheaper routes to synthetic Tyrian purple. However, this still expensive dye has not been commercialized because the cost of synthetic Tyrian purple is still higher than other purple dye alternatives. Mauveine was the first synthetic organic dye in the world, developed by Henry Perkin in 1856. The dye is a mixture of 4 compounds with any combination of R_1 & R_2 = H / Me. Tyrian purple is not used as a dye-stuff in the present day.

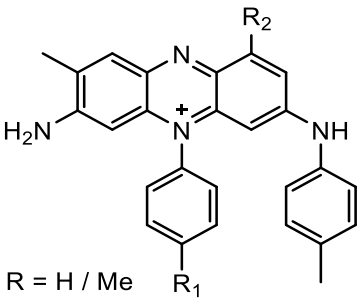

Mauveine

1.3 The structure and shape of an indigo

1.3.1 Structure of indigo

The structure of indigo was originally suggested by Baeyer who was first to synthesise indigo. However, he incorrectly assumed that indigo would have a *cis* structure as (Z) configuration as molecule 6.[10]

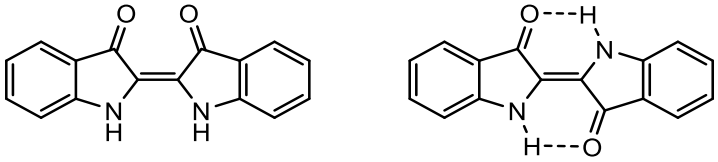

cis trans

6, indigo (**cis**, suggested by Baeyer); **indigo** (**trans**, determined by X-ray)

With the help of X-ray crystallographic analysis, indigo's structure was confirmed as the *trans*-structure that has been understood.[5,11] These more stable configurations attribute in part to the stabilisation from the two O···H—N hydrogen bonds.

The indigo molecule is completely flat where all the atoms on this molecule are exactly on the same plane and has cis symmetry. Each indigo is a dimer of two oxidised indole moieties (**3**) that are connected by a double bond. All of the non-hydrogen atoms on the rings have sp^2 hybridisation. The conjugation of all these empty non-hybridised p orbitals creates a well extended π-conjugation that locked the shape of an indigo molecule.

To explain the packing of indigo systems, the coordinate axis of each molecule will be defined as shown below in Figure 5. The molecule is placed in the x-y plane. For indigo, the direction perpendicular to the plane is defined as Z-axis and the direction of the double bond joint will be X-axis. Lastly, the axis on the plane perpendicular to the double bond will be Y.

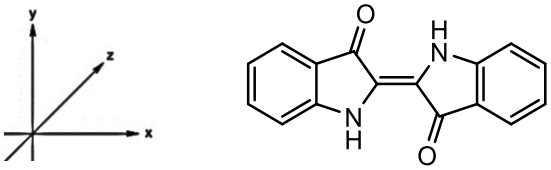

Figure 5 – Indigo and its system's coordinate axis definition

The conjugation also makes it possible for electrons to delocalise across the molecule by resonance. This decreases the polarity of heteroatom sites and makes the entire molecule more inert, behaving as a non-polar molecule. As a result, the molecule is more stable and less likely form hydrogen bond with water, which decreases its solubility and increases its stability.

The significance of these facts makes it such a good vat dye that is resistant to fade or lose its colour in a solvent or even during washing.

1.3.2 H-chromophore of indigo

For indigo, the molecule's colour and absorption are dominated by the intramolecular and intermolecular hydrogen bonds among the oxygen and nitrogen sites. In the gaseous state, indigo has an absorption maximum of 539 nm at 385 °C (Figure 10, pg. 17, curve 1), and when it is dissolved in DMSO, the wavelength of absorption that shifts to 619 nm.[12] Thus, dissolving in DMSO gives a red shift of, $\Delta\lambda_{DMSO\text{-}gas}$ = 80 nm.

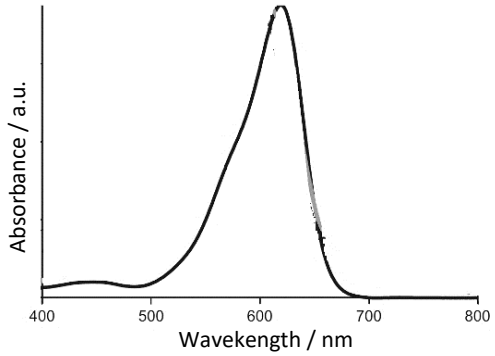

Figure 6 – UV-Vis absorption spectrum of indigo in DMSO. (the figure was reproduced with permission)[12]

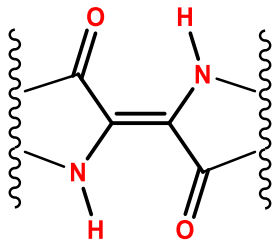

Figure 7 – The indigoid system's H-chromophore

Indigo has a symmetrical system where two coupled merocyanine chains can be found. The merocyamine is a polymethine chain that has the " – NH – C = C – C = O" linkage. Next to the junction of the indoles, there are two N-H electron-donating groups and two C=O electron-accepting groups. This H-shape junction creates a "cross-conjugation" through this double bond.

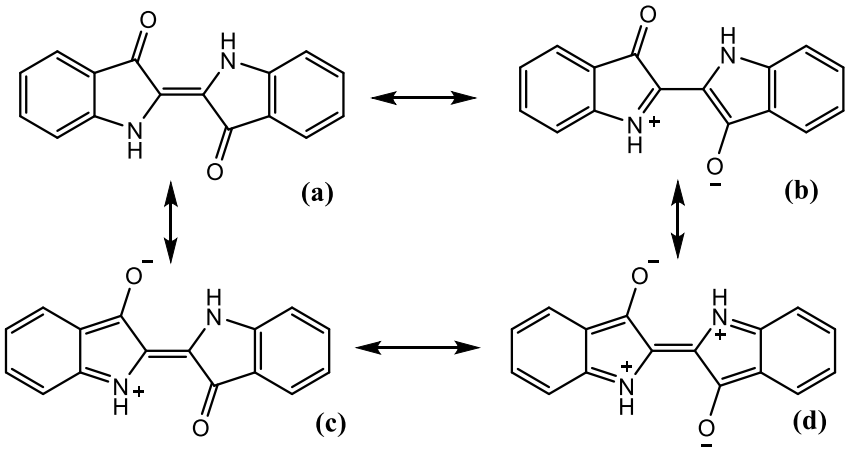

Figure 8 – Resonance H-chromophore of indigo molecules.

"H-chromophore": The concept of the H-chromophore arises from these liked merocyanine chines, linked and cross conjugated by the double bond connecting the two indole rings of the indigo, with the horizontal bar of the 'H" representing the double bond (Figure 7). Hydrogen bonding between the adjacent C=O and N-H groups of the chromophore further stabilise the indigo molecule. The dipole is created by itself can stabilise the hydrogen bonding intramolecularly and intermolecularly.

The H-chromophore of the indigo molecule have extensive resonance and this reduce the energy of the transition and introduce a red shift during absorption (Figure 8). Assuming the ground state is the neutral form as (**a**) and the excited states of the molecule comprise the less stable resonance forms **b-d**. Planck's relationship suggested that the dominating excitation always occurs from the ground state to the first excited state.[13] The excited states with the charge separation create a dipole or quadrupole structure which will be stabilized by the extension of the conjugation of the π system. This is one the reasons of why indigo can absorb light efficiently, and the energy was red-shifted from gas to solid-state.

1.3.3 H-chromophore from other molecules

Apart from indigo, the H-chromophore motif can be found in other molecules as well. For example, indigo's isomer indirubin has half of the "H-chromophore".

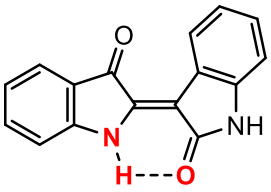

4

Analysis of indirubin also showed that it is moderately flat, but not as flat as the indigo. Structural data showed that the two indole planes still have an angle of 3.97 ° to one another. This small distortion can be explained by a comparison of structure between indigo and indirubin.

Indirubin also has but only one merocyanine chain (- NH – C = C – C = O). The conjugation of the molecule is less than that of indigo and it was limited to half of the molecule (CSD code: INDRUB)[14]. The stabilisation of indirubin by resonance would require a geometrically possible charge transfer. The merocyanine chain formed a head-to-tail ring to form intramolecular hydrogen bonds, which also allows the molecule to interact extensively with two adjacent molecules with those heteroatoms. Indirubin has a shorter wavelength of light absorption, λ_{max} = 540 nm in DMSO[15], (cf. indigo, 620 nm).

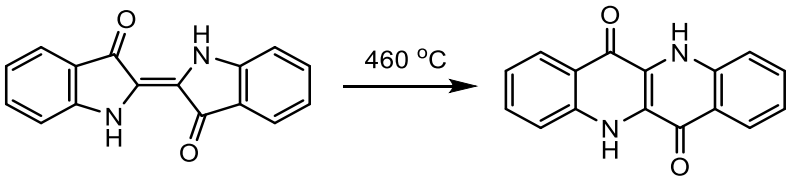

7, Epindolidione

Scheme 5 – Conversion of indigo to epindolidione[12]

Epidolidione, 7, also has the "H-chromophore" within the molecule. Epidolidione can be made by a ring re-arrangement of gaseous indigo at above 460 °C.[12] However, in epidolidione the H-chromophore is no longer a linkage between the two aromatic rings, but a shared double bond. Therefore, its orientation of the H-chromophore is perpendicular to the long axis of the molecule, contrary to that of indigo where is it parallel to the long axis. Its UV-Vis spectrum shows that it has an absorption in DMSO at 446 nm (Figure 9). The UV-Vis spectra showed that epidolidione may have an absorption peak that is similar to indigo and indirubin but occurring at much higher energy and shorter wavelength.

The intramolecular hydrogen bond of epidolidione is geometrically less stable than the hydrogen bond of indigo. The hydrogen bond of the indigo's system forms two 6-membered rings that can push the hydrogen atom towards the oxygen. However, for epindolidione, although the oxygen and hydrogen are in close proximity, the geometry makes the N-H and C=O bond almost parallel and the interaction of the sp^2 of nitrogen and carbonyl carbon atom require some distortion.

The difference among these absorption wavelengths may due to the rigidity of the molecule and the orientation of the H-chromophore that changed the direction of transition dipole moment when it was excited by a photon.

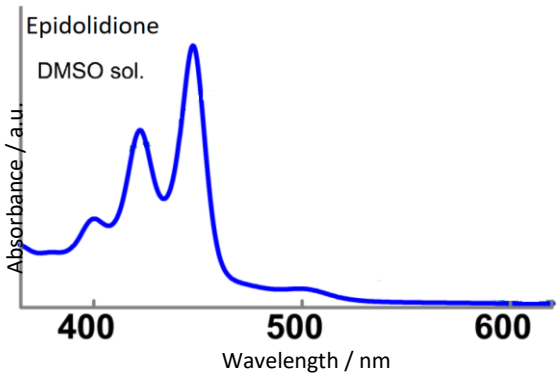

Figure 9 – The UV-Vis spectra of **7** in DMSO (blue)[16]

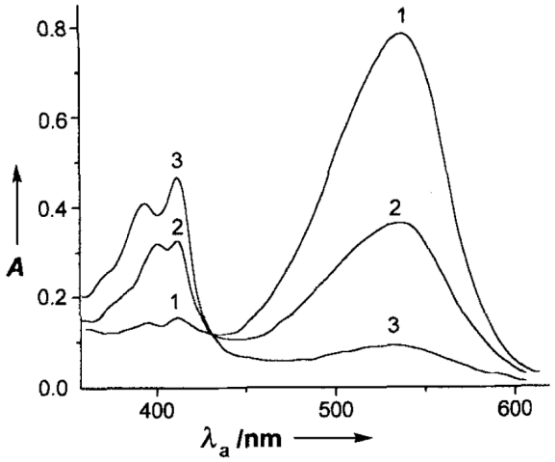

Figure 10 – UV-Vis spectra of gaseous phase conversion from indigo to epindolidione (1) is at the beginning of the reaction of indigo at 430 °C; (2) is a mixture of indigo and **7** at 480 °C at 5 min reaction; (3) is mainly **7** at 500 °C after 10 min of reaction (the figure was adapted with permission)[12]

From Figure 8, the form b can improve the intramolecular hydrogen bonding between the two monomers of the same indigo molecule. Figure 8(c) shows an improvement of the intermolecular hydrogen bonding along the "line" of packing.

1.4 Packing of indigoid

1.4.1 Kasha's exciton model

Michael Kasha's exciton model can be used to explain the spectral shift in the absorption spectrum of indigo.[17] Firstly, it is important to define the terminologies used to analyse the relative arrangement of indigo molecules and their interaction. To simplify the problem, a scenario of the dimer is considered as two individual molecules as light-absorbing monomers that interact with each other.

When a molecule is excited by a photon it is the transition dipole moment that interacts with the approaching photon: there is a resonance between the electronic transition dipole of the molecule and the incoming light's oscillating electric field, which has to have some parallel component. Because the wavelengths of ultraviolet and visible light are at a much larger scale than a molecule, two adjacent molecules would effectively experience the same electrical field as the light passes past them. Therefore, to be quantum mechanically allowed, both of the molecules would be excited with the same orientated electrical field of the light.

Kasha listed a few possible scenarios as shown in the following diagrams in Figure 11. The ovals represent the structure of the molecular monomers and the double-headed arrow correspond to the polarisation axis of the transition dipole moment of the molecules.

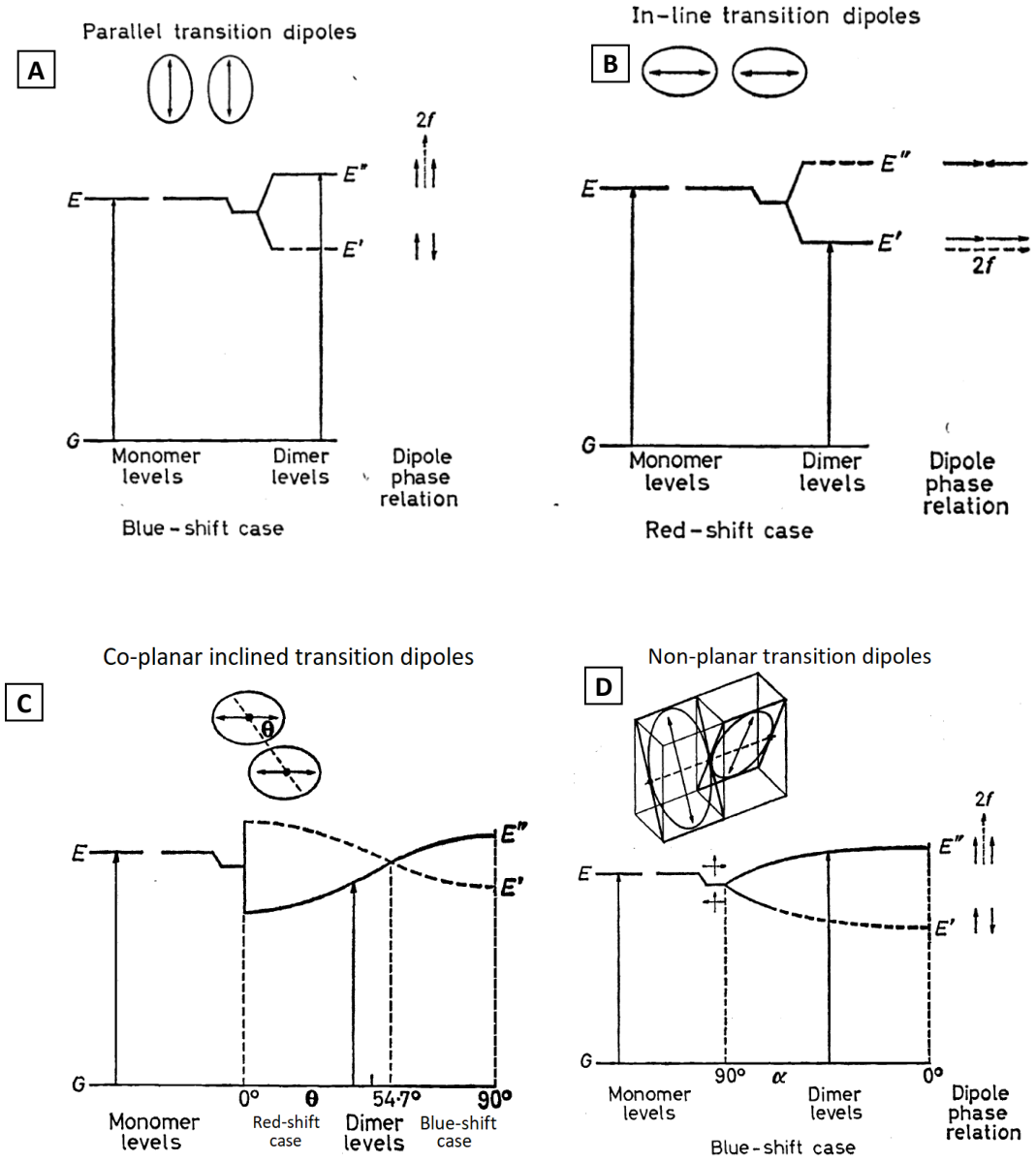

Figure 11 – Kasha's exciton energy diagrams of dimers for a different arrangement of composite molecules. (A): a blue shift of the absorption when the transition dipole is side-by-side parallel; (B) a red shift of the absorption when the transition dipole is co-linear; (C) a correlation function of absorption when the transition dipole is parallel but staggered; (D) a correlation function of the blue shift of the absorption when the transition dipole is pointing towards different directions.[17]

When the two molecules are arranged side by side as Figure 11A, the same orientation as the incoming photon means an in-phase transition dipole. In this configuration the energy level of the dimer splits into two levels of different energies, corresponding to the case in which the two transition dipole moments are anti-parallel (lower energy level) or parallel (upper energy level). In this case, only the transition from the ground state to higher E'' has a finite transition dipole moment and therefore is the only allowed transition. Because the lower state has a zero transition dipole moment overall the transition is forbidden. Therefore, in the spectrum of a sample with this arrangement of dimers a blue shift is observed for the dimer compared to the monomer.

Similarly, when the two molecules are arranged head to tail, the two oscillations lie in the same direction, Figure 11B. Using the same logic, the monomer's excited states are split in the dimer, but now the transition to the lower E' is the allowed transition. Therefore, a red shift is observed in the spectra in this case.

The same idea applies again in Figure 11C where the molecules are shown with a varying angle between the two centres, representing the intermediate stages between A and B. The change of energy would become a correlation function of the angle between the two coplanar transition dipole moments. Figure 11D also shows the change as a function of a torsional angle between two parallel orientated vectors of two transition dipole moments. In these examples, the situation is more complex since the magnitude of the splitting energy and the degree of allowedness of the transitions varies continuously with angles.

As the compound packs into an aggregate constituted of more than two molecules, the splitting would exist in a form of many similar energy levels centred about the monomer's wavelength of absorption and degeneration would overlap and form allowed two states that are responsible for red and blue-shifted absorption. Typically two types of aggregate commonly form, referred to as. H-aggregate or J-aggregates (Figure 12).

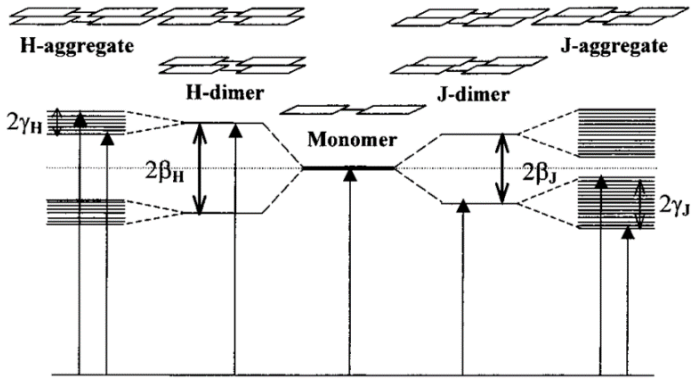

Figure 12 – H & J aggregate of absorption[17]

1.4.2 Indigoid's packing

The crystal packing of indigo can be found in the Cambridge Structure Database (CSD) with a reference code of INDIGO03.[18] It is reported to have a monoclinic crystal system where its cell parameters are: a = 5.8 Å, b = 9.2 Å, c = 11.5 Å, α = 108.7°, β = γ = 90.0°. [18] When the indigo molecules pack they have two orientations with an angle of 70.1° between one another of the molecular planes and each orientation has half of the indigo. The molecules interact via the hydrogen bonds of the oxygen and nitrogen parts. For molecules parallel to each other, their distance is large enough to avoid interaction of the molecular orbital and therefore give rise to

splitting.

For indigo molecules, the $S_1 \leftarrow S_0$ transition occurs with the polarisation of the transition dipole moment along the length of the molecule. The Kasha and H/J-aggregation explanation can be used straight away by treating the double-headed arrows as the direction of polarisation of indigo.

The problem can be analysed from the perspective of the indigo molecule in the red circle (RedIDG)in Figure 13A. This molecule has three types of neighbouring indigo that are in blue, green, and orange circles respectively.

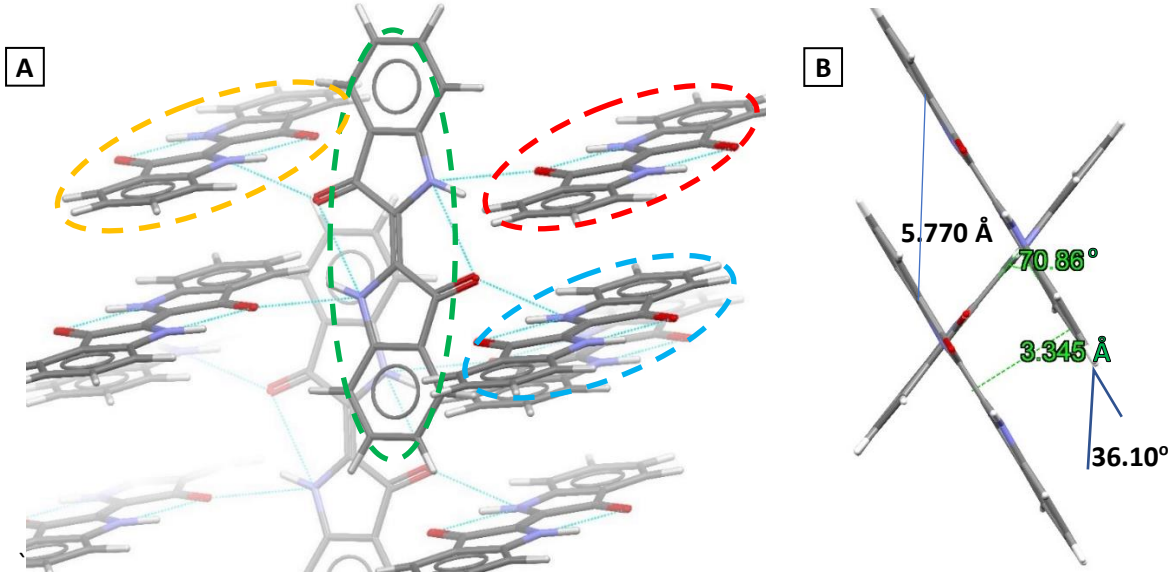

Figure 13 – Cambridge Structural Database of the packing of indigo from two different angles.[18] (The figure was reproduced with permission) (A) a view of the packing of indigo; (B) a view of the adjacent indigo molecules along their Y-axis

The closest neighbour is the molecule (BlueIDG) above and below each other. They have the coplanar orientation and their distance is 3.35 Å and the centroids' line has an angle of 36° with their planes. This relative position can be assigned using the J-aggregate model. This staggered arrangement would lead the molecule to have a red shift.

When the HOMO-LUMO transition occurs, the contributing orbitals are all on the Z-axis, (the molecular orbitals of indigo will be discussed in Section 1.5). The directions mean BlueIDG have the best chance of orbital overlap with neighbouring molecules and have coupling, which determined that BlueIDG may dominate the shift.

The second closest interaction is with GreenIDG. It is a molecule with a different orientation but has a hydrogen bond between the C=O and N-H of the two molecules. The distance between the two centroids is 6.8 Å and the angle of the two indigo planes is 71°. The direct distance from the RedIDG's oxygen to the hydrogen of the GreenIDG is just 2.1 Å. However, this distance is less significant as Kasha's exciton model focus on the centre of the transition dipole moment's interacting orbitals and the direct distance would show more influence on molecular interactions such as hydrogen bonds.

For Green IDG, Kasha's non-planar inclined model shows that the molecule may have only a blue shift because of this type of arrangement. This position has a poor overlap of neighbouring molecules, which limits the orientation of the dipole. However, the magnitude would be limited to

the projection of the vector of transition moment in the direction of light. This means the contribution would be equal or even lower by a factor of cos 71° = 0.326.

The furthest interaction is with the molecule that is in the same plane and arranged side by side (OrangeIDG). The centroid-centroid distance is 12.2 Å and the inclined angle between the two is 85°, which may have a tiny blue shift based on the parallel model. However, OrangeIDG is at a large distance and might be considered too far to have a strong interaction thus the impact on the splitting from the exciton model's perspective would be less significant.

Overall, due to the dominance of the red shift from BlueIDGs and the counter-blue-shift from the other two types of arrangement, the net effect of the indigo's aggregation would be red-shifted. This simple approach then can explain the shift of wavelength that causes a colour change from the red gas to the blue solid.

1.4.3 Distortion of the indigo skeleton

As mentioned, indigo is completely flat. However, when the molecule is substituted, steric interaction may distort the ring systems. Since the indole rings are relatively rigid, this distortion occurs at the connected double bond.

There are three types of possible distortion of the indigo skeleton (Figure 14) and they were explained by Dirk Blunk who was working on the semi-conductor and liquid crystal properties of indigo.[19] The distortion is labelled as twisted, buckled, or skew structures. The change in structure and spectral behaviour was first noticed for *N, N'* –dimethyl indigo[20] and confirmed for *N, N'*-diacetyl indigo, **8**.

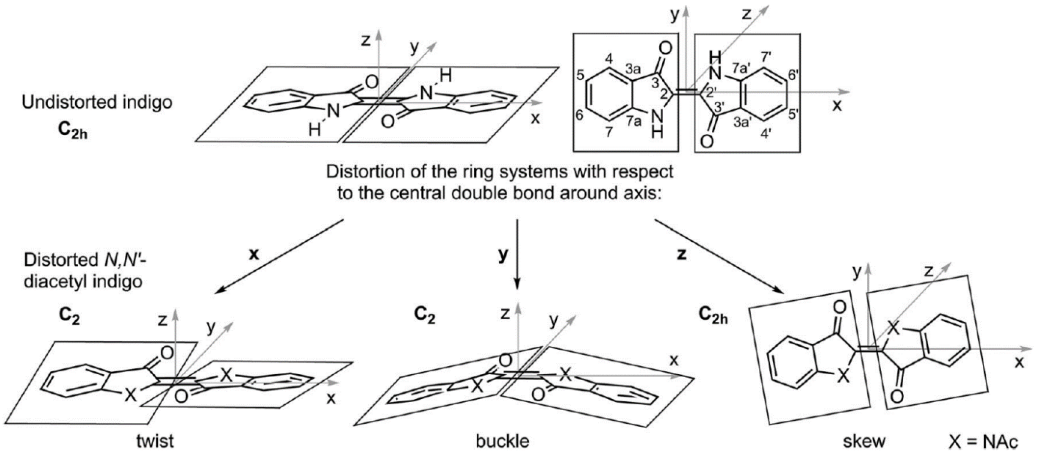

Figure 14 – distortion of indigo's ring system[19]

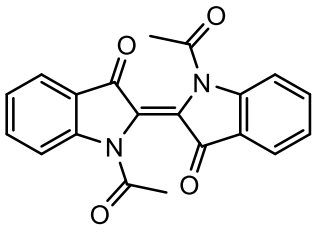

8, *N,N*'-diacetyl-indigo

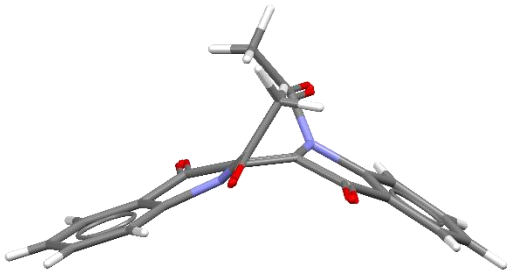

Figure 15 – N, N'-diacetyl-indigo's ChemDraw and CSD structure.[21] (The figure was reproduced with permission)

The structure shows that in this compound, the indigo skeleton is buckled, and the colour of this N-substituted indigo,**8**, has a blue shift that yields a spectrum that is closer to the absorption of gaseous indigo.[8] The solution of **8** absorbs light at 561 nm in toluene. A further experiment was done by making **9**, substituted by two long-chain alkoxy groups. This was reported to be more stable than **8** due to the aliphatic chains' Van der Waal interaction. In both cases, the two indole rings were bent with a dihedral angle of 20° of distortion by experimental measurement. As a result, the entire molecule behaves as a C_2 symmetry and the 5-member rings' conjugated π-systems were deformed and re-hybridised with a greater degree of p-character that shifted towards sp^3. The molecule also experiences more flexibility in all dimensions as a result of the weaker double bond. The UV-Vis spectrum shows that the molecule has a significance of the reduction of the intensity of absorption at around 600 nm, which is the characteristic peak for planar indigo.

In terms of Kasha's exciton model, the presence of the aliphatic groups means that the packing results in reduced intermolecular interactions that would prevent the blue-shifted splitting. Apart from this, the buckled distortion also weakens the H-chromophore linkage as the double bond shows reduced conjugation. The absorption maximum also had blue-shifted to 579 nm and it was closer to the true red colour of gaseous indigo.

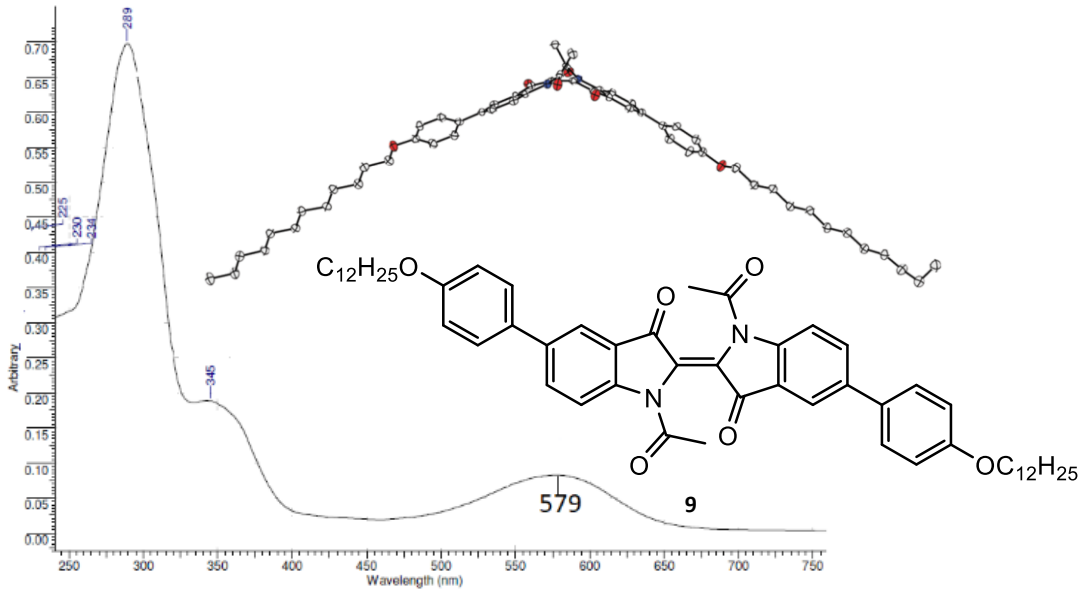

Figure 16 – **9**'s chemical and CSD structures and its UV-Vis spectrum in NMP.

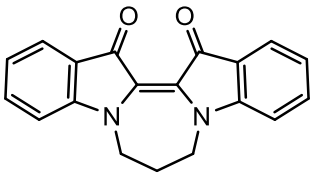

10

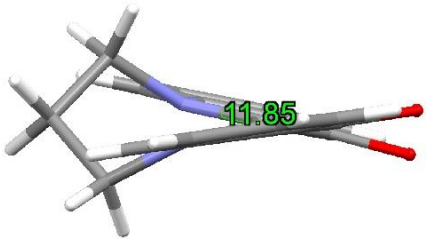

Figure 17 – CSD structure of **10**. [22] (The figure was reproduced with permission)

Another example of a twisted indigo derivative is **10, which** has a propyl-bridge linking the two nitrogen atoms, resulting in a twisted and cis structured indole ring. This combination of effects causes a blue shift relative to indigo and the UV-Vis spectra showed that it has an absorption at 578 nm when it is dissolved in triethylamine.

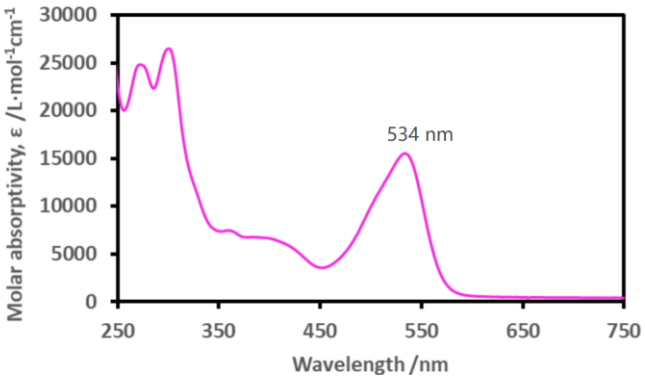

Figure 18 - UV-Vis spectrum of **11** in acetonitrile at room temperature

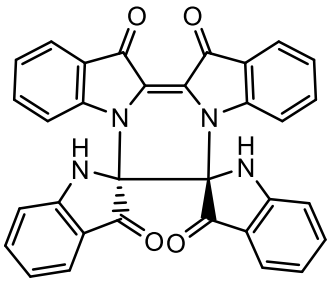

11

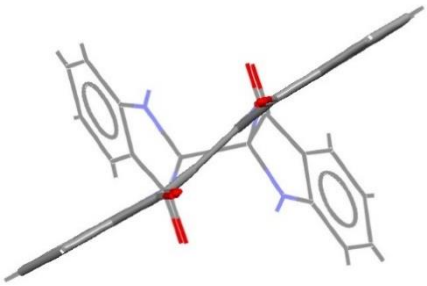

Figure 19 – CSD structure of **11**.[23] (The figure was reproduced with permission)

Compound 11 is an example of skewed indigo that was made by the dimerization of indigo. This molecule has four indoles, including two that are not conjugated. The main skeleton motif is a cis-indigo. The CSD database shows that the two indole rings are almost parallel with an angle of 3.3°. This UV-Vis showed a blue-shifted peak attributed to the distortion and cis-structure interfering with the conjugation of the indigo's π-system and transition dipole. The other two non-conjugated indole rings have no significant contribution of absorption in the visible portion of the spectrum.

1.4.4 Indirubin's packing

Indirubin is an isomer of indigo and it has a related but different packing. The packing of indirubin can be seen from the CSD structure (Figure 20). Unlike indigo, although indirubin has an equal number of each functional group as indigo, the intermolecular hydrogen bonds are also limited geometrically. As a result, indirubin can only bond to two other indirubin molecules rather than the four experienced by indigo. This decreased conjugation restricts indirubin to having a cross-linked lattice structure, and only hydrogen-bond-linked chains are allowed to exist as a more random overall structure. For indigo, it has two orientations for the entire lattice while indirubin has two orientations per chain.

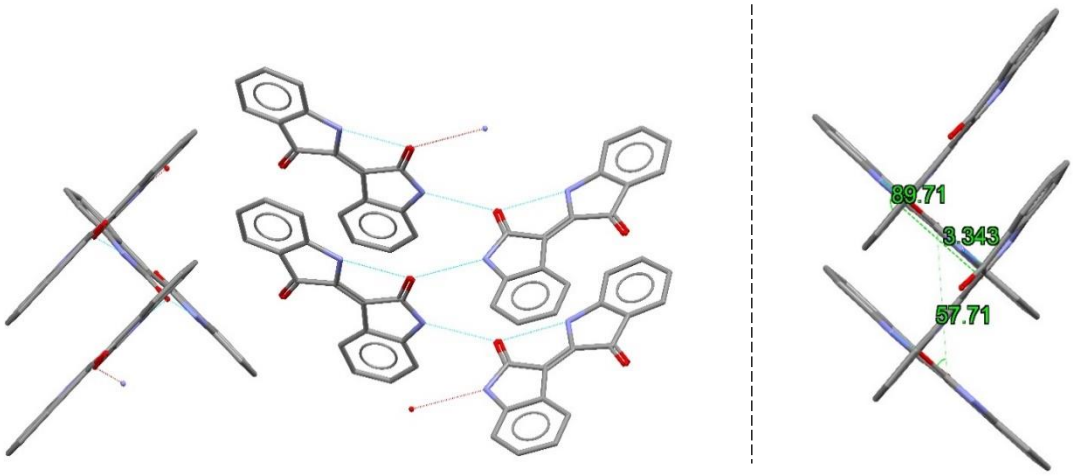

Figure 20 – CSD structure of indirubin, **4**.[24] (The figure was reproduced with permission)

For indirubin, Kasha's exciton model only has the J-aggregate model left, which causes a red shift from its gaseous phase. Also, the non-planar inclined angle of 90° means that there is no splitting, and the random packing due to less hydrogen bonding removes the possibility of the tiny blue shift from the remote "inline". The transition dipole moment of indirubin is not parallel to X-axis as in indigo is because the asymmetrical shape causes the HOMO-LUMO transition to have introduced a node that is neither parallel to X nor Y, which means the splitting was further reduced.

1.5 Orbital energies of indigo

1.5.1 Photophysical response of indigo

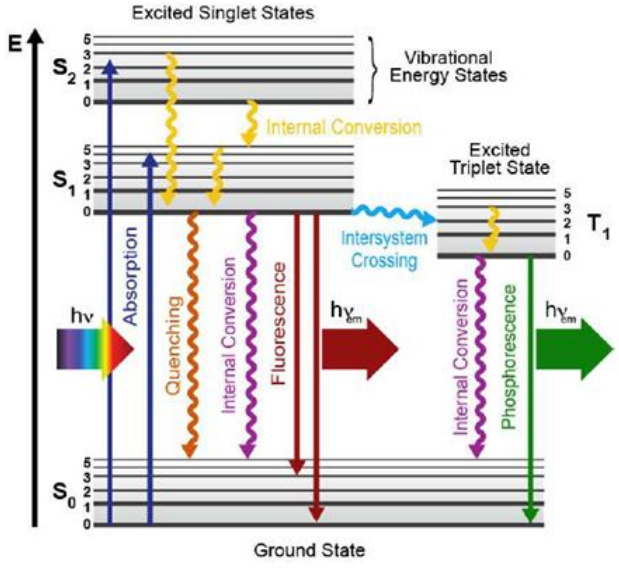

Figure 21 – Jablonski diagram of excitation and relaxation of molecules [25]

Indigo has attracted a lot of research interest for more than a century. In the solid state, indigo has an intense blue colour. This can also be explained by its absorption spectra which shows a maximum, λ_{max}, between 600 to 620 nm in most of the common solvents, which originates from a very strong band $S_1 \leftarrow S_0$ transition, which corresponds to $\pi^* \leftarrow \pi$ transition.

Indigo has a large extinction coefficient, ε = 17708 $M^{-1}cm^{-1}$ in chloroform[26] which indicates a moderately strong absorption. Despite having a highly allowed $S_1 \leftarrow S_0$, indigo has a low fluorescence quantum yield, $\Phi_F = 0.0023$[27], and the intersystem crossing is also inactive.[28] This means, after the absorption, there is barely any emission, but that the excited S_1 state undergoes internal conversion from S_1 back to S_0 decaying via a non-radiative pathway.

Therefore, the physical appearance of the indigo can be considered as just purely affected by the absorption that shows its compensated colour. This same concept also applies to all the other indigo derivatives or indigoids as well.

1.5.2 Electrostatic potential of indigo

The electron density of indigo is shown in Figure 22 as its electrostatic potential surface (ESP). [29] The red zone represents negatively charged areas that are electron-rich, the blue zones corresponds to a positively charged area that has a deficiency of electrons, and the green means neutral. The result proved indigo's quadrupole character with two partially negative centres on carbonyl oxygen and two partially positive centres of the amine groups.

Additionally, it can also be noticed that the 5 and 5'-positions are slightly more positively charged yellow zone from re-centralised aromatic areas and the 6 and 6' positions are slightly more negatively charged around the edges than the 4, 5, or 7 positions. The result indicated the potential difference which can support and explain the effects of substitution around the ring upon the absorption spectra and colour.

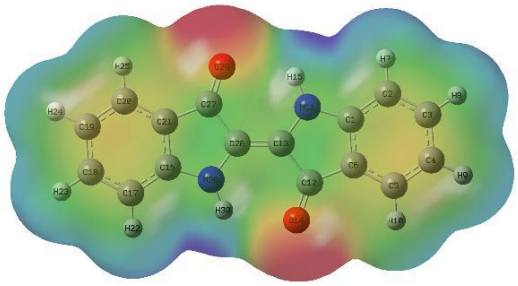

Figure 22 – indigo's molecular electrostatic potential surface[29]

1.5.3 Molecular modelling of indigo excited states

Z. Ju and co-workers reported a calculation of the frontier orbitals of indigo with B3LYP / 6-311G(d,p) (Figure 23).[29] The HOMO-LUMO gap is 2.5035 eV, which is 495.2 nm for discrete indigo molecules. The absorption of indigo comes from this HOMO-LUMO transition minus a pairing energy compensation during excitation.

After the HOMO-LUMO excitation, the greatest change is the extra node introduced to the centre of the molecule, which created an inversion centre to change the π_u HOMO to π_u* LUMO. Since the node is on the y-z plane, the transition dipole is on the x-axis which lies along with the double bond. Therefore, the photon must have a component on the x-axis to have effective activation of the molecule.

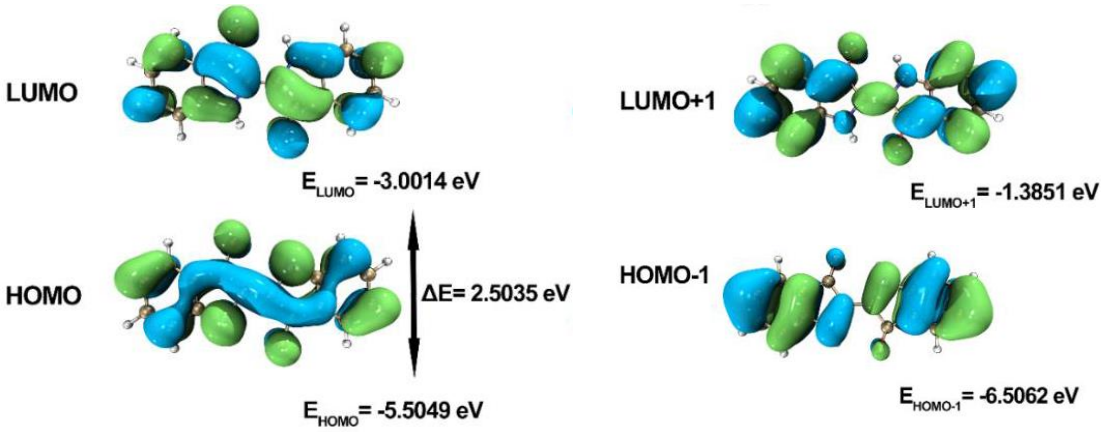

Figure 23 – Frontier orbitals of indigo[29]

The experimental result also showed that a change of orbital contribution of nitrogen and oxygen. The size of the nitrogen orbitals almost halved and the oxygen orbitals increased when they changed from HOMO to LUMO. This corresponds to a charge separation due to resonance and the change from an uncharged molecule as the ground state's form to a zwitterion's excited state.

1.5.4 indirubin

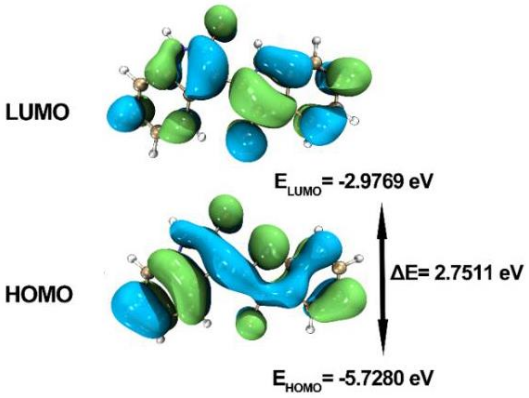

Figure 24 – indirubin and indigo's LUMO and HOMO comparison[29]

Indirubin has a very similar energy gap and contributing orbitals as indigo due to the similarity of the indole fragment and how they are connected.

This can be noticed from its frontier orbitals in Figure 24. The right-hand side of HOMO and LUMO are normal indole rings that have the double bond linkage on the 2nd position and the left-hand side are the rearranged indole system jointed from the 3rd position.

The right-hand side is almost identical to indigo in terms of the size of each orbital and their sign. However, although the left-hand-side LUMO was still similar to indigo but flipped, the HOMO of indirubin was more like a mixed state of HOMO and HOMO+1 of indigo.

Apart from this, for indirubin's HOMO and LUMO orbitals, the top-most green orbitals that correspond to the 2-position carbonyl oxygen has little change during the excitation because it has no neighbouring amine group to share charges. This means a less effective resonance can be expected from indirubin.

This can be shown from indirubin' UV-Vis absorption (450.7 nm), which is observed a shorter wavelength than indigo. The unavailable carbonyl and amine were unable to introduce as much shifts as what the indoles can do within an indigo molecule.

1.6 UV-Vis absorption of indigos

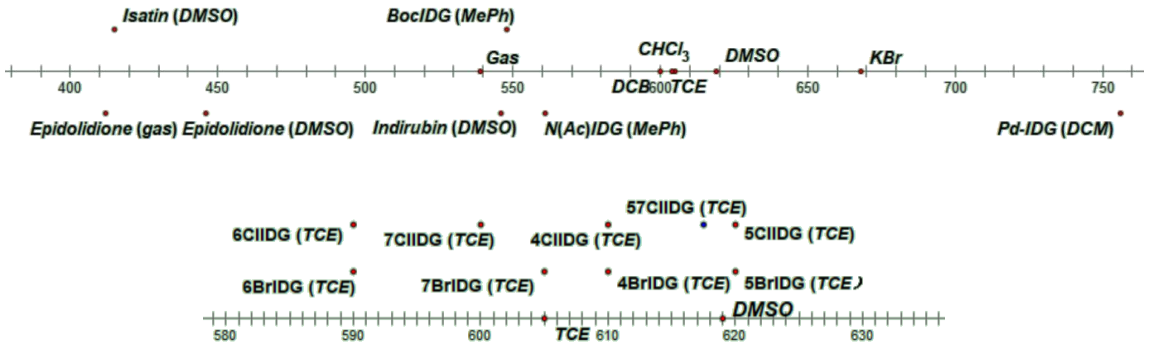

Figure 25 – Literature λ_{max} / nm for indigo and its derivatives the indigo derivative and solvent in brackets. [30]

1.6.1 The UV-Vis absorption when changing indigo's physical state or solvent.

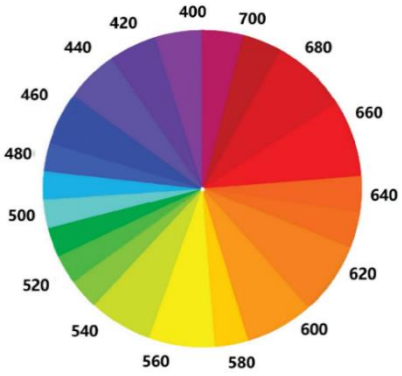

Figure 26 – Complementary colour wheel of light of absorption in its wavelength (in nm) [31]

In the gaseous phase, the absorption spectrum of indigo has a maximum absorption at 539 nm (Figure 10, curve 1).[5] In this state the indigo is present as an individual molecule, meaning there are no significant intermolecular interactions, i.e. hydrogen bonds. The red colour can be seen as the "true" colour of each molecule as their original but a mixed-up band of the wavelength of energy of absorption.

In the condensed phase, as either the pure solid or as a solute, indigos are expected to behave as aggregates due to strong indigo-indigo interactions. This leads to a redshift in the absorption spectrum compared to the gaseous spectrum. The greater the degree of aggregation, the greater the red shift is. In this case, it would be 668 nm as a solid or 590-630 nm in a solution.

1.6.2 Properties of indigo in a different solvent.

Indigo is essentially insoluble in water and it has very poor solubility in common organic solvents such as ethanol, acetone, DCM and DMSO.

UV-Vis spectroscopic analysis of indigo showed that the pigment exhibits a positive net solvatochromism, a red shift to increase its absorption wavelength as the solvent's polarity increases. As it dissolves in a non-polar solvent, the solution can be observed as bluish-purple, e.g. in CCl_4 (λ_{max} = 590 nm). When indigo was dissolved in DMSO, a polar aprotic solvent, its colour is a deeper blue with λ_{max} = 620 nm. This solvatochromism has been widely noticed as a result of H-bond or dipole interaction with the solvent.[32,33]

1.6.3 Indigo's functional group substitution on the aromatic ring.

Indigo's absorption properties are more interesting when its aromatic hydrogens are replaced by other groups. This has been commonly observed and tested when the groups have a strong electron-withdrawing/donating capability in the indigo system. These groups would change the electron density on the heterocycle, particularly at the nitrogen and carbonyl groups, which changes the energy levels. Early research found that there are few changes in the ground state of indigo and the shifts arise from the change of the excited state levels. The most famous example is Tyrian purple, 6,6'-dibromoindigo, which is a vivid deep purple colour. However, all other isomers of 4,4', 5,5' and 7,7'-dibromoindigos are all blue. Therefore, the colour of the substituted indigos' colour is found to be highly dependent upon the combination of position and the nature of the group.

Generally, research interest has focused on 5- and 6- substituted indigos. Because the properties of 4 and 7 substituted indigos are very similar, and their behaviours are normally in between 5- or 6-cases. Additionally, 4- and 7-substituted indigos are more difficult to prepare, and there are fewer available literature examples.

The shift in the absorption spectrum arsing from a 5 or 6-substituent can be correlated by the Hammett σ values of the group in an aromatic system. For example, the Br group is a para-directing group, which has its $\sigma_m > \sigma_p$. In this case, Br substituent would cause a lower absorption at 6 than 5.

The methoxy group also has $\sigma_m > \sigma_p$, which also leads to a red-shift in the 5 substituted indigo and a blue-shift for the 6 substituted indigo. The nitro group is the opposite where it has $\sigma_m < \sigma_p$ and the shifts are also opposed to the other two. [5]

It is also interesting that the 5 or 6 substituted indigos diverge from the absorption maxima of indigo. They did not have both of the maxima to increase or decrease with changes of one greater than the other. Surprisingly, the wavelength changes were also similar in magnitude but in a different direction, which made the average of 5 and 6 similar to that of the parent.

However, the σ value's prediction would fail to predict an accurate shift when the $\Delta\sigma_{m-p}$ is small because the σ values are for a real aromatic system rather than an indigo system. Therefore, the *tert*-butyl group substitution has been noticed as an exception.

Table 1 – $\sigma_{m/p}$ values of substituent and their position of corresponding indigo's UV-Vis absorption wavelength[5,30,34, 35]

σ or Substituent	σ_m	σ_p	5,5'	6,6'
H (DCE or TCE)	-	-	605	
Br (TCE)	+0.37	+0.24	620	590
OMe (DCE)	+0.10	-0.12	645	570
^{t}Bu (TCE)	-0.09	-0.15	592	607
Me (TCE)	-0.06	-0.14	620	595
NO_2 (DCE)	+0.71	+0.81	580	635

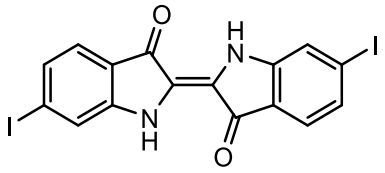

12

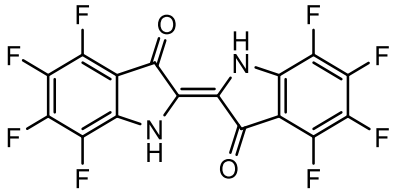

13

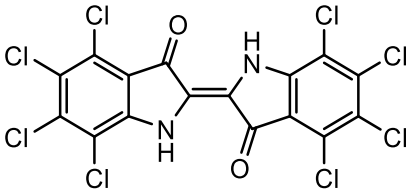

14

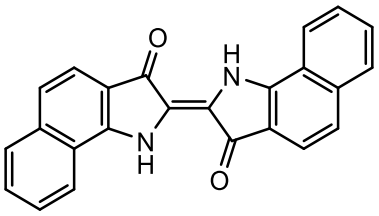

15

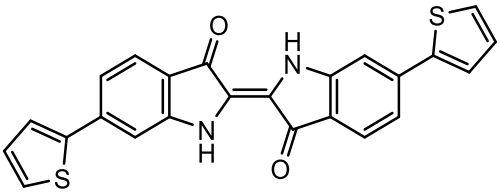

16

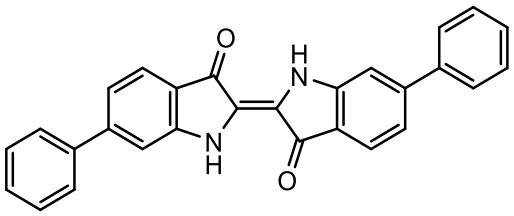

17

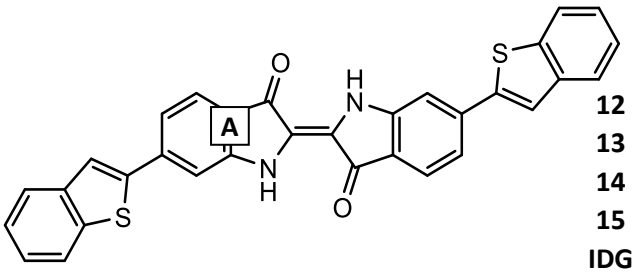

12
13
14
15
IDG

18

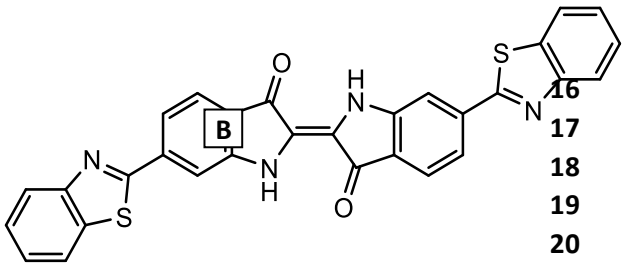

16
17
18
19
20
IDG

19

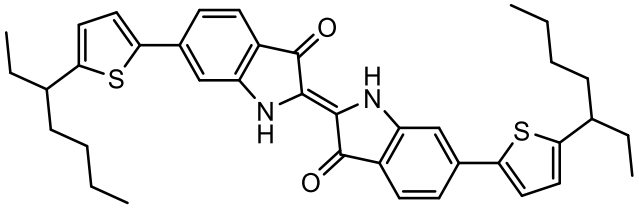

20

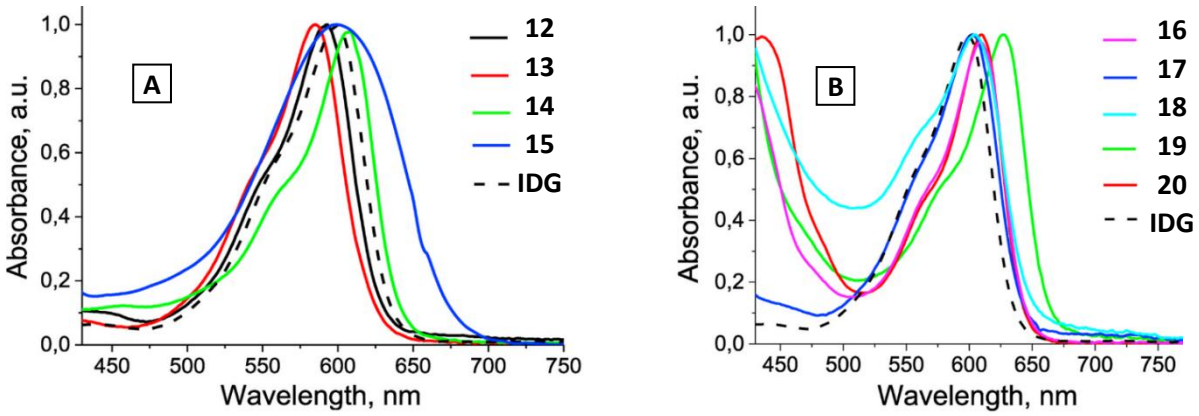

Figure 27 (A)&(B)– Normalized UV-Vis spectra of indigo and its derivatives that dissolved in 1,2-dichlorobenzene (the black broken line is the spectrum of indigo with a max absorption of 600 nm)[36]

Irina V. Klimovich and her team have made a range of indigo derivatives substituted with heterocyclic groups. The absorption spectra recorded in hot 1,2-dichlorobenzene, DCB, are shown in Figure 27.[36] Surprisingly, most of these compounds had similar absorption maxima apart from a significant red shift of the 5,5'-thioindole substituted indigo that increased 28 nm from indigo. From the data, it can be seen that the indigo's absorption spectrum is relatively resilient to change without distortion of the indigo skeleton.

Table 2 – Wavelength of indigos of **12-20** in hot ortho-dichlorobenzene [36]

Molecule	**IDG**	**12**	**13**	**14**	**15**
Wavelength / nm	600	593	584	607	600
Molecule	**16**	**17**	**18**	**19**	**20**
Wavelength / nm	609	602	628	606	610

1.6.4 Indigo in a metal complex

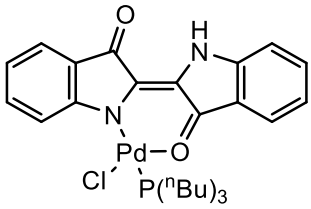

21

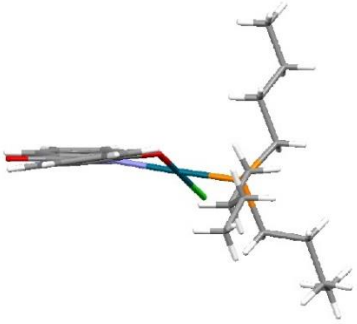

Figure 28 – CSD structure of **21** (indigo acts as a ligand on the left) [37]

Deprotonated indigo can as a bidentate or a tetradentate bridge to form a metal complex with transition metal and lanthanide ions. This complex formation brings about subtle changes in the shape of the indigo frame.

21 is an example of the indigo-based complex in which the indigo is bonded to Pd(II) forming a d^8 square planar complex: the N-Pd-O angle was 91.7° The presence of the metal ion and other ligands caused a twist of the indigo with an angle of 8.8° between the two indole planes. The UV-Vis absorption spectrum of the complex has a maximum of 756 nm in DCM, a red shift of 150 nm. The shift was attributed by the authors to originate from a metal-to-ligand charge transfer (MLCT) between the Pd(II) and heterocycle.[38] The group also prepared and measured the absorption

spectra of other complexes with Pd and Pt with different branching ligands but on the other side of the metal. All of the UV-Vis results are consistent with **21**, which had absorption within a range of 720 to 800 nm.

Other complexes have been prepared in which the characteristic absorption band of indigo may close to disappearing[39] as shown by compound **22**. The calculated spectrum showed tiny absorptions at 667 nm and 708 nm and the measured absorption were at 578 nm, 820 nm and 1002 nm. The spectrum calculated by molecular modelling showed that the complex has a triplet ground state and a low-lying excited ionic state. The complex has a triplet-triplet absorption which is spin allowed metal-to-ligand-charge transfer. Additionally, the indigo was in its cis configuration, which was suggested to correspond to the 578 nm maximum that was from a blue shift of the original 665 nm of free trans-indigo.

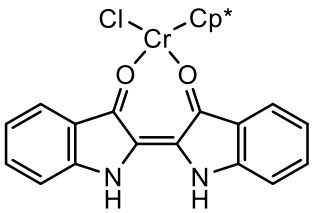

22

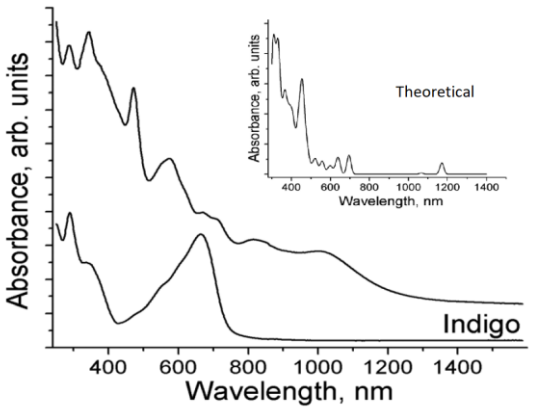

Figure 29 – indigo and complex **21**'s UV-Vis-NIR spectrum in KBr pellets. The right corner is complex **21**'s theoretical spectrum for the same condition.[39]

1.6.5 Indigo isomers

Indigo exists as trans-structure and the free cis-structure is hard to identify as it is assumed to convert back to the trans. Molecular modelling of the cis-indigo yields a UV-Vis absorption maximum of 526 nm compared to a similar calculation of trans-indigo which yields a value of 621 nm.[39] The result showed again that the intramolecular hydrogen bonding within the H-chromophore can have a redder shifted indigo from the gaseous state. Another well-studied example is indirubin, which is blue-shifted from indigo and has been discussed in the previous sections.

An indigo isomer, isoindirubin, **23**, also has but only one merocyanine chain (high-lighted in red). The chain was locked by the alkene bond and it is unable to form any kind of intramolecular hydrogen bond linkage. This compound also has a red colour with an absorption maximum of 552 nm when dissolved in DMSO. [40]

This can be explained by the presence of the merocyanine chain which determined the wavelength would be similar to indirubin. However, due to the lack of direct hydrogen bonding, the conjugation was weaker which increased the absorption wavelength.

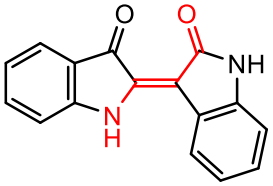

23, Isoindirubin

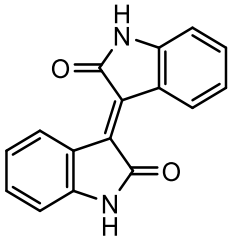

24, Isoindigo

Another example is isoindigo, which is brown. In this compound, two amide groups linked an alkene bond and the merocyanine chain does not exist anymore. At the same time, the intramolecular hydrogen bond became unavailable. As a result, the conjugation of the two indoles was weaker and the resultant UV-Vis spectrum was 490 nm.[40]

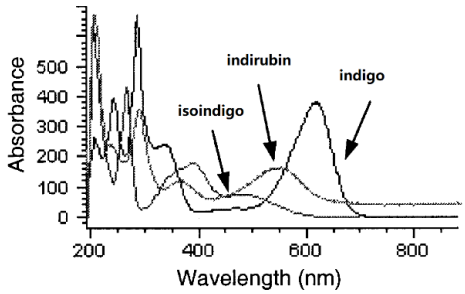

Figure 30 – UV-Vis spectroscopy of indigo, indirubin, and isoindigo. (The figure was adapted with permission)[40]

In Figure 30, the three isomers were tested and showed that indigo has the highest absorbance as a characteristic of its merocyanine chains. As the number of chains decreased from 2 to 1, the absorbance dropped to a half and eventually went down to a quarter.

1.6.6 Properties of other indigoid-skeleton systems

Table 3 – UV-Vis absorption Maxima of indigoid system

Name	Solvent	Absorption Maxima / nm	Colour
Indigo	DMSO	620[41]	blue
Selenoindigo	EtOH	559[42]	red-brown
Thioindigo	MeCN	542[43]	red
Oxindigo	cyclohexane	413[44]	yellow

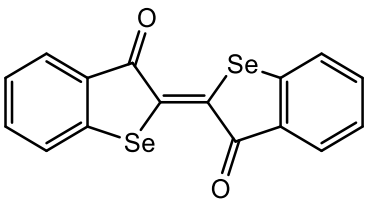

25, Selenoindigo

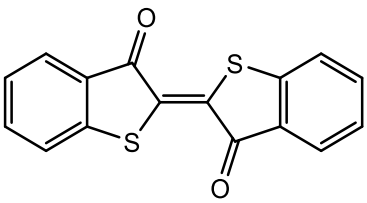

26, Thioindigo

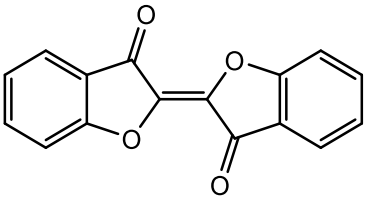

27, Oxindigo

A number of indigo analogues are known in which the nitrogen atoms have been replaced with other elements. It is found that the absorption wavelength of indigo was significantly longer than those containing group-6 substituted indigoid systems. This was dominated by the extra hydrogen on nitrogen atoms, which provided a considerable red shift to the absorption band.

Among the group 6 indigoids, the absorption wavelength increases down the group corresponding to the elements becoming more metallic in character, which makes them better at electron-donating like nitrogen and therefore to have charge separation within the molecule. Therefore, the absorption wavelength was longer.

1.7 The interest of this research

Indigo and analogues have deep and vivid colours with their exact hue depending upon the substitution of the indole ring. Previous research has investigated the effect of changing the electronic distribution of the indigos by adding an electron-donating group or electron-withdrawing groups to the benzene ring.

The research described in this thesis focuses upon the investigation of whether the extended conjugation of indigo affect the colour and/or physical properties and how they could be controlled and modified. This was done by the preparation of indigo derivatives decorated with aryl and arylethynyl groups.

During this research, a family of compounds substituted around the benzene ring of the indole were prepared. These indigos were made by Suzuki or Sonaogashira coupling reactions of the commercially available bromoindoles to obtain the substituted indoles. These were converted to the 3-acetoxy-indole precursors from which the indigo derivatives were prepared by hydrolysis and oxidation. The final products were collected and their UV-Vis spectra were measured in DMSO or DCM at room temperature.

In parallel to the synthetic work, molecular modelling was used to model the electronic structure of the di(p-tolyl)-indigo derivatives using Gaussian-16 with CAM-B3LYP (6-31g + d) to simulate their frontier orbitals and UV-Vis absorption maximum as discrete molecules.

The research also noticed a few indigo samples that would undergo degradation to isatin in the presence of oxygen. This observation was studied and investigated.

2. Overview of synthesis

2.1 Laboratory synthetic method of indigo

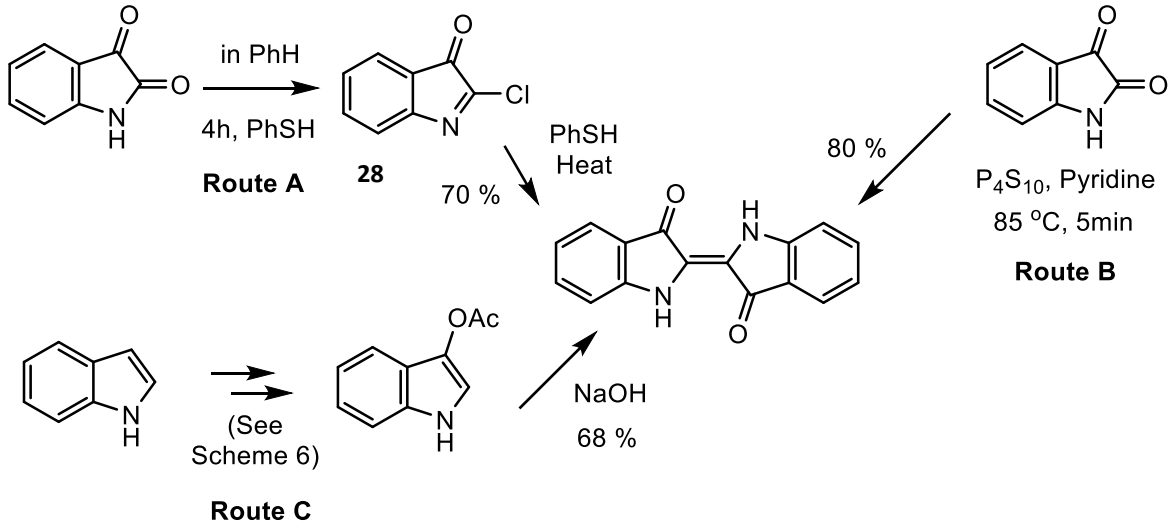

Figure 31 – Laboratory indigo synthesis methods with their condition and their literature yields. [45-47]

Different routes to the substituted indigo derivatives were explored, as shown in Figure 31.

2.1.1 Route A of indigo synthesis

Route A takes 2-chloro-3H-indol-3-one (28) as the precursor of indigo synthesis, a route created by Alan Katrizky.[45] The reaction of 28 with thiophenol in refluxing benzene for 4 hours in the presence of thiophenol gave a reported yield of 70% of the desired indigo.

The greatest challenge for this synthetic pathway is the stability of (**28**): it was reported as an extremely reactive compound that can be easily and completely hydrolysed by the water vapour in the air. Even the report of the successful synthesis had recorded trials where no indigo had been formed. Also because of the sensitivity of the chemical, it is not commercially and has to be made from isatin, the difficulty to handle the chemical made this route unlikely to fulfil the need for this research.

2.1.2 Route B of indigo synthesis

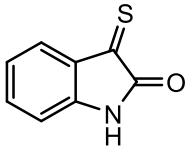

29

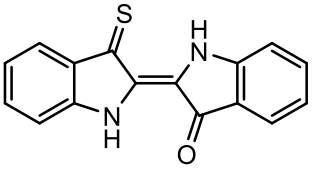

30

Route B was the method described by Adolf Baeyer in 1879 but he failed to obtain indigo. The practical success of this method was not achieved until 1994 by Jan Bergan.[46] The reaction reacts to isatin and di-phosphorus pentasulfide (P_4S_{10}) in pyridine at 85 °C for 5 minutes to form indigo with a

good yield of 90%. However, this reaction scheme would also have a side reaction. When the reaction mixture was heated to a high temperature, coupling and extrusion of sulphur would occur simultaneously. This means sulphur may replace the oxygen on position 3 of the isatin. Therefore, the product would be a mixture of indigo and 3-thioisatin (**29**). Additionally, since the optimum result requires the reaction to be precisely controlled to react for 5 minutes and at 85 degrees. Insufficient reaction would have a poor yield. When it is over reacted, the product would continue to react with phosphorus pentasusulfide (P_4S_{10}) to replace one but only one oxygen of the indigo to give a mono-thionated impurity as (**30**). After around 30 minutes of reaction, more mono-thionated indigo can be found in the mixture, as well as indirubin as another by-product. Therefore, Route B was not a suitable route for this research.

2.1.3 Route C of indigo synthesis

Because of the challenge of routes A & B, the synthesis of indigo by the spontaneous oxidative coupling of 3-hydroxyindole, formed by the in situ hydrolysis of 3-acetoxy indole was chosen. Although the overall yield is slightly lower than the other two methods, the reaction conditions are simpler and the intermediates are readily purified and characterised. These stable intermediates can then be taken through to the indigo under mild and facile conditions.

The parent 3-acetoxy indole is commercially available, however, substituted derivatives are not. Therefore, the preparation of substituted acetoxy indoles was further considered, giving the flexibility to allow a wider range of indigo derivatives to apply for such a synthetic method. This will be discussed in the next section.

2.2 Indole and acetoxy indole synthesis

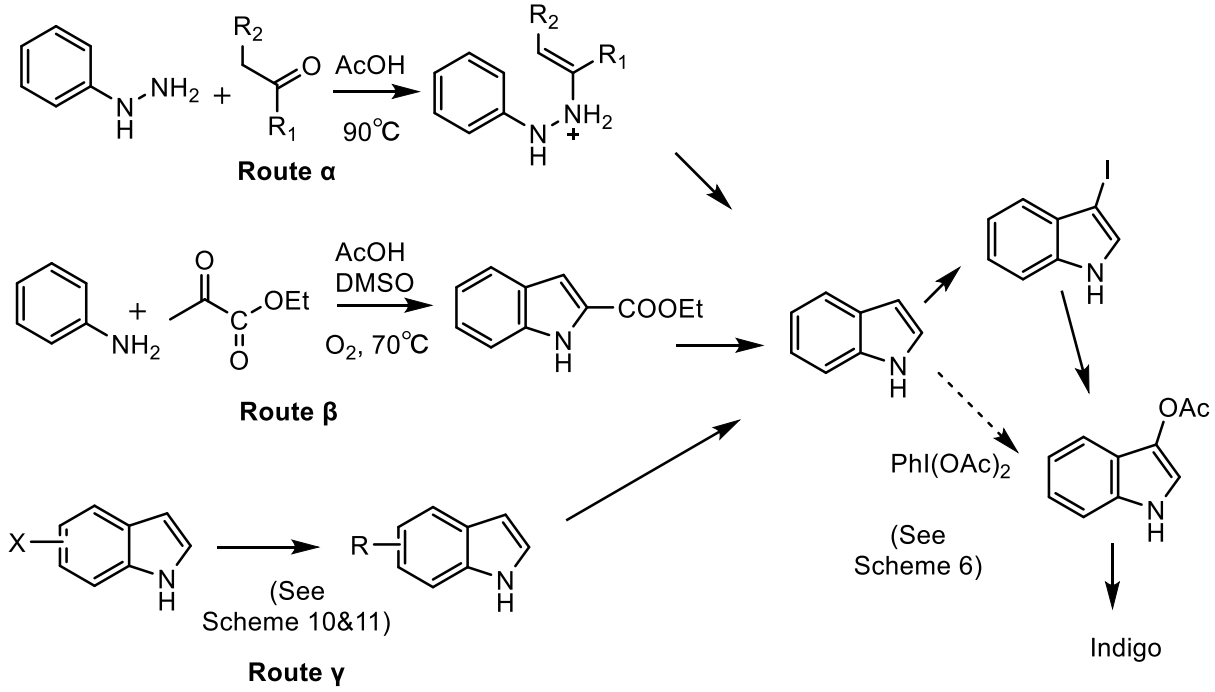

Figure 32 – synthesis plans of indole and acetoxy indole. [48-50,54,55]

To complete the synthesis of indigo by Route C, the indole precursor's synthetic plan was investigated as shown below.

2.2.1 Indole to acetoxy indole

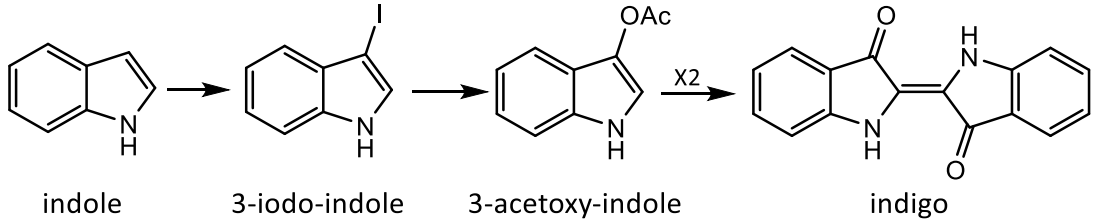

Scheme 6 – A brief indigo synthesis plan that starts from indole (right-hand-side of Figure 32, the details can be found in Chap.6.2, Scheme 8 and Scheme 9)

The most widely reported method is a multi-step synthesis that starts from indole (Scheme 6) and is the method adopted in this research. The practical detail of this scheme will be discussed as a generic method in Sections 6.2.1 & 6.2.2.

Based on the result of this research, the average yield of the reaction from indole to acetoxy indole is just around 40 %. Although it is lower than the other methods, the reaction is mild and easy to control. Additionally, because both indole and acetoxy indole have moderate solubility, the purification of the product can be easily done by column chromatography.

Although some indigo derivatives can be made through Suzuki or Sonogashira couplings that start from a dibromo-indigo. The solubility of the dibromo-indigo made it hard to react. Although adding bulky Boc groups on the nitrogen atoms does make the indigos soluble for a reaction and the Boc group can be removed by thermal-decomposition, the price to buy the commercially available dibromo-indigo or to add the Boc the chemical would make the reaction unaffordable if a range of indigos is needed.

A direct route from indole to acetoxy indole by reaction with diacetoxy iodobenzene(diacetate) method was reported by Guosheng Huang in 2010, which was shown by the dotted line that point from indole to acetoxy indole. [47] The reported yield is higher than the two-step method used in this research but with a cheaper reagent, $PhI(OAc)_2$ and it can react under a lower temperature. This route has the potential to be a better method, however, due to a lack of consistent data of the same method from other scientists and the limitation of time of this research, this method was not attempted.

2.2.2 Route α of indole synthesis (Fischer indole synthesis)

Route α is known as the Fischer indole synthesis, which is one of the most popular methods to form an indole from an aromatic system. [48] However, although Fischer indole synthesis may react completely, most of the successful examples require the R2 position (position 3 of the indole) as a non-hydrogen group.[49] However, having hydrogen at position-3 of the indole is key for the following indole to acetoxy indole to react as it will be substituted by the iodo group. An additional step for R2 group cleavage would potentially introduce impurities and lower the yield.

If other indole derivatives are attempted for this method, apart from 5-substituted indole that would start from para-substituted aniline, another attempt would unavoidably create products that were mixtures of indole isomer with potentially very similar properties and hence hard to separate.

As a result, this route via the Fischer indole synthesis method was abandoned.

2.2.3 Route β of indole synthesis

Route β also being with a substituted aniline, yielding the 2-carboxylic ester of the indole.[50] This route was investigated and attempted once in this project to prepare 5-bromoindole. However, this trial showed that the attempted yield was less than 40 % for the first step and, as for the Fischer indole synthesis it cannot be readily used for asymmetric anilines, meaning that routes to more complicated indole/indigo derivatives were expected to have an even lower yield. The yield was also hugely affected by the usage of the 4 Å molecular sieve.

Additional consideration of isomer product also involves the same reason for Route α in Section 2.2.3 and Route β was also abandoned.

2.2.4 Route γ of indole synthesis as the method for this research

This route starts with the commercially available bromo-substituted indoles and uses palladium(0) catalysed Suzuki or Sonogashira coupling to generate aryl or arylethynyl substituted indoles.[54,55] These can then be taken forwards to the corresponding indigos via the 3-iodo and 3-acetate derivatives that are then hydrolysed and undergo spontaneous oxidation in the air to the symmetrically substituted indigos.

3. Spectroscopy of indigo

3.1 Table of synthesis

During this research, indole and indigo samples were synthesised. The structures and absorption λ_{max} can be found in Tables 4 & 5. The synthesis process can be found in Chapter 6.

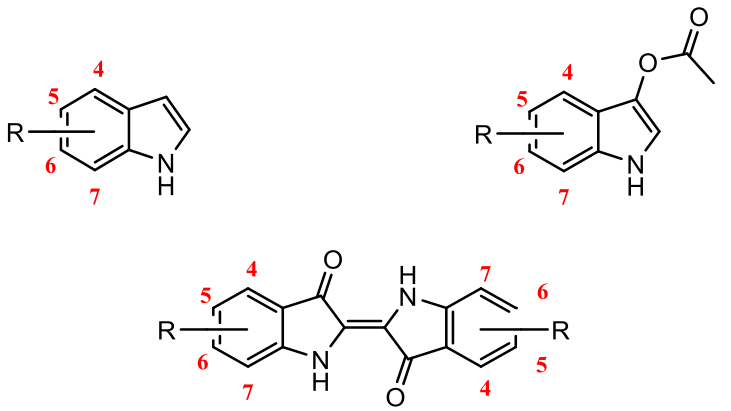

Table 4 – the indole, acetoxy indole and indigo were made during this research and their corresponding molecule caption number and their UV-Vis spectroscopy maxima absorption wavelength in DMSO

R group	Position	indole	Acetoxy indole	indigo	λ_{max} in DMSO / nm
-Br	4	Bought as Commercial product	**31**	Not attempted	-
	5		**32**		-
	6		**33**		-
	7		**34**		-
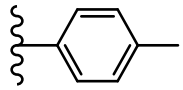	4	**36**	**40**	**44**	637
	5	**37**	**41**	**45**	605
	6	**38**	**42**	**46**	622
	7	**39**	**43**	**47**	617
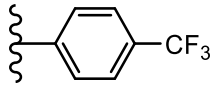	5	**48**	**50**	**52**	636
	6	**49**	**51**	**53**	601
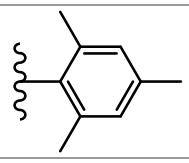	5	**54**	**56**	**58**	634
	6	**55**	**57**	**59**	599
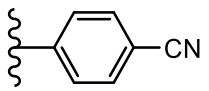	5	**60**	Failed	-	-
	6	**61**	Failed	-	-

R group	Position	indole	Acetoxy indole	indigo	λ_{max} in DMSO / nm
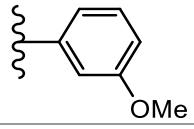	5	**62**	**64**	Failed	-
	6	**63**	**65**	**66**	627
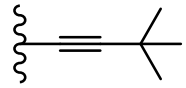	5	**67**	**73**	**79**	627
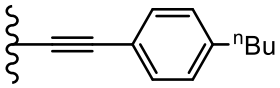	5	**68**	**74**	**80**	607
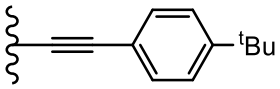	4	**69**	**75**	Failed	-
	5	**70**	**76**	**81**	641
	6	**71**	**77**	**82**	614
	7	**72**	**78**	**83**	607
N,N'-diBoc-indigo Boc = COO^tBu R = -Br	N/A	N/A		**84**	552
	5			**85**	561
	6			**86**	565

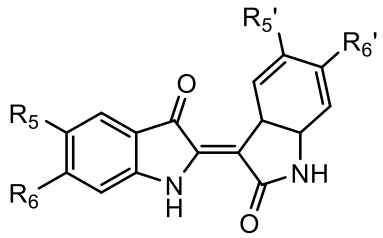

Table 5 – Dibromoindirubin made in this research and their corresponding molecule caption number and their UV-Vis spectroscopy maxima absorption wavelength in DMSO

R_5	**R_6**	**R_5'**	**R_6'**	**Indirubin**		**λ_{max} in DMSO**
Br	H	Br	H	5,5'	**87**	558
H	Br	H	Br	6,6'	**88**	556
Br	H	H	Br	5,6'	**89**	573
H	Br	Br	H	6,5'	**90**	545

3.2 Experimental UV-Vis spectra

NB *Due to the poor solubility of indigos, the solution was filtered before the measurement. The product was low quantity that is hard to be weighed on balance. The concentration was not recorded. Therefore, the extinction coefficients were not calculated.*

To overview absorption behaviours of samples listed in Tables 4 & 5, their final indigo products' UV-Vis spectra were measured in DMSO at room temperature and pressure. Their λ_{max} were plotted and combined on an axis of absorption wavelength in nm (Figure 33).

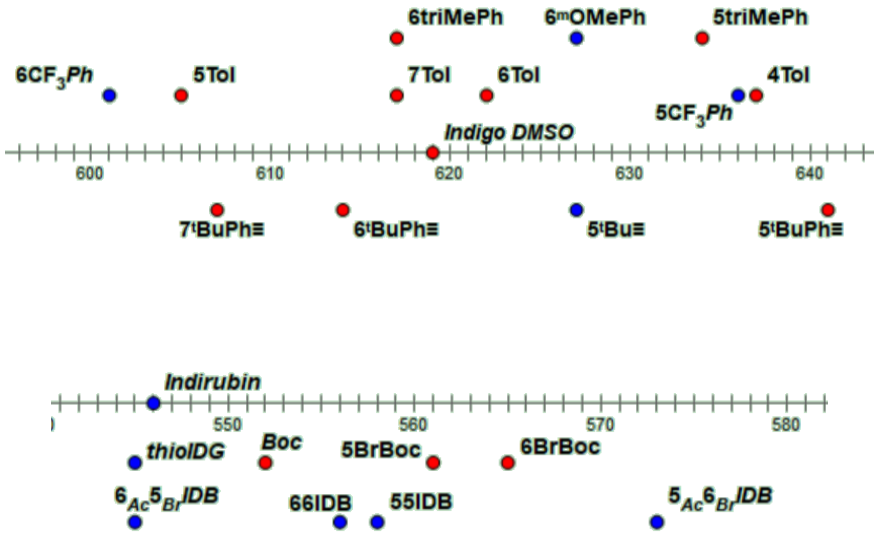

Figure 33 - Experimental λ_{max} of samples made during this research in DMSO at room temperature (The abbreviations are substituted group followed by its position, more abbreviations can be found on pg.3) (The detailed structure and value can be found in Table 4 and Table 5; The y-coordinates and colour of the dots have no implication)

For all of the UV-Vis spectra of the compounds prepared during this work, the absorption maxima were represented as dots on a number line in Figure 33 for comparison and they were dissolved in DMSO at room temperature. The more detailed plots can be found below and the exact values of each can be found in the table of synthesis (Section 3.3). Additional UV-Vis spectra acquired in DCM can also be found below. Generally, the indigo's derivatives were are around ± 20 nm of indigo.

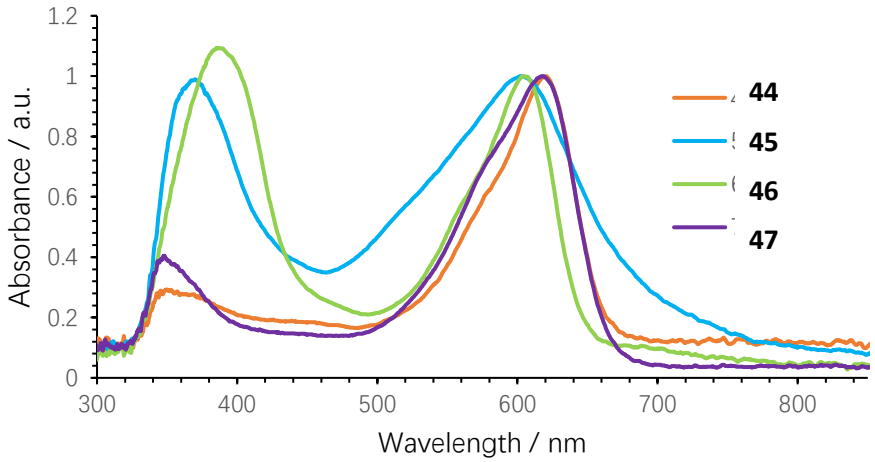

Figure 34 – Normalised UV-Vis spectra for ditoly-indigo derivatives in DCM

Table 6 – UV-Vis absorption Maxima of di(p-tolyl)-indigo in DCM

Name		Solvent	Absorption Maximum / nm
4,4'-di(p-tolyl)-indigo	**44**	DCM	620
5,5'-di(p-tolyl)-indigo	**45**	DCM	602
6,6'-di(p-tolyl)-indigo	**46**	DCM	604
7,7'-di(p-tolyl)-indigo	**47**	DCM	618

This result is showing a different trend to the bromo substituted indigos where the 6-bromo-indigo (Tyrian purple) stood out to have a smaller blue shift than the absorption spectra of 4, 5, or 7-derivatives. This is attributed to the bromo group being a weak electron-withdrawing group, whereas the tolyl group is a weak electron-donating group. In this case, 6-bromo-indigo shows its electronic characteristic which made the dye looks more purple.

For tolyl-indigos, the σ-donating/withdrawing effects of the group are negligible. However, the presence of this bulky substituent can hugely affect the hydrogen bonds that connect indigo molecules. As the packing of indigo discussed in the previous section 1.4.2 and Figure 13, the presence of the tolyl groups are attached on 4 or 7 positions would sit very close to either the O or N of the indole ring. Then, when the tolyl groups are on either 4 or 7, the aromatic group would lie parallel to the hydrogen bond, but longer than O-H hydrogen bond interaction. Therefore, the hydrogen bonds are geometrically forbidden and this means a considerable number of hydrogen bonds will be disconnected or distorted due to the steric repulsion from the bulkier tolyl group. For 5 or 6 positions, the tolyl groups cannot reach the binding site, which would have minimal impact on the absorption spectrum.

When the indigo derivatives are dissolved in solution, this would not just apply to the hydrogen bond but also interaction from the solvent molecule if they interact with the N or O. Hence this explains why 5 and 6 substituted indigos are similar as less steric with a difference to 4 and 7 indigo.

Therefore, as explained previously with examples of indigo's derivatives and isomers. The reduced availability of hydrogen bonds would cause a shift in the indigo's absorption spectrum shorter wavelength.

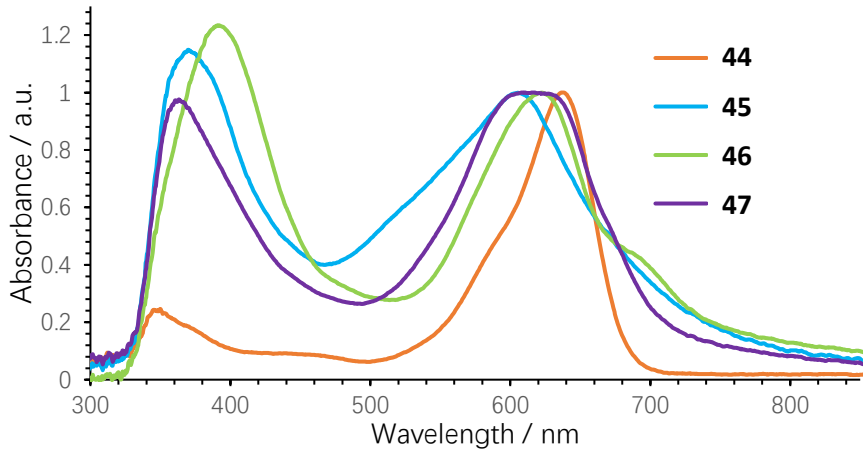

Figure 35 – Normalised UV-Vis spectra for ditolyl-indigos in DMSO

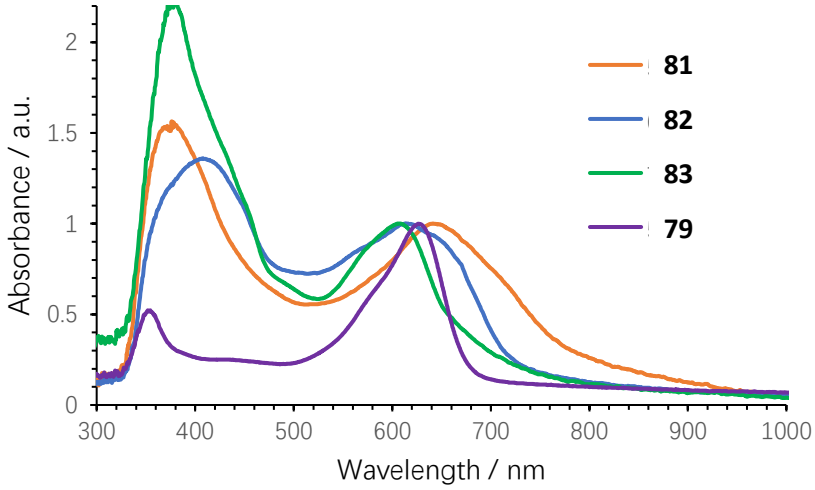

Figure 36 – Normalised UV-Vis spectra of 4-(*tert*-butyl-phenyl-ethynyl)- and 3,3-dimethyl-but-1-ynyl indigo derivatives in DMSO solution

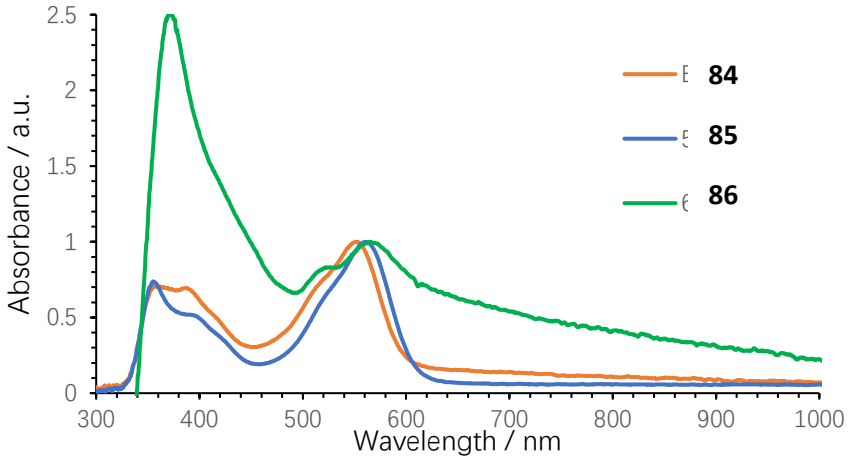

Figure 37 – Normalised UV-Vis spectra of *N,N*'-diBocindigo and its dibromo derivatives in DMSO

From Figure 37, the spectra of the *N,N*'-diBoc-dibromoindigos with the 5 and 6 positions have a red shift compared to the original *N,N*'-diBoc-indigo. This demonstrates that after the indigo skeleton has been distorted from the planar conformation, and the electrons are less delocalised that the 5th or the 6th position substitution cause less shift of absorption. The fact that both shifts were in the same direction indicated the nature of the electron-withdrawing bromo group on the indole system.

The dibromoindirubin's UV-Vis absorption spectra (Figure 38) showed that the compound with the longest wavelength absorption is **89** (the product of the reaction of 3-acetoxy-5-bromoindole and 6-bromoisatin, 573 nm), and the shortest one is **90** (the product between 3-acetoxy-6-bromoindole and 5-bromoisatin, 545 nm). The result means that the position of the H-chromophore is influenced by the relative position to the double-bond linking the two indoles, rather than the substituents on the indole's aromatic ring.

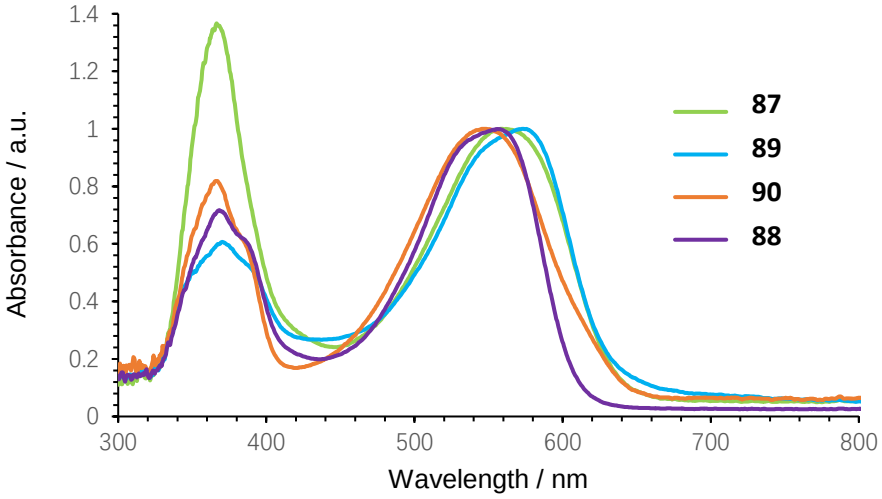

Figure 38 - Normalised UV-Vis spectra of dibromoindirubin in DMSO

3.3 Degradation of indigo derivative

3.3.1 Observations of degradation

Surprisingly, although indigo is known as a stable chemical for centuries, during this research, it has been found that some of the indigo derivatives rapidly degraded after they were dissolved in different solvents (i.e. acetone, DCM, water, MeOH).

The observation is that the fresh indigo derivative solution would gradually undergo a colour change from blue to green to yellow and that this process may occur over a period of hours or days until it the solution is finally colourless.

The degradation was firstly noticed from 4,4'-di(p-tolyl)-indigo's solution in its acetone washing that was left outside, further trials showed that it may decompose in other solvents. Some other samples has also been noticed with the same behaviour. For instance, 6,6'-Bis(trimethylphenyl)-indigo showed its labile character and has been further tested. The recorded phenomena are listed in Table 7. All the solutions were from the same sample of **44** or **59**.

The table lists the sample that was used and the solvent of the sample that had shown degradation. Air exposure was estimated as the time taken during the preparation of the solutions, which had all of them under room conditions. The time-taken and colour changes for the degradation were also estimated.

It was confirmed qualitatively that the degradation correlated with the exposure of the solution to the air and light, but that these may speed up the degradation but are not a requirement of the degradation. In the solid-state of 4,4'-di(p-tolyl)-indigo may degrade after time, but there was no observable difference after the solid-state was kept at room temperature for a few months and the correlation between the solid-state and degradation was unable to be concluded.

The same solution (Trial No. 4) was measured before and after degradation, the original peak of absorption at 637 nm disappeared, and it was replaced by a smoother peak at 423 nm.

Two possible degradations are reported in the literature and are considered here, in which the indigo may degrade to isatin or leuco indigo.

Table 7 – degraded samples summary

Trial	Chemicals and their initial colour	Solvent	Estimated Duration of air exposure	Time-taken (corresponding colour changes)	Result and additional information
1	4,4'-di(p-tolyl)-indigo, **44**, blue	Acetone	2 h	After opened, 3d (green) 14d (colourless)	Maintained blue for 28d before opened and degraded after opened
2		Acetone	10 min	Maintained blue for at least 28d	Covered with foil
3		DCM	1 h	7d (yellow)	Room temperature
4		DMSO	1 h	3h (green) 3d (yellow)	Dark at 4 °C
5	6,6'-di(trimethylphenyl)-indigo, **59**, greenish blue	Solid	2 d	14d (greenish grey)	Room temperature
6		DMSO	1 s	1s (Blue to green to yellow)	0.5 mL DMSO was added to 1 mg of **59**
7		DMSO	1s	1s (Blue to green to yellow)	1 mg of solid **59** was added to 0.5 mL DMSO

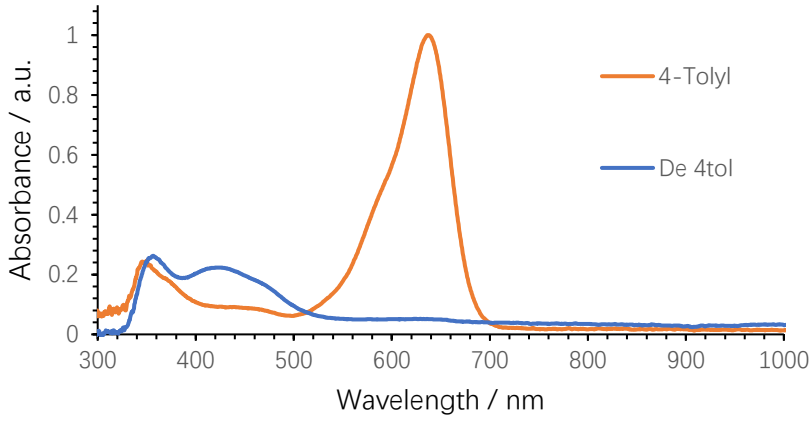

Figure 39 – UV-Vis spectra of 4,4'-di(p-tolyl)indigo in DMSO with similar estimated concentration when it is fresh (red) and after degradation (blue).

3.3.2 Degradation to isatin

In the cases of our research, the degradation formed isatin, in which the double bond linking the two indole rings has been cleaved and replaced by carbonyl groups in the two fragments.

The reaction mechanism has not been confirmed and a possible explanation is oxidation by the oxygen in the air, and then analysing the end products by accurate mass spectroscopy, which supported the hypothesis. The absorption spectrum also agreed with the literature and experiemental absorption of isatin (Figure 33).[51] For simpler indigoids like indigo, this oxidation

process is negligible, and more forcing conditions are required, a strong oxidising agent like potassium dichromate or nitric acid is needed to degrade. The great stability of indigo is one of the important reasons why examples of indigo used by the ancients still survive as a vibrant blue material. However, there are limited researches on indigo's decomposition in air.

Since the indigo-to-isatin route can only happen in the presence of an oxidising agent and the only possible oxidising agent is oxygen, this research suggests a possibility that the indigos had gone through decomposition in air.

3.3.3 Degradation to leuco indigo

Another possible degradation has been reported in which indigo can degrade to leuco indigo. The phenomenon was observed as a photo-decomposition of indigo in the presence of UV. [52]

The leuco-indigo produced in this way may undergo oxidation back to indigo in a vessel exposed to the air. However, although leuco indigos are generally known as an unstable species, for molecules such as **10**, where the shape and conjugation to be constrained, it may remain as the relatively stable leuco indigo form.Their experimental data showed that for indigo itself the leuco indigo can only be generated following exposure to UV, and it will be oxidised back to indigo-form spontaneously unless the structure is locked.

In this work, all of the indigos had full H-chromophore stabilisation and none were locked as cis-structure. In addition to the results obtained from mass spectrometry of the degraded samples, the degradation to the leuco-form of our indigos degradation was not the pathway in this work.

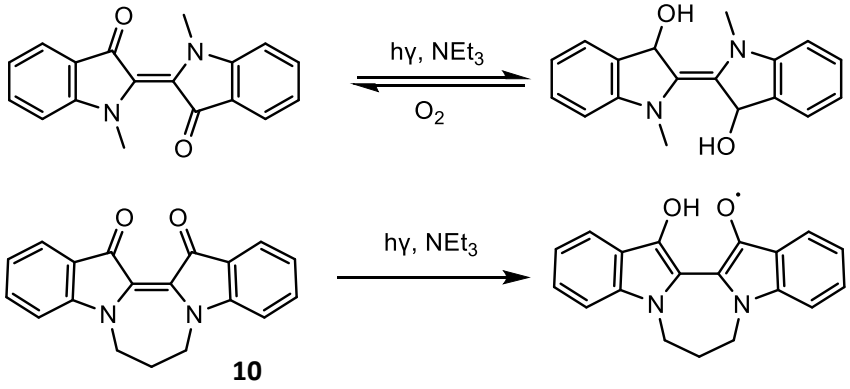

Scheme 7 – Photo-decomposition of *N,N*'-dimethyl-indigo and **10** [52]

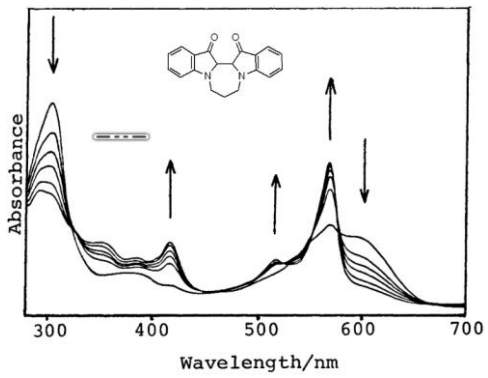

Figure 40 – UV-Vis Spectra of **10** in NEt_3 at 0, 15, 30, 45 75, 105 min.[47]

4. Molecular modelling of indigo derivatives

4.1 Calculation of electronic structure of bis(p-tolyl)-indigo derivatives

The electronic structure of indigo derivatives was carried out using Gaussian-16, employing a CAM-B3LYP functional and 6-31g+d basis set. Structures were first optimised then followed by the first excited state calculated using TD-DFT. These calculations allowed the nature of the transition to the first excited state to be described, which in each case was dominated by a LUMO-HOMO transition. The calculated HOMO & LUMO's (Table 8) and predicted UV-Vis absorption spectra, calculated in the gas phase (Table 9).

Table 8 – Results of Gaussian-16 calculation of di(p-tolyl)-indigos

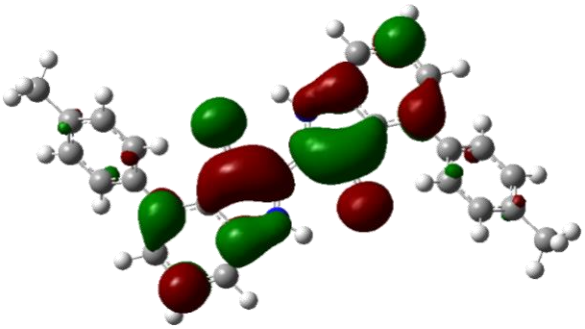

LUMO (E = -1.941 eV)

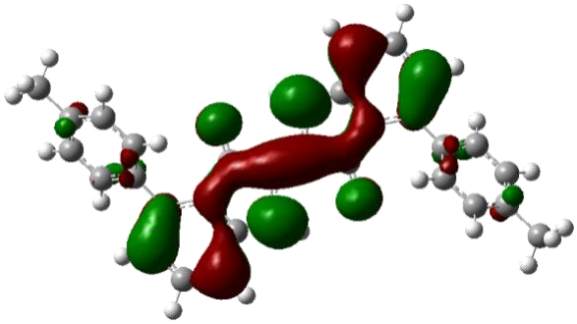

HOMO (E = -6.656 eV)

4,4'-di(p-tolyl)-indigo

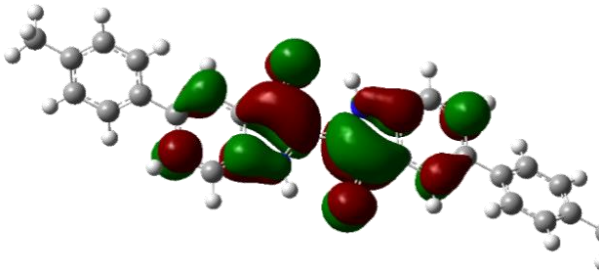

LUMO (E = -2.006 eV)

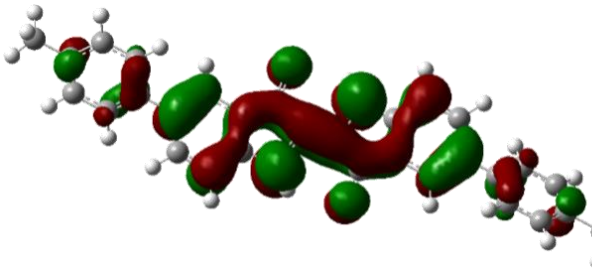

HOMO (E = -6.664 eV)

5,5'-di(p-tolyl)-indigo

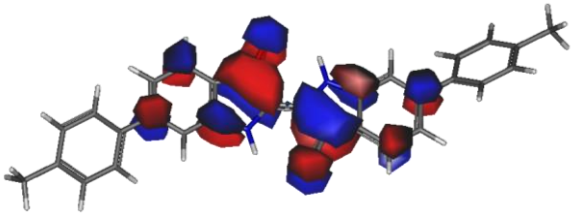

LUMO (E = -2.122 eV)

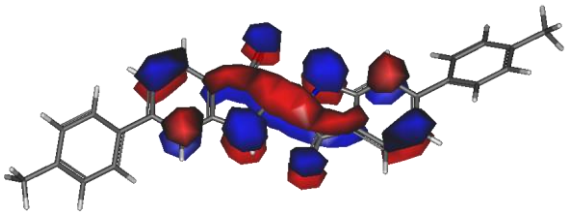

HOMO (E = -6.810 eV)

6,6'-di(p-tolyl)-indigo

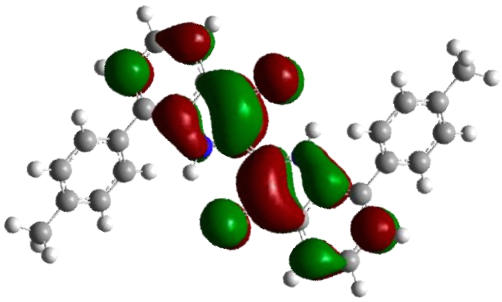

LUMO (E = -1.927 eV)

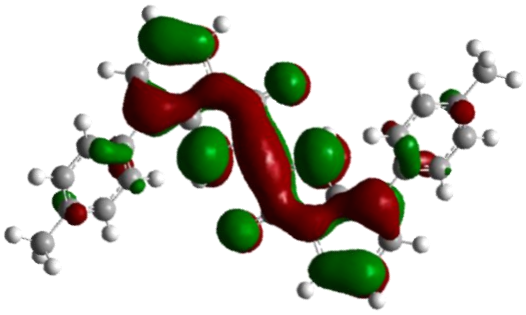

HOMO (E = -6.378 eV)

7,7’-di(p-tolyl)-indigo

Table 9 – Predicted UV-Vis spectra of di(p-tolyl)-indigos by gaussian calculation

4,4’-di(p-tolyl)-indigo	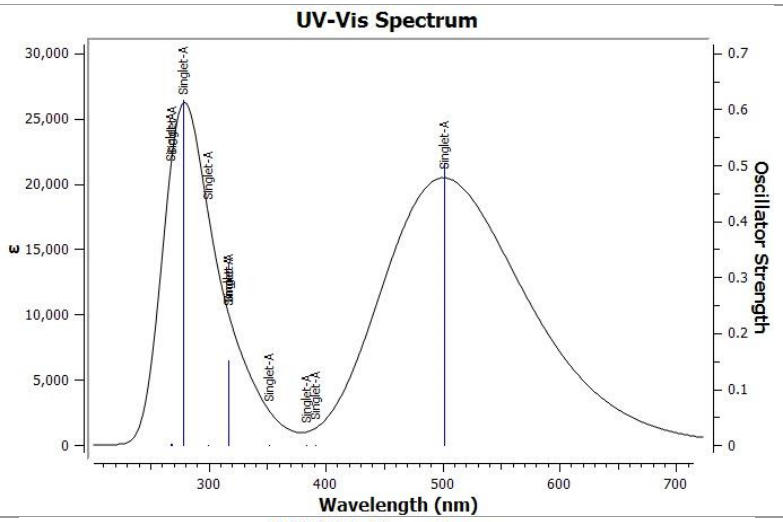
λ_{max} = 496.70 nm (singlet)	
oscillator strength = 0.5041	
5,5’-di(p-tolyl)-indigo	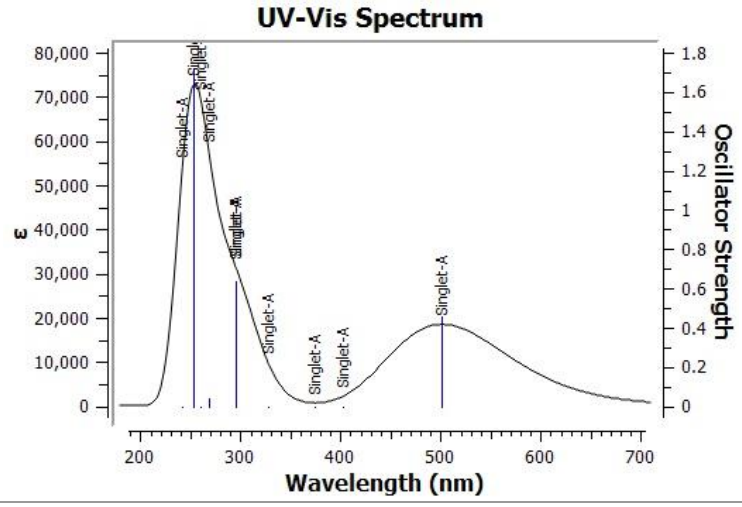
λ_{max} = 502.29 nm (singlet)	
oscillator strength = 0.4551	

6,6'-di(p-tolyl)-indigo	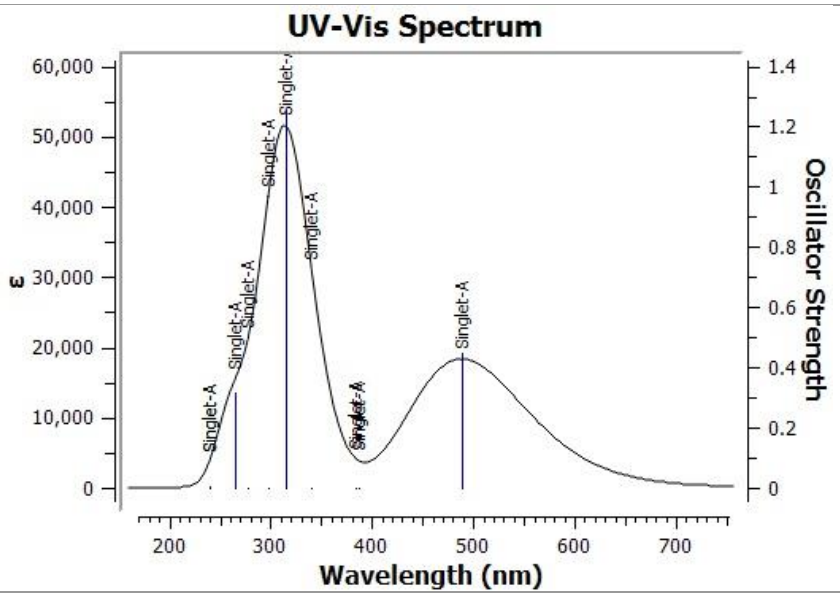
λ_{max} = 491.20 nm (singlet)	
oscillator strength = 0.4510	
7,7'-di(p-tolyl)-indigo	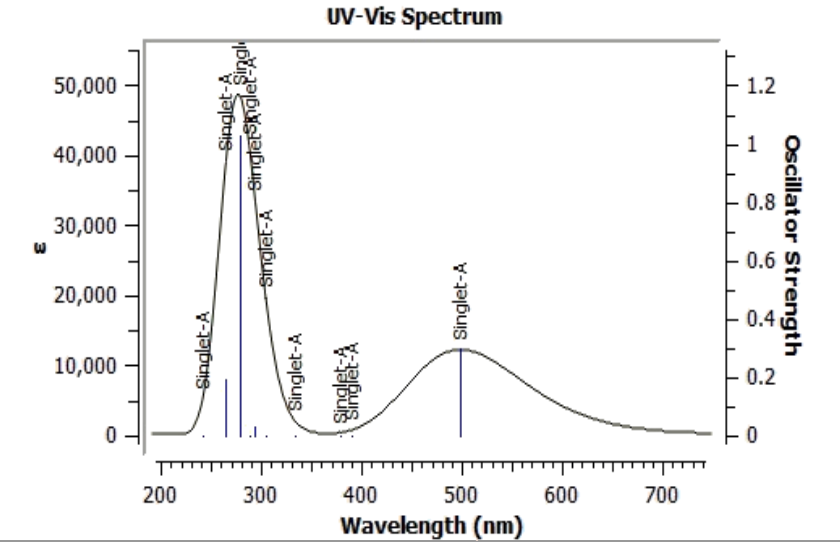
λ_{max} = 497.58 nm (singlet)	
oscillator strength = 0.2991	

Calculations reveal that none of the di(p-tolyl)-indigos are planar. The substituted tolyl rings are twisted away from the indole and indigo planes. This is a result of steric interactions between the 2,6-hydrogen atoms and the indole aromatic ring. The twist also causes the substituted aromatic orbitals to have less contribution in the frontier orbitals, and especially in the LUMOs.

Therefore, comparing the HOMO and LUMO of di(p-tolyl)-indigos with those of the parent molecule, indigo, their orbital contribution of all the indigo-skeleton atoms are very similar in terms of their sign and magnitude. This means the optical properties of di(p-tolyl)-indigos are dominated by the character of the indigo core when the excitation happens. A similar HOMO shows that the highest occupied electrons can move mostly within the indigo group with occasional changes in the tolyl groups, while they would be only limited in the indigo part with an extra node after the photo-excitation. Regardless, all those transitions have a phase change of half of the molecule. This means the transition dipole moment lies on the long side of the molecules. The results consist of the parent molecule, indigo. Therefore, the ditolyl-indigos have a wavelength that is close to indigo.

Since the simulation determining the molecular and electronic structures were made on single molecules in the gas phase, the results have no shifts induced by solvent or aggregation effects. The

prediction of the UV-Vis absorption maxima are also consistent with the value observed for gaseous indigo, which is all in the same range, but the di(p-tolyl)-indigos are red-shifted due to having a raised HOMO level compared to indigo itself. However, the LUMO energy levels for the di(p-tolyl)-indigo are very similar. In terms of the HOMO, the aromatic contribution can be observed with a ranking that is consistent with UV-Vis as the following:

Table 10 – Calculated HOMO aromatic contribution and UV-Vis spectra for di(p-tolyl)-indigo with a comparison with literature dibromoindigo in tetrachloroethane at 20 °C. [30]

Substituted position:	**5**	**7**	**4**	**6**
Calculated contribution of the aromatic orbital	5 > 7 > 4 > 6			
Calculated UV-Vis spectra of ditolyl-indigo's maxima /nm	502	498	497	491
Observed UV-Vis absorption of ditolyl-indigo in DCM /nm	602	618	620	604
Observed UV-Vis absorption of ditolyl-indigo in DMSO /nm	605	613	637	622
Literature UV-Vis absorption of dibromo-indigo in C_2Cl_4 /nm	620	605	610	590

This calculated result is very similar to the observed UV-Vis trend of dibromo-indigos. The transition wavelengths reflect the electronic activity and contribution of each site with the trend of 5 > 7 > 4 > 6.

However, the calculated UV-Vis results' trend does not agree with the observed UV-Vis result of di(p-tolyl)-indigo in solution: the trend is more random. A possible explanation can be the effect of the solvent upon J-aggregation. This comes from the geometry of the molecules. The 4 or 7 positions are very close to the N and O site of the indigo skeleton and when groups are placed in these positions they lay close to where the neighbouring H-bonded molecules should be. Theoretically, 4th or 7th substitution would introduce a steric that blocks some of the hydrogen bond formations and reduce the interaction of neighbouring molecule's interactions. This geometrical challenge becomes more significant as the tolyl groups are much larger than a hydrogen bond where a bromo group's size is smaller. Overall, when substituents are tolyl groups, the influence can be observed from the subtle change of the ranking, but not significant because the change of wavelength was dominated by the J-aggregation.

4.2 N,N'-diBoc-indigo

Table 11 – Gaussian calculation result of the frontier orbitals of *N,N*'-diBoc-indigo

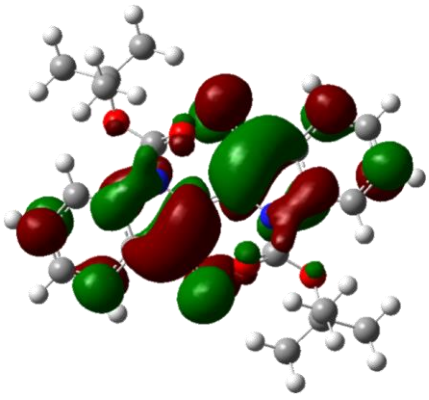

LUMO (E = -2.047 eV)

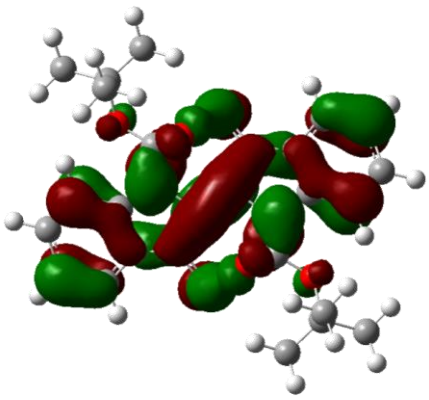

HOMO (E = -7.318 eV)

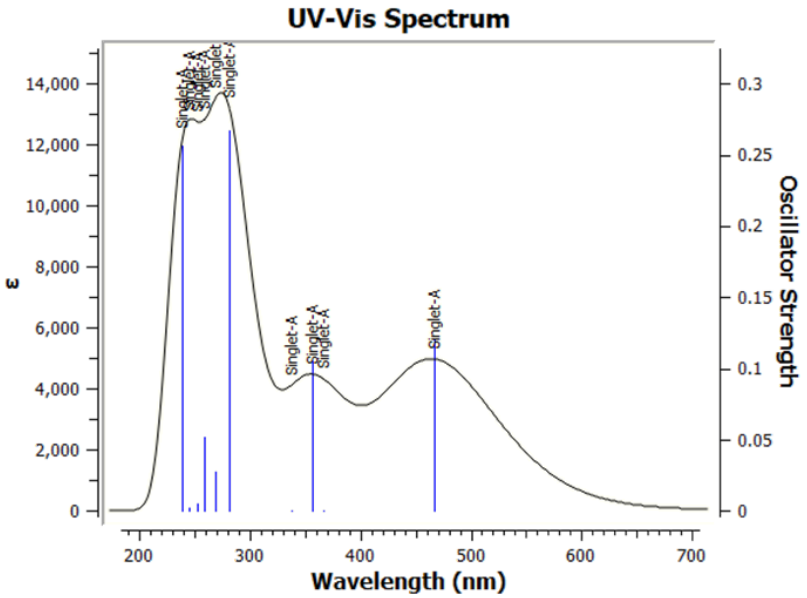

Figure 41 - Calculated UV-Vis: 360.57, 468.12 nm, singlet

The calculations show that the lowest energy conformation of this molecule was not flat. The distortion caused by the two Boc groups twists the molecule and resulted in a blue shift, similar to that observed for *N,N*'-diacetyl-indigo.

The frontier orbitals' calculation showed that the orbital contribution of each atom was again similar to indigo, but the similarity was not as good as the di(p-tolyl)-indigos. Both HOMO and LUMO have their skeleton extended to the carbonyl group from the branched Boc. The continuity of the HOMO was also affected due to the twist of the skeleton and redistribution of the electron density. Breaks can be noticed from the bond between the skeleton carbonyl carbon and the indole aromatic ring. Additionally, the charge transfer is still noticeable with a change of orbital size of nitrogen and oxygen even although the molecule is not flat.

The calculated UV-Vis spectrum of *N,N*'-diBoc-indigo agrees with the measured absorption in solution. Although the calculation of diBoc-indigo can also be considered as gaseous state estimation, the agreement showed that the impact on absorption by solvation or aggregation of *N,N*'-diBoc-indigo was not as significant as the flat indigo derivatives. This twisted shape limited the chance of in-phase transition dipoles and J-aggregation.

5. Summary

During this research, the optical properties of indigo were reviewed and a range of aryl and arylethynyl substituted indigos were made, in addition to *N,N*'-di-Boc-dibromo-indigo and dibromoindirubin.

In the first chapter, indigo's history, molecular structure, solid-state packing model, orbital energies, and absorption were reviewed with an association of other molecules that either had indigo as the skeleton structure or were otherwise similar to indigo.

Recent studies have shown that indigo has a flat structure with a fully conjugated π structure. The molecule has an 'H-chromophore' describing the two crossed donor-acceptor groups that effectively allows intermolecular and intramolecular hydrogen bonding. This structure of indigo in the solid-state, known as J-aggregation, leads to exciton coupling, which has a selection rule that prefers a red-shifted transition in the absorption spectrum compared to the isolated monomeric unit.

Therefore, it is a combination of the increased level of hydrogen bonds, flatness, H-chromophore, and aggregation that would make indigo have a more red-shifted absorption.

For most of those molecules sharing a similar skeleton, since the structural change is most likely to let their skeletons deviate from those factors, they tend to have a shorter absorption wavelength than solid indigo and are close to the gaseous indigo.

The electronic structures of indigo's derivatives were further explored using electron and energy calculations. The HOMO and LUMO are largely localised on the H-chromophore, extending to the N and O-atoms as well as onto the benzene ring. Calculations also reveal a noticeable difference in orbital contribution between the 5 and 6 positions. During excitation, which is primarily described by a LUMO <- HOMO transition the molecule orbitals indicate that the is some degree of charge separation during excitation. The additional node in the LUMO of the molecule showed the direction of the transition dipole moment, is along the length of the molecule, indicating the polarisation of the transition.

The UV-vis absorption spectrum of indigo is strongly affected by its physical state, solvent, substituents, complexation, isomerisation, and N-substitution. The physical state and solvent effect are dominated by aggregation and interaction with neighbouring molecules. The substituents' effect is related to its position and electron-donating/withdrawing capability, which would affect the electron distribution of the entire molecule. The complexation can cause a considerable blue shift of the molecule. The isomerisation is a change of the H-chromophore.

Our experiments were designed to extend the indigo's conjugated ring system by using aromatic or arylethynyl substituents. Among the aromatic substituents, the group were selected with extra functionality that affected the geometric or electronic structure which potentially had influence over the spectroscopic and structural properties of the new compounds. Overall, the indigo derivatives did not have a significant change of indigo skeleton's shift, which was shown by their absorption spectra in DMSO. Interestingly, some of the new substituted compounds exhibited significantly greater lability than the parent, undergoing oxidative degradation to the isatins.

6. Experimental procedure

6.1 Introduction

Chemicals were purchased from Fluorochem, Acros Organics, Sigma Aldrich, Alfa Aesar and used without further purification. Solvents were purchased from Fischer Scientific. 5-Bromoindole was a gift from Prof Ian Baxendale.

Any reaction without specification of the temperature or pressure can be assumed as room temperature and atmospheric pressure. For reaction conditions that require an inert environment, they were performed under an atmosphere of dry nitrogen with a standard Schlenk line setup.

All of the reaction progress and column chromatography was monitored by thin-layer chromatography (TLC) with fluorescent silica plate (Polygram® Sil G/UV_{254} 0.2 mm silica) and visualised under UV light at 254 nm . Column chromatography was carried out on silica gel 60 (230-400 mesh) from Merck.

Routine NMR spectra were collected using either a Varian Unity 300, Mercury 400, Bruker Avance 400 MHz Bruker, Varian Inova 500 or Varian 700 MHz instrument, and spectra were analysed using MestReNova. Chemical shifts are referenced to the residual in the deuterated solvent (^{1}H) or the ^{13}C shift of the solvent (^{13}C). Solvent ^{1}H shifts (ppm): $CDCl_3$ ^{1}H 7.27 (s). Solvent ^{13}C shifts (ppm): $CDCl_3$, 77.2 (t). All the reported NMR chemical shifts were in ppm and all the J coupling were in Hz.

Mass spectroscopy (MS) was performed either by atmospheric solids analysis probe (ASAP) or gas chromatography-mass spectroscopy (EI GC-MS). ASAP mass spectrometry was performed on either a Xevo QToF mass spectrometer (Waters Ltd, UK) equipped with an Agilent 7890 GC (Agilent Technologies UK Ltd, UK) with a default temperature of 450 °C, or by an LCT Premier XE mass spectrometer combined with an Acquity UPLC (Waters Ltd, UK) with a temperature of 350 °C. Accurate Mass analysis for the peak of $[M+H]^+$ was performed on the LCT Premier XE system as described. Electron ionization of Non-polar Gas chromatography-mass spectroscopy (Ultra) (EI GC-MS) was also used several times during this research as purity assessment of the compound by EI GC-MS QP2010-Ultra. EI was carried at 70 eV fitted with a Rxi-17Sil MS (0.15µm x 10m x 0.15 mm) column. Helium was the carrier gas of EI GC with a speed of 0.41 mL / min. Both ASAP and GC-MS results were analysed by MestReNova.

UV-Vis absorption spectroscopies were performed with a tungsten-halogen lamp and spectrograph-CCD camera (Ocean Optics MAYPro) and the spectra were analysed by SpectraSuite. The pre-set parameter was kept the same for all the measurements. The spectra were recorded with an integration time of 25 ms and the spectra were averaged per 25 data points.

Molecular modelling was carried out using Gaussian-16 Ver B-01, and visualised using GaussView 5.{Gaussian 16, Revision C.01, M. J. Frisch, G. W. Trucks, H. B. Schlegel, G. E. Scuseria, M. A. Robb, J. R. Cheeseman, G. Scalmani, V. Barone, G. A. Petersson, H. Nakatsuji, X. Li, M. Caricato, A. V. Marenich, J. Bloino, B. G. Janesko, R. Gomperts, B. Mennucci, H. P. Hratchian, J. V. Ortiz, A. F. Izmaylov, J. L. Sonnenberg, D. Williams-Young, F. Ding, F. Lipparini, F. Egidi, J. Goings, B. Peng, A. Petrone, T. Henderson, D. Ranasinghe, V. G. Zakrzewski, J. Gao, N. Rega, G. Zheng, W. Liang, M. Hada, M. Ehara, K. Toyota, R. Fukuda, J. Hasegawa, M. Ishida, T. Nakajima, Y. Honda, O. Kitao, H. Nakai, T. Vreven, K. Throssell, J. A. Montgomery, Jr., J. E. Peralta, F. Ogliaro, M. J. Bearpark, J. J. Heyd, E. N. Brothers, K. N. Kudin, V. N. Staroverov, T. A. Keith, R. Kobayashi, J. Normand, K.

Raghavachari, A. P. Rendell, J. C. Burant, S. S. Iyengar, J. Tomasi, M. Cossi, J. M. Millam, M. Klene, C. Adamo, R. Cammi, J. W. Ochterski, R. L. Martin, K. Morokuma, O. Farkas, J. B. Foresman, and D. J. Fox, Gaussian, Inc., Wallingford CT, 2016.} After creation of the molecular structures the structures were first optimised using the CAM-B3LYP functional and a 6-31g* basis set. The vibrational spectra for this optimised structure were also calculated, and the discovery of the global energy minimum assured on the basis of there being no vibrations with negative frequencies. The optimised structres were then used to calculate the excited states of the molecules at this geometry uisng the same functional and basis sets wuth TD-DFT, calculating the electronic structure for the first 10 excited states to ensure the correct identification of the lowest excited state. The electronic structure of the ground state and the identificaiotn of the excited state, in terms of the ground-state orbitals, was then visualised using GaussView.

6.2 Generic methods being used:

6.2.1 Indigo synthesis

The general procedure of indigo synthesis is adapted from work by Y. Tanoue et al. (Scheme 8*).* [53]

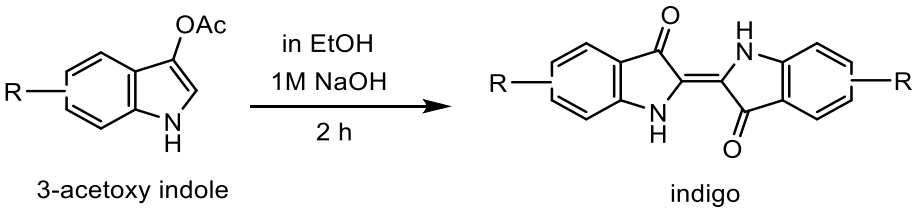

Scheme 8 - Indigo synthesis[53]

Acetoxy-indole (10 mg) was dissolved in ethanol (1 mL). 1M NaOH (aq, 2 mL) was poured into the indole at room temperature for 2 h to give a strong blue precipitate. After centrifuging the solution, most of the solvent was removed and discarded. The precipitate was resuspended in ethanol (10 mL) and water (2 × 10 mL) and the precipitate was collected by centrifugation (112 g, 10 min) each time. The solid was collected and dried *in vacuo* at 50 °C.

Due to the poor solubility of the indigo products, the only practical way to identify them was by using high resolution mass spectroscopy. Since the theoretical conversion rate was high and there was a significant difference of the solubility between the product and the others, it was assumed that most of the impurities were washed off during the washings.

6.2.2 Synthesis of 3-acetoxy-indole

The generic method of 3-acetoxy-indole was adapted from work by Y. Tanoue et al. (Scheme 9*).*[53]

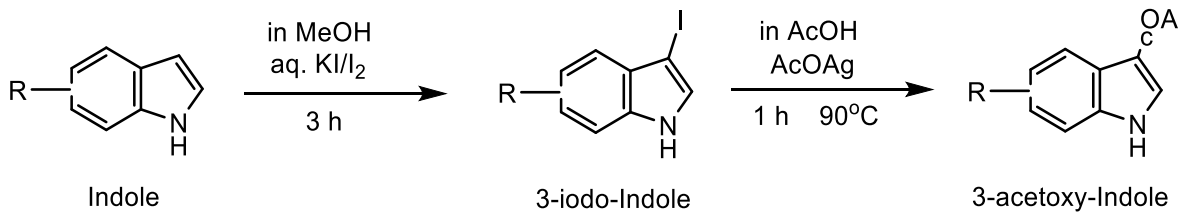

Scheme 9 - Synthesis of 3-acetate-indole[53]

A solution of iodine (1 eq.) in 0.5 M potassium iodide (1 eq.) was added dropwise to a stirred solution of the indole (1 eq.) dissolved in 0.1 M methanolic sodium hydroxide (1 eq.). Upon completion of the addition, the lightly coloured solution was stirred for a further 3 hours at room temperature. After this period, water was added to double the volume of the solution, precipitating the 3-iodoindole. The precipitate was isolated by filtration and dried *in vacuo* and used without further characterisation.

The crude iodo-indole was dissolved in acetic acid (8 mL per mmol) and stirred and silver acetate (2 eq.) was added in one portion. The mixture was heated to 90 °C for 1 h. The mixture was cooled and the solvent was removed *in vacuo*. The residue was purified by column chromatography on silica gel eluting with dichloromethane/hexane 2:1 to yield the pure 3-acetoxyindole. The products have an R_f value of 0.25-0.5 in DCM.

3-iodo-indole is a labile molecule. The purification and spectroscopic analysis of 3-iodo indole were skipped to maximize the yield and purity of the acetoxy-indole and indigo. The experimental section of this thesis combined the first two steps into one, which was shown as indole to 3-acetoxy-indole.

6.2.3 Aromatic-indole synthesis by Suzuki Coupling

The generic method of 3-acetoxy-bromoindole was adapted from work by C. Shao et al. (Scheme 10).[54]

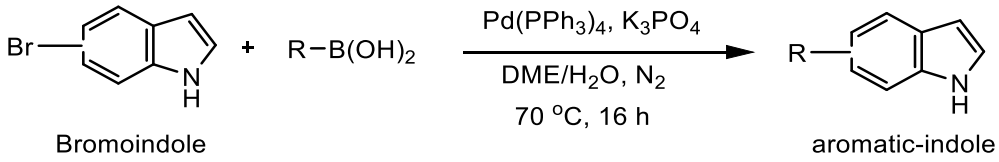

Scheme 10– Synthesis of aromatic indole by Suzuki Coupling from bromoindole

The bromoindole (1.00 g, 5.1 mmol, 1 eq.), boronic acid (2 eq.), K_3PO_4 (2 eq.) were dissolved in a mixed solvent of DME (18 mL) and water (4.5 mL) in a Schlenk tube. The mixture was degassed by a freeze-pump-thaw cycle and back-filled with N_2 four times. Under a positive pressure of supply of N_2, $Pd(PPh_3)_4$ (4 mol%) was added to the system. The solution was kept closed under a blanket of N_2 and stirred at 70 °C for 5 – 20 h. The reaction was monitored by TLC for the presence of starting materials. Upon completion of the reaction, the mixture was left to cool down to room temperature and the solvent was removed *in vacuo*. The residue was dissolved in ethyl acetate (30 mL) and washed with a saturated aqueous solution of $NaHCO_3$ and NaCl (3 $\times$ 10 mL). The combined aqueous washing was re-extracted by ethyl acetate (3 $\times$ 10 mL). All of the ethyl acetate fractions were combined and dried over anhydrous K_2CO_3, filtered, and the solvent was removed *in vacuo*. The crude product was filtered through a short silica plug with DCM and further purified by column chromatography on silica gel with DCM/hexane (1:3 to 2:1) to give the desired product. The products have an R_f value of 0.4-0.6 in DCM or 0.2-0.4 in DCM/hexane (1:1).

6.2.4 Acetylenyl-indole synthesis by Sonogashira Coupling

The generic method of 3-acetoxy-indole was adapted from work by H. Hénon et al.(Scheme 11). [55]

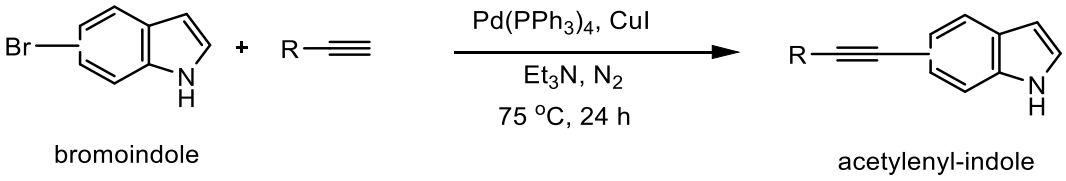

bromoindole acetylenyl-indole

Scheme 11 - Synthesis of ethynyl-indole by Sonogashira Coupling from bromoindole

The bromoindole (1.00 g, 1 eq.) was dissolved in Et_3N (12 mL) in a Schlenk tube. The mixture was degassed by a freeze-pump-thaw cycle and back-filled with N_2 three times. The acetylene (1.6 eq.) was added by syringe and followed by another evacuation and back-fill of N_2 2 times. CuI (10 mol% eq.) and $Pd(PPh_3)_4$ (7 mol% eq.) were added under a positive pressure of N_2. The mixture was kept closed under a blanket of N_2 and stirred at 70 °C for 5 – 20 h. The reaction was monitored by TLC for the presence of starting materials. Upon completion of the reaction, the solution was left to cool to room temperature and the solvent was removed *in vacuo*. The crude product was filtered through a short silica plug with DCM and further purified by column chromatography on silica gel with DCM/hexane (1:3 to 2:1) to give the desired product. The products have an R_f value of 0.4-0.6 in DCM or 0.2-0.4 in DCM/hexane (1:1).

6.2.5 Boc-indigo synthesis

The generic method of Boc-indigo was adapted from work by H. Wolfgang et al.(Scheme 12). [56]

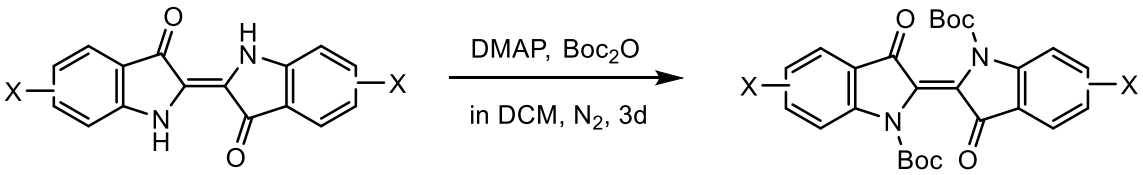

indigo N,N'-diBoc-indigo

Scheme 12 – *N,N*-diBoc-indigo synthesis (X = H or Br)

Indigo (X = H or Br, 1 eq.), DMAP (2 eq.) was mixed in DCM (50 mL per mmol of indigo) at 0 °C. The mixture was degassed by a freeze-pump-thaw cycle and back-filled with N_2 two times. Boc_2O (3 eq.) was added to the solution and the mixture was stirred at room temperature under N_2 for 2-3 days. The mixture was evaporated to dryness and purified by column chromatography on silica with DCM/hexane (1:1) to give the final product.

6.2.6 "Symmetrical indirubin" synthesis

The above generic method of Boc-indigo was adapted from work by H. Wolfgang et al.(Scheme 13).[57]

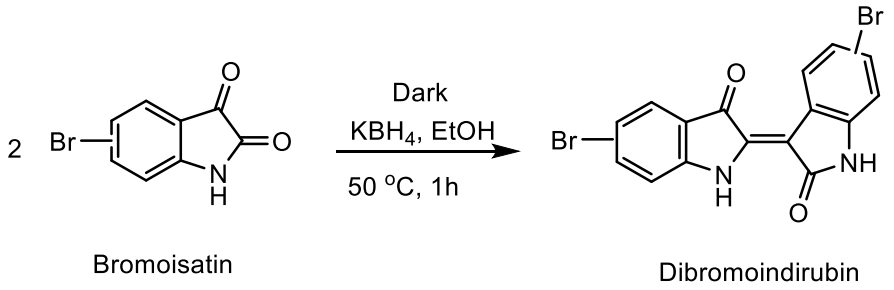

Scheme 13 – "Symmetrical indirubin" synthesis

Isatin (X = Br, 1 eq.) was dissolved in EtOH (5 mL per mmol of reactant) in a dark environment. The solution was cooled to 0 °C and KBH_4 (0.5 eq.) was added. The yellow solution was heated to 50 °C for 1h and formed a violet precipitate. The mixture was left to cool to room temperature and stirred for 24h. 2-fold of water was added to the system. After centrifuging the solution, most of the solvent was removed. Water (10 mL per mmol of product) was added to wash the residue and removed by centrifuge three times. The solid was collected and dried *in vacuo* at 50 °C to give the final violet solid as the product.

6.2.7 "Asymmetrical indirubin" synthesis

The above generic method of asymmetrical indirubin *was adapted from work by T. Maugard et al. (Scheme 14).* [58]

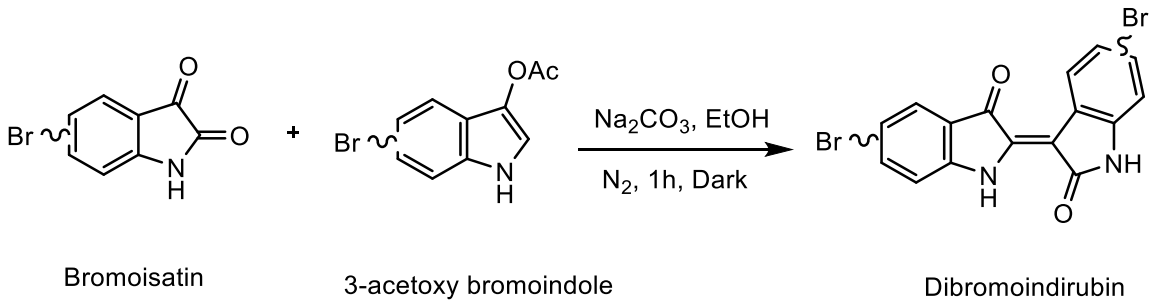

Scheme 14 – "asymmetrical indirubin" synthesis

The Isatin (1 eq.) and 3-acetoxy-haloindole (1 eq.) were dissolved in EtOH (5 mL per mmol of reactant) in a dark environment and cooled to 0 °C. The mixture was degassed by a freeze-pump-thaw cycle and back-filled with N_2 3 times. Under a positive pressure of supply of N_2, Na_2CO_3 (2.5 eq.) was added to the system. The solution was kept closed under a blanket of N_2 and stirred at room temperature for 24 h and the yellow solution typically form a violet precipitate. After centrifuging the solution, most of the solvent was removed. Water (10 mL per mmol of product) was added to wash the residue and removed by centrifuge three times. The precipitate was collected and dried *in vacuo* at 50 °C to give the final violet solid as the product.

6.3 Synthesis of 3-acetoxy-haloindole

6.3.1 3-acetoxy-4-bromoindole synthesis

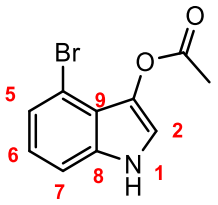

31

Formula:
$C_{10}H_8O_2NBr$

M_r = 254.08 g mol^{-1}

The generic method (Section 6.2.2) was used, employing 4-bromo-indole (0.300 g, 1.53 mmol) as the starting material. The product was purified as described to give final product (**31**), 3-acetoxy-4-bromo-indole (0.22 g, 0.87 mmol, 57 %)

^{1}H NMR (400 MHz, $CDCl_3$) δ 8.09 (brs, 1H, H-N), 7.26 (d, *J* = 7.9 Hz, 2H, H-5&7), 7.16 (d, *J* = 2.7 Hz, 1H, H-2), 7.03 (t, *J* = 7.9 Hz, 1H, H-6), 2.41 (s, 3H, CH_3).

^{13}C NMR (101 MHz, $CDCl_3$) δ 170.29 (C=O), 134.72 (C-8), 129.63 (C-3), 124.26 (C-9), 123.65 (C-6), 119.09 (C-5), 115.63 (C-4), 111.59 (C-7), 110.88 (C-2), 21.18 (CH_3).

Acc. ASAP-MS, *m/z*: 253.9813 $[M+H]^+$; Calc. for $[C_{10}H_9O_2NBr]^+$ = 253.9817.

The result is consistent with the literature.[59]

6.3.1 3-acetoxy-5-bromoindole synthesis

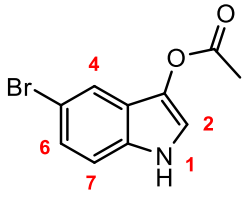

32

Formula:
$C_{10}H_8O_2NBr$

M_r = 254.08 g mol^{-1}

The generic method (Section 6.2.2) was used, employing 5-bromo-indole (0.500 g, 2.55 mmol) as the starting material. The product was purified as described to give final product (**32**), 3-acetoxy-5-bromo-indole (0.33 g, 1.30 mmol, 51 %)

^{1}H NMR (400 MHz, $CDCl_3$) δ 8.07(brs, 1H, H-N), 7.70 (d, *J* = 2.0 Hz, 1H, H-4), 7.30-7.27 (m, 2H, H-2 and H-6), 7.16 (d, *J* = 8.6 Hz, 1H, H-7), 2.39 (s, 3H, OAc).

Acc. ASAP-MS, *m/z*: 253.9817 $[M+H]^+$; Calc. for $[C_{10}H_9O_2NBr]^+$ = 253.9817.

The result is consistent with the literature. [59,60]

6.3.1 3-acetoxy-6-bromoindole synthesis

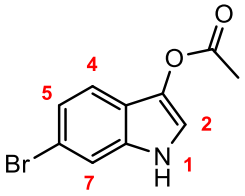

33

Formula:
$C_{10}H_8O_2NBr$

M_r = 254.08 g mol^{-1}

The generic method (Section 6.2.2) was used, employing 6-bromo-indole (0.500 g, 2.55 mmol) as the starting material. The product was purified as described to give final product (**33**), 3-acetoxy-6-bromo-indole (0.36 g, 1.42 mmol, 55 %)

^{1}H NMR (400 MHz, $CDCl_3$) δ 7.92, (s, 1H, N-H), 7.49 (d, *J* = 1.6 Hz, 1H, H-7), 7.44 (d, *J* = 8.5 Hz, 1H, H-4), 7.33 (d, *J* = 2.6 Hz, 1H, H-2), 7.26 (dd, *J* = 8.5, 1.6 Hz, 1H, H-5), 2.39 (s, 3H, OAc).

Acc. ASAP-MS, *m/z*: 253.9813 $[M+H]^+$; Calc. for $[C_{10}H_9O_2NBr]^+$ = 253.9817.

The result is consistent with the literature.[53]

6.3.1 13-acetoxy-7-bromoindole synthesis

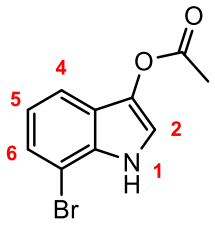

34

Formula:
$C_{10}H_8O_2NBr$

M_r = 254.08 g mol^{-1}

The generic method (Section 6.2.2) was used, employing 7-bromo-indole (0.300 g, 1.53 mmol) as the starting material. The product was purified as described to give final product (**34**), 3-acetoxy-7-bromo-indole (0.26 g, 1.02 mmol, 66 %)

^{1}H NMR (400 MHz, $CDCl_3$) δ 8.18 (s, 1H, NH), 7.54 (d, *J* = 7.7, 1H, H-6), 7.44 – 7.37 (m, 2H, H-2&4), 7.04 (dd, *J* = 7.8, 7.7 Hz, 1H, H-5), 2.40 (s, 3H, OAc).

^{13}C NMR (101 MHz, $CDCl_3$) δ 168.68 (C=O), 131.57 (C-8), 131.02 (C-3), 125.13 (C-9), 121.29 (C-4), 121.01 (C-5), 116.91 (C-6), 114.33 (C-7), 105.25 (C-2), 20.98 (CH_3).

Acc. ASAP-MS, *m/z*: 253.9816 $[M+H]^+$; Calc. for $[C_{10}H_9O_2NBr]^+$ = 253.9817.

6.3.2 3-acetoxy-6-chloroindole synthesis

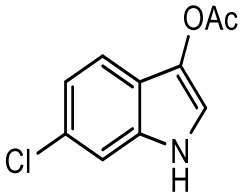

35

Formula:
$C_{10}H_8O_2NCl$

M_r = 209.63 g mol^{-1}

The generic method (Section 6.2.2) was used, employing 5-chloro-indole (0.500 g, 3.30 mmol) as the starting material. The product was purified as described to give final product (**35**), 3-acetoxy-6-chloro-indole (0.35 g, 1.67 mmol, 51 %)

^{1}H NMR (400 MHz, $CDCl_3$) δ 7.94 (s, 1H, N-H), 7.48 (d, *J* = 8.5, 1H, H-4), 7.34 – 7.25 (m, 2H, H-2&7), 7.13 (dd, *J* = 8.5, 1.8 Hz, 1H, H-5), 2.39 (s, 3H, Me).

Acc. ASAP-MS, *m/z*: 210.0315 $[M+H]^+$; Calc. for $[C_{10}H_9O_2NCl]^+$ = 210.0322.

6.4 Synthesis of (p-tolyl)-indoles

6.4.1 4-(p-tolyl)-indole synthesis

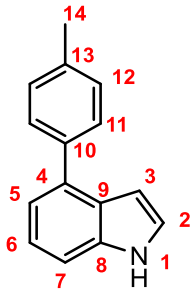

36

Formula:

$C_{15}H_{13}N$

M_r = 207.27 g mol^{-1}

The generic method (Section 6.2.3) was used, employing 4-bromo-indole (1.000 g, 5.101 mmol) as the starting material to react with p-tolyl boronic acid. The product was purified as described to give the final product (**36**), 4-(p-tolyl)-indole (0. 843 g, 4.07 mmol, 80 %)

^{1}H NMR (400 MHz, $CDCl_3$) δ 8.23 (s, 1H, N-H), 7.70 (d, *J* = 8.1 Hz, 2H, H-11), 7.43 – 7.32 (m, 4H, H-5,7&12), 7.30 – 7.24 (m, 2H, H-2&6), 6.81 (tt, *J* = 2.3, 1.0 Hz, 1H, H-3), 2.51 (s, 3H, H-14).

^{13}C NMR (101 MHz, $CDCl_3$) δ 138.45 (C- Ar-Tolyl), 136.68 (C-Ar-Tolyl), 136.30 (C-Ar-Tolyl), 134.50 (C-8), 129.29 (C-Ar-Tolyl), 128.70 (C-9), 126.17 (C-4), 124.44 (C-2), 122.36 (C-5), 119.64 (C-6), 110.08 (C-7), 102.23 (C-3), 21.28 (C-14).

Acc. ASAP-MS, *m/z*: 208.1114 $[M+H]^+$; Calc. for $[C_{15}H_{14}N]^+$ = 208.1126.

The result is consistent with the literature.[61]

6.4.2 5-(p-tolyl)-indole synthesis

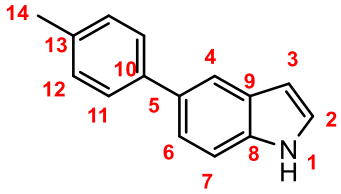

37

Formula:

$C_{15}H_{13}N$

M_r = 207.27 g mol^{-1}

The generic method (Section 6.2.3) was used, employing 5-bromo-indole (1.000 g, 5.101 mmol) as the starting material to react with p-tolyl boronic acid. The product was purified as described to give final product (**37**), 5-(p-tolyl)-indole (0.515 g, 2.48 mmol, 49 %)

^{1}H NMR (400 MHz, $CDCl_3$) δ 8.30 (brs, 1H, N-H), 7.90 (s, 1H, H-4), 7.62 (d, *J* = 8.0 Hz, 2H, H-11), 7.48 (s, 2H, H-12), 7.31 (d, *J* = 7.7 Hz, 2H, H-2&6), 7.25 (t, *J* = 2.8 Hz, 1H, H-7), 6.64 (ddd, *J* = 3.0, 2.0, 0.8 Hz 1H, H-3), 2.46 (s, 3H, H-14).

Acc. ASAP-MS, *m/z*: 208.1114 $[M+H]^+$; Calc. for $[C_{15}H_{14}N]^+$ = 208.1126.

The result is consistent with the literature.[62]

6.4.3 6-(p-tolyl)-indole synthesis

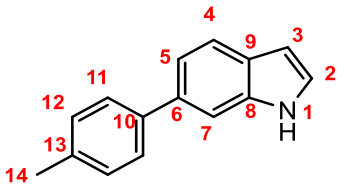

38

Formula:

$C_{15}H_{13}N$

M_r = 207.27 g mol^{-1}

The generic method (Section 6.2.3) was used, employing 6-bromo-indole (1.000 g, 5.101 mmol) as the starting material to react with p-tolyl boronic acid. The product was purified as described to give final product (**38**), 6-(p-tolyl)-indole (0.482 g, 2.323 mmol, 46 %)

^{1}H NMR (400 MHz, $CDCl_3$) δ 8.28 (s, 1H, N-H), 7.74 (dt, *J* = 8.3, 0.8 Hz, 1H, H-7), 7.60 (d, *J* = 7.9 Hz, 2H, H-11), 7.55 (d, *J* = 8.2 Hz, 1H, H-4), 7.43 (dd, *J* = 8.2, 1.6 Hz, 1H, H-5), 7.31 (d, *J* = 7.8 Hz, 2H, H-12), 7.23 (dd, *J* = 3.2, 2.4 Hz, 1H, H-2), 6.61 (ddd, *J* = 3.1, 2.0, 1.0 Hz, 1H, H-3), 2.46 (s, 3H, H-14).

^{13}C NMR (101 MHz, $CDCl_3$) δ 139.47 (C-8), 136.32 (C-9), 135.48 (C-Ar-Tolyl), 129.47 (C-Ar-Tolyl), 128.77 (C-Ar-Tolyl), 127.26 (C-Ar-Tolyl), 127.03 (C-2), 124.79 (C-5), 120.86 (C-4), 119.68 (C-6), 109.37 (C-7), 102.44 (C-3), 21.15 (C-14).

Acc. ASAP-MS, *m/z*: 208.1114 $[M+H]^+$; Calc. for $[C_{15}H_{14}N]^+$ = 208.1126.

The result is consistent with the literature.[63]

6.4.4 7-(p-tolyl)-indole synthesis

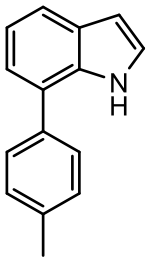

39

Formula:

$C_{15}H_{13}N$

M_r = 207.27 g mol^{-1}

The generic method (Section 6.2.3) was used, employing 7-bromo-indole (1.000 g, 5.101 mmol) as the starting material to react with p-tolyl boronic acid. The product was purified as described to give the final product (**39**), 7-(p-tolyl)-indole (0.648 g, 3.126 mmol, 61 %)

Acc. ASAP-MS, *m/z*: 208.1125 $[M+H]^+$; Calc. for $[C_{15}H_{14}N]^+$ = 208.1126.

6.5 Synthesis of 3-acetoxy-p-tolylindoles

6.5.1 3-acetoxy-4-(p-tolyl)-indole synthesis

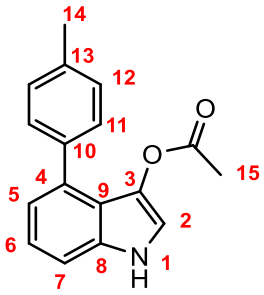

40

Formula:

$C_{17}H_{15}NO_2$

M_r = 265.31 g mol^{-1}

The generic method (Section 6.2.2) was used, employing 4-(p-tolyl)-indole (**36**, 0. 843 g, 4.067 mmol) as the starting material. The product was purified as described to give final product (**40**), 3-acetoxy-4-(p-tolyl)-indole (0.553 g, 2.08 mmol, 51 %)

^{1}H NMR (400 MHz, $CDCl_3$) δ 8.02 (s, 1H, N-H), 7.41 (d, *J* = 8.0 Hz, 2H, H-11), 7.34 (dd, *J* = 8.3, 1.0 Hz, 1H, H-7), 7.26 (d, *J* = 7.1 Hz, 3H, H-2&12), 7.19 (d, *J* = 2.7 Hz, 1H, H-5), 7.07 (dd, *J* = 7.2, 1.0 Hz, 1H, H-6), 2.44 (s, 3H, H-15), 1.81 (s, 3H, H-14).

^{13}C NMR (101 MHz, $CDCl_3$) δ 169.49 (C=O), 137.39 (C-Ar-Tolyl), 136.35 (C-Ar-Tolyl), 134.22 (C-Ar-Tolyl), 134.08 (C-8), 130.41 (C-Ar-Tolyl), 129.44 (C-3), 128.30 (C-9), 122.80 (C-6), 121.66 (C-5), 117.69 (C-4), 114.47(C-7), 110.50 (C-2), 21.22 (C-15), 20.34 (C-14).

Acc. ASAP-MS, *m/z*: 266.1181 $[M+H]^+$; Calc. for $[C_{17}H_{16}NO_2]^+$ = 266.1181.

6.5.2 3-acetoxy-5-(p-tolyl)-indole synthesis

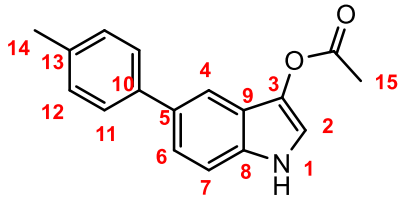

41

Formula:
$C_{17}H_{15}NO_2$

M_r = 265.31 g mol^{-1}

The generic method (Section 6.2.2) was used, employing 5-(p-tolyl)-indole (**37**, 0.515 g, 2.48 mmol) as the starting material. The product was purified as described to give final product (**41**), 3-acetoxy-5-(p-tolyl)-indole (0.151 g, 0.569 mmol, 23 %)

^{1}H NMR (400 MHz, $CDCl_3$) δ 7.87 (s, 1H, N-H), 7.75 (s, 1H, H-4), 7.57 (d, *J* = 7.9 Hz, 2H, H-11), 7.52 – 7.36 (m, 4H, H-2,6&12), 7.26 (s, 1H, H-7), 2.43 (s, 3H, H-15), 2.41 (s, 3H, H-14).

^{13}C NMR (101 MHz, $CDCl_3$) δ 168.65 (C=O), 139.30 (C-Ar-Tolyl), 136.18 (C-Ar-Tolyl), 133.59 (C-Ar-Tolyl), 132.47(C-8), 130.95 (C-Ar-Tolyl), 129.38 (C-3), 127.25 (C-6), 122.72 (C-9), 120.52 (C-4), 115.67 (C-2), 113.89 (C-5), 111.56 (C-7), 21.08 (C-15), 21.05 (C-14).

Acc. ASAP-MS, *m/z*: 266.1180 $[M+H]^+$; Calc. for $[C_{17}H_{16}NO_2]^+$ = 266.1181.

6.5.3 3-acetoxy-6-(p-tolyl)-indole synthesis

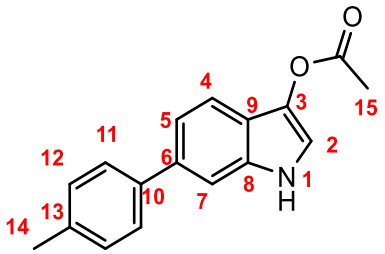

42

Formula:
$C_{17}H_{15}NO_2$

M_r = 265.31 g mol^{-1}

The generic method (Section 6.2.2) was used, employing 6-(p-tolyl)-indole (**38**, 0.482 g, 2.323 mmol) as the starting material. The product was purified as described to give the final product (**42**), 3-acetoxy-6-(p-tolyl)-indole (0.123 g, 0.464 mmol, 20 %)

^{1}H NMR (400 MHz, $CDCl_3$) δ 7.93 (s, 1H, N-H), 7.62 (d, *J* = 8.3 Hz, 1H, H-4), 7.55 (d, *J* = 7.7 Hz, 2H, H-11), 7.49 (s, 1H, H-2), 7.42 (d, *J* = 8.2, 1H, H-7), 7.33 (d, *J* = 2.6 Hz, 1H, H-5), 7.28 (d, *J* = 7.1, 2H, H-12), 2.44 (s, 3H, H-15), 2.41 (s, 3H, H-14).

^{13}C NMR (101 MHz, $CDCl_3$) δ 168.91 (C=O), 139.09 (C-Ar-Tolyl), 136.56 (C-Ar-Tolyl), 136.34 (C-Ar-Tolyl), 133.73 (C-8), 130.49 (C-Ar-Tolyl), 129.49 (C-3), 127.24 (C-5), 119.86 (C-9), 119.11 (C-4), 117.70 (C-6), 113.90 (C-7), 109.70 (C-2), 21.13 (C-15), 21.07 (C-14).

Acc. ASAP-MS, *m/z*: 266.1178 $[M+H]^+$; Calc. for $[C_{17}H_{16}NO_2]^+$ = 266.1181.

6.5.4 3-acetoxy-7-(p-tolyl)-indole synthesis

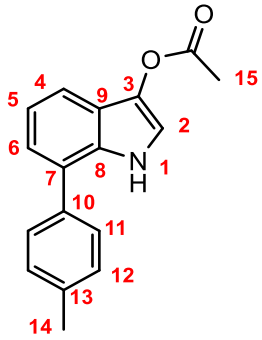

43

Formula:
$C_{17}H_{15}NO_2$

M_r = 265.31 g mol^{-1}

The generic method (Section 6.2.2) was used, employing 7-(p-tolyl)-indole (**39**, 0.648 g, 3.126 mmol) as the starting material. The product was purified as described to give the final product (**43**), 7-acetoxy-7-(p-tolyl)-indole (0.135 g, 0.694 mmol, 22 %)

^{1}H NMR (400 MHz, $CDCl_3$) δ 8.10 (s, 1H, N-H), 7.54 (d, *J* = 8.1 Hz, 2H, H-11), 7.39 (d, *J* = 2.7 Hz, 1H, H-6), 7.35 (d, *J* = 7.7 Hz, 2H, H-12), 7.29-7.20 (m, 3H, H-2,4&5), 2.46 (s, 3H, H-15), 2.41 (s, 3H, H-14).

^{13}C NMR (101 MHz, $CDCl_3$) δ 168.73 (C=O), 137.43 (C-Ar-Tolyl), 135.46 (C-Ar-Tolyl), 130.98 (C-Ar-Tolyl), 130.94 (C-8), 129.92 (C-Ar-Tolyl), 128.13 (C-9), 125.78 (C-3), 122.60 (C-4), 120.44(C-5), 120.34 (C-6), 116.52 (C-7), 113.47 (C-2), 21.24 (C-15), 21.02 (C-14).

Acc. ASAP-MS, *m/z*: 266.1175 $[M+H]^+$; Calc. for $[C_{17}H_{16}NO_2]^+$ = 266.1181.

6.6 Synthesis of (p-tolyl)-indigos

6.6.1 4,4'-di(p-tolyl)-indigo synthesis

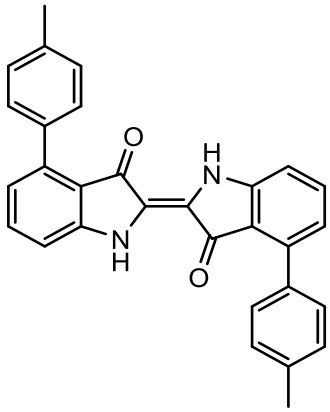

44

Formula:
$C_{30}H_{22}N_2O_2$

M_r = 442.51 g mol^{-1}

The generic method (Section 6.2.1) was used, employing 3-acetoxy-4-(p-tolyl)-indole (**40**, 0.553 g, 2.08 mmol) as the starting material. The product was purified as described to give the final product as a dark blue solid(**44**), 4,4'-di(p-tolyl)-indigo (0.234 g, 0.529 mmol, 51 %)

Acc. ASAP-MS, *m/z*: 443.1761 $[M+H]^+$; Calc. for $[C_{30}H_{23}N_2O_2]^+$ = 443.1760.

6.6.2 5,5'-di(p-tolyl)-indigo synthesis

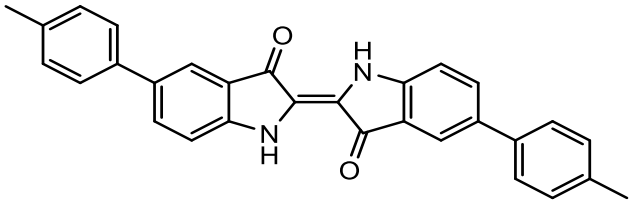

Formula:
$C_{30}H_{22}N_2O_2$

M_r = 442.51 g mol^{-1}

45

The generic method (Section 6.2.1) was used, employing 3-acetoxy-5-(p-tolyl)-indole (**41**, 0.151 g, 0.569 mmol) as the starting material. The product was purified as described to give the final product (**45**), 5,5'-di(p-tolyl)-indigo (0.067 g, 0.151 mmol, 66 %)

Acc. ASAP-MS, *m/z*: 443.1757 $[M+H]^+$; Calc. for $[C_{30}H_{23}N_2O_2]^+$ = 443.1760.

6.6.3 6,6'-di(p-tolyl)-indigo synthesis

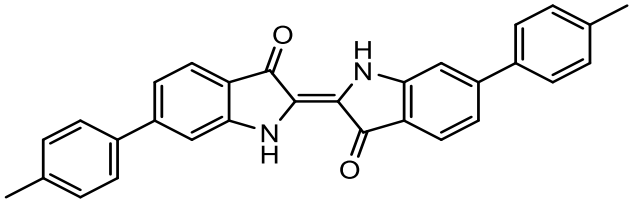

Formula:
$C_{30}H_{22}N_2O_2$

M_r = 442.51 g mol^{-1}

46

The generic method (Section 6.2.1) was used, employing 3-acetoxy-6-(p-tolyl)-indole (**42**, 0.151 g, 0.569 mmol) as the starting material. The product was purified as described to give the final product (**46**), 6,6'-di(p-tolyl)-indigo (0.067 g, 0.151 mmol, 66 %)

Acc. ASAP-MS, *m/z*: 443.1752 $[M+H]^+$; Calc. for $[C_{30}H_{23}N_2O_2]^+$ = 443.1760.

6.6.4 7,7'-di(p-tolyl)-indigo synthesis

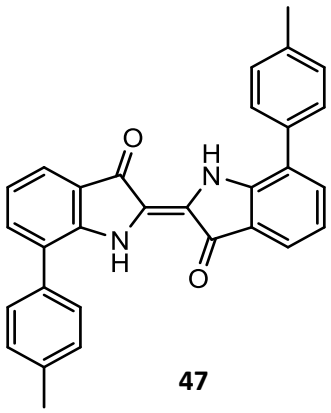

Formula:
$C_{30}H_{22}N_2O_2$

M_r = 442.51 g mol^{-1}

47

The generic method (Section 6.2.1) was used, employing 3-acetoxy-7-(p-tolyl)-indole (**43**, 0.123 g, 0.464 mmol) as the starting material. The product was purified as described to give the final product (**47**), 7,7'-di(p-tolyl)-indigo (0.088 g, 0.199 mmol, 86 %)

Acc. ASAP-MS, *m/z*: 443.1757 $[M+H]^+$; Calc. for $[C_{30}H_{23}N_2O_2]^+$ = 443.1760.

6.7 Synthesis of (p-trifluoromethylphenyl)-indoles

6.7.1 5-(p-trifluoromethylphenyl)-indole synthesis

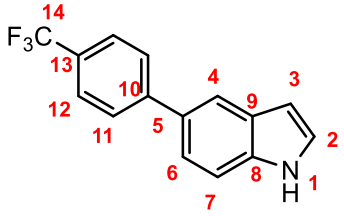

Formula:

$C_{15}H_{10}NF_3$

M_r = 261.24 g mol^{-1}

48

The generic method (Section 6.2.3) was used, employing 5-bromo-indole (1.000 g, 5.101 mmol) as the starting material to react with p-trifluoromethyl-phenyl boronic acid. The product was purified as described to give the final product (**48**), 5-(p-trifluoromethylphenyl)-indole (0.815 g, 3.12 mmol, 61 %)

^{1}H NMR (400 MHz, $CDCl_3$) δ 8.26 (s, 1H, NH), 7.94 – 7.88 (m, 1H, H-4), 7.78 (d, *J* = 8.1 Hz, 2H, H-11), 7.71 (d, *J* = 8.3 Hz, 2H, H-12), 7.52 (d, *J* = 8.4 Hz, 1H, H-2), 7.48 (dd, *J* = 8.5, 1.7 Hz, 1H, H-6), 7.31 (dd, *J* = 8.5, 2.2 Hz, 1H, H-7), 6.66 (ddd, *J* = 3.0, 2.0, 0.9 Hz, 1H, H-3).

^{13}C NMR (101 MHz, $CDCl_3$) δ 146.05 (C-14), 135.70 (C-Ar-Tolyl), 131.90 (C-Ar-Tolyl), 128.46 (C-Ar-Tolyl), 127.50 (C-8), 125.60 (q, *J* = 3.7 Hz, 1C, C-13), 125.57 (C-9), 125.19 (C-2), 124.88 (C-4), 121.77 (C-6), 119.62 (C-5), 111.50 (C-7), 103.21 (C-3).

Acc. ASAP-MS, *m/z*: 262.0851 $[M+H]^+$; Calc. for $[C_{15}H_{11}NF_3]^+$ = 262.0844.

The result is consistent with the literature.[64]

6.7.2 6-(p-trifluoromethylphenyl)-indole synthesis

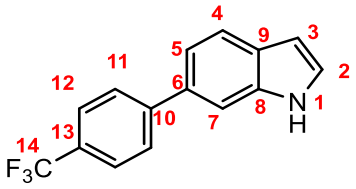

Formula:

$C_{15}H_{10}NF_3$

M_r = 261.24 g mol^{-1}

49

The generic method (Section 6.2.3) was used, employing 6-bromo-indole (1.000 g, 5.101 mmol) as the starting material to react with p-trifluoromethyl-phenyl boronic acid. The product was purified as described to give the final product (**49**), 6-(p-trifluoromethylphenyl)-indole (0.887 g, 3.40 mmol, 67 %)

^{1}H NMR (400 MHz, $CDCl_3$) δ 8.29 (s, 1H, N-H), 7.77 (dt, *J* = 8.1, 6.4 Hz, 3H, H-7&11), 7.73 (d, *J* = 1.1 Hz, 2H, H-12), 7.65 (dt, *J* = 1.7, 0.8 Hz, 1H, H-4), 7.42 (dd, *J* = 8.2, 1.6 Hz, 1H, H-5), 7.31 (dd, *J* = 3.2, 2.4 Hz, 1H, H-2), 6.63 (ddd, *J* = 3.1, 2.0, 1.0 Hz, 1H, H-3).

^{13}C NMR (101 MHz, $CDCl_3$) δ 145.83 (C-14), 136.28 (C-8), 133.98 (C-9), 129.01, (C-Ar-Tolyl) 127.89 (C-Ar-Tolyl), 127.54 (C-Ar-Tolyl), 125.64 (q, *J* = 3.8 Hz, 1C, C-13), 125.59 (C-2), 125.40 (C-5), 121.23 (C-4), 119.68 (C-6), 109.82 (C-7), 102.72 (C-3).

Acc. ASAP-MS, *m/z*: 262.0835 $[M+H]^+$; Calc. for $[C_{15}H_{11}NF_3]^+$ = 262.0844.

6.8 Synthesis of 3-acetoxy-(p-trifluoromethylphenyl)-indole

6.8.1 3-acetoxy-5-(p-trifluoromethylphenyl)-indole synthesis

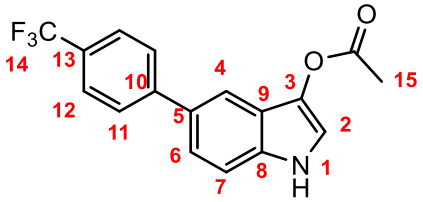

50

Formula:

$C_{17}H_{12}NO_2F_3$

M_r = 319.28 g mol^{-1}

The generic method (Section 6.2.2) was used, employing 5-(p-trifluoromethylphenyl)-indole (**48**, 0.815 g, 3.12 mmol) as the starting material. The product was purified as described to give the final product (**50**), 3-acetoxy-5-(p-trifluoromethylphenyl)-indole (0.451 g, 1.41 mmol, 39 %)

^{1}H NMR (400 MHz, $CDCl_3$) δ 8.03 (s, 1H, N-H), 7.80 – 7.75 (m, 3H, H-4&11), 7.73 – 7.67 (m, 2H, H-12), 7.54 – 7.40 (m, 3H, H-2, 6&7), 2.42 (s, 3H, H-15).

^{13}C NMR (101 MHz, $CDCl_3$) δ 168.74 (C=O), 145.69 (C-14), 132.95 (C-8), 132.04 (C-Ar-Tolyl), 130.92 (C-Ar-Tolyl), 128.69 (C-3), 127.56 (C-6), 125.78 (C-Ar-Tolyl), 125.60 (q, *J* = 3.7 Hz, 1C, C-13), 122.57 (C-9), 120.57 (C-4), 116.35 (C-2), 114.52 (C-5) 111.95 (C-7), 21.05 (C-15).

Acc. ASAP-MS, *m/z*: 320.0905 $[M+H]^+$; Calc. for $[C_{17}H_{13}NO_2F_3]^+$ = 320.0898.

6.8.2 3-acetoxy-6-(p-trifluoromethylphenyl)-indole synthesis

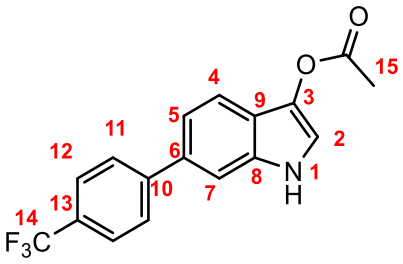

51

Formula:

$C_{17}H_{12}NO_2F_3$

M_r = 319.28 g mol^{-1}

The generic method (Section 6.2.2) was used, employing 6-(p-trifluoromethylphenyl)-indole (**49**, 0.887 g, 3.40 mmol) as the starting material. The product was purified as described to give the final product (**51**), 3-acetoxy-6-(p-trifluoromethylphenyl)-indole (0.561 g, 1.76 mmol, 52 %)

^{1}H NMR (400 MHz, $CDCl_3$) δ 8.03 (s, 1H, N-H), 7.73 (d, *J* = 8.3 Hz, 4H, H-11&12), 7.66 (dt, *J* = 8.4, 0.7 Hz, 1H, H-4), 7.57 (dd, *J* = 1.5, 0.7 Hz, 1H, H-2), 7.44 (d, *J* = 2.7 Hz, 1H, H-7), 7.42 (dd, *J* = 8.3, 1.5 Hz, 1H, H-5), 2.42 (s, 3H, H-15).

^{13}C NMR (101 MHz, $CDCl_3$) δ 168.76 (C=O), 145.50 (C-14), 134.84 (C-Ar-Tolyl), 133.55 (C-8), 130.58 (C-3), 127.58 (C-Ar-Tolyl), 127.58 (C-Ar-Tolyl), 125.68 (d, *J* = 3.8 Hz, 1C, C-13), 119.93 (C-5), 119.81 (C-9), 118.14 (C-4), 115.64 (C-6), 114.54,(C-7) 110.19 (C-2), 20.69 (C-15).

Acc. ASAP-MS, *m/z*: 320.0907 $[M+H]^+$; Calc. for $[C_{17}H_{13}NO_2F_3]^+$ = 320.0898.

6.9 Synthesis of di(p-trifluoromethylphenyl)-indigos

6.9.1 5,5-di(p-trifluoromethylphenyl)-indigo synthesis

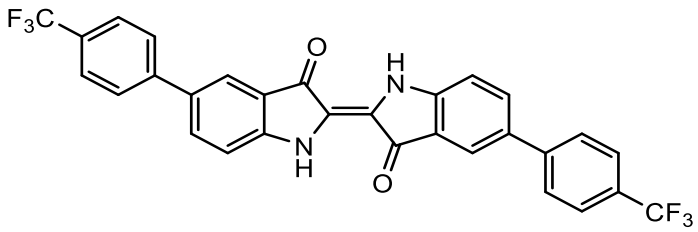

Formula:

$C_{30}H_{16}N_2O_2F_6$

M_r = 550.45 g mol^{-1}

52

The generic method (Section 6.2.1) was used, employing 3-acetoxy-5-(p-trifluoromethylphenyl)-indole (**50**,0.451 g, 1.41 mmol) as the starting material. The product was purified as described to give the final product as a dark blue solid(**52**), 5,5-di(p-trifluoromethylphenyl)-indigo (0.218 g, 0.396 mmol, 71 %)

Acc. ASAP-MS, *m/z*: 551.1188 $[M+H]^+$; Calc. for $[C_{30}H_{17}N_2O_2F_6]^+$ = 551.1194.

6.9.2 6,6'-di(p-trifluoromethylphenyl)-indigo synthesis

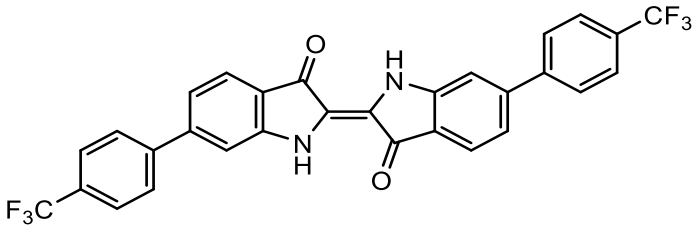

Formula:

$C_{30}H_{16}N_2O_2F_6$

M_r = 550.45 g mol^{-1}

53

The generic method (Section 6.2.1) was used, employing 3-acetoxy-6-(p-trifluoromethylphenyl)-indole (**51**, 0.561 g, 1.76 mmol) as the starting material. The product was purified as described to give the final product as a greenish-blue solid(**53**), 5,5-di(p-trifluoromethylphenyl)-indigo (0.197 g, 0.358 mmol, 41 %)

Acc. ASAP-MS, *m/z*: 551.1192 $[M+H]^+$; Calc. for $[C_{30}H_{17}N_2O_2F_6]^+$ = 551.1194.

6.10 Synthesis of (2,4,6-trimethylphenyl)-indoles

6.10.1 5-(2,4,6-trimethylphenyl)-indole synthesis

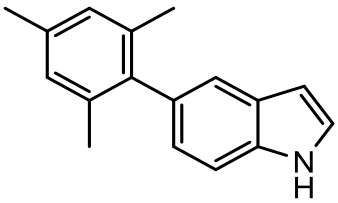

Formula:

$C_{17}H_{17}N$

M_r = 235.32 g mol^{-1}

54

The generic method (Section 6.2.3) was used, employing 5-bromo-indole (1.000 g, 5.101 mmol) to react with 2,4,6-trimethylphenyl boronic acid. The product was purified as described to give the final product (**54**), 5-(2,4,6-trimethylphenyl)-indole (0.804 g, 3.42 mmol, 67 %)

^{1}H NMR (400 MHz, $CDCl_3$) δ 8.22 (s, 1H, N-H), 7.47 (dt, *J* = 8.3, 0.9 Hz, 1H, H-2), 7.42 (t, *J* = 0.7 Hz, 1H, H-3), 7.29 (s, 1H, H-4), 6.99 (s, 2H, H-12), 6.99 (dd, *J* = 8.2, 1.6 Hz, 1H, H-6), 6.60 (ddd, *J* = 3.1, 2.1, 1.0 Hz, 1H, H-7), 2.38 (s, 3H, H-14), 2.05 (s, 6H, H-16).

Acc. ASAP-MS, *m/z*: 236.1432 $[M+H]^+$; Calc. for $[C_{17}H_{18}N]^+$ = 236.1439.

6.10.2 6-(2,4,6-trimethylphenyl)-indole synthesis

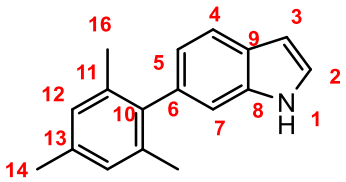

55

Formula:

$C_{17}H_{17}N$

M_r = 235.32 g mol^{-1}

The detailed procedure of the generic method can be found in Section 6.2.3. 6-bromo-indole (1.000 g, 5.101 mmol) as the starting material to react with 2,4,6-trimethylphenyl boronic acid. The product was purified as described to give the final product (**55**), 6-(2,4,6-trimethylphenyl)-indole (0.847 g, 3.60 mmol, 71 %)

^{1}H NMR (400 MHz, $CDCl_3$) δ 8.80 (s, 1H, N-H), 7.67 (d, *J* = 8.1 Hz, 1H, H-4), 7.22 (dd, *J* = 3.3, 1.8 Hz, 1H, H-3), 7.16 (s, 1H, H-7), 6.96 (s, 2H, H-12), 6.88 (dd, *J* = 8.1, 1.4 Hz, 1H, H-5), 6.58 (d, *J* = 3.0 Hz, 1H, H-2), 2.35 (s, 3H, H-14), 2.03 (s, 6H, H-16).

^{13}C NMR (101 MHz, $CDCl_3$) δ 139.99 (C-8), 136.50 (C-9), 136.19 (C-Ar), 136.18 (C-Ar), 134.77 (C-Ar), 127.90 (C-Ar), 126.35 (C-2), 124.26 (C-5), 121.47 (C-4), 120.41 (C-6), 111.54 (C-7), 102.13 (C-3), 58.17 (C-16), 18.26 (C-14).

Acc. ASAP-MS, *m/z*: 236.1434 $[M+H]^+$; Calc. for $[C_{17}H_{18}N]^+$ = 236.1439.

6.11 Synthesis of 3-acetoxy-(2,4,6-trimethylphenyl)-indoles

6.11.1 3-acetoxy-5-(2,4,6-trimethylphenyl)-indole synthesis

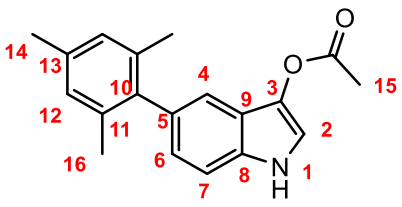

56

Formula:

$C_{19}H_{19}NO_2$

M_r = 293.36 g mol^{-1}

The generic method (Section 6.2.2) was used, employing 5-(2,4,6-trimethylphenyl)-indole (**54**, 0.804 g, 3.33 mmol) as the starting material. The product was purified as described to give the final product (**56**), 3-acetoxy-5-(2,4,6-trimethylphenyl)-indole (0.351 g, 1.20 mmol, 36 %).

^{1}H NMR (400 MHz, $CDCl_3$) δ 7.89 (s, 1H, N-H), 7.42 (d, *J* = 2.7 Hz, 1H, H-4), 7.40 (dd, *J* = 8.4, 0.8 Hz, 1H, H-6), 7.33 (t, *J* = 0.8 Hz, 1H, H-2), 7.02 (dd, *J* = 8.3, 1.6 Hz, 1H, H-7), 6.98 (s, 2H, H-12), 2.37 (s, 3H, H-15), 2.35 (s, 3H, H-14), 2.04 (s, 6H, H-16).

Acc. ASAP-MS, *m/z*: 294.1475 $[M+H]^+$; Calc. for $[C_{19}H_{20}NO_2]^+$ = 294.1494.

6.11.2 3-acetoxy-6-(2,4,6-trimethylphenyl)-indole synthesis

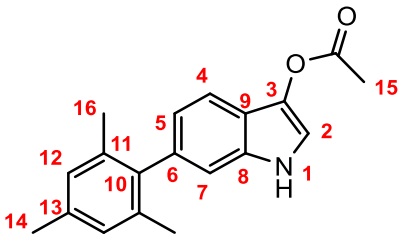

57

Formula:

$C_{19}H_{19}NO_2$

M_r = 293.36 g mol^{-1}

The generic method (Section 6.2.2) was used, employing 6-(2,4,6-trimethylphenyl)-indole (**55**, 0.847 g, 3.60 mmol) as the starting material. The product was purified as described to give the final product (**57**), 3-acetoxy-6-(2,4,6-trimethylphenyl)-indole (0.486 g, 1.66 mmol, 46 %).

^{1}H NMR (400 MHz, $CDCl_3$) δ 7.87 (s, 1H, N-H), 7.61 (dt, *J* = 8.1, 0.8 Hz, 1H), 7.38 (d, *J* = 2.6 Hz, 1H, H-2), 7.11 (t, *J* = 1.0 Hz, 1H, H-7), 6.98 (s, 2H, H-12), 6.94 (dd, *J* = 8.1, 1.3 Hz, 1H, H-4), 2.41 (s, 3H, H-15), 2.37 (s, 3H, H-14), 2.03 (s, 6H, H-14).

^{13}C NMR (101 MHz, $CDCl_3$) δ 168.82 (C=O), 139.53 (C-Ar), 136.43 (C-Ar), 136.41 (C-Ar), 135.92 (C-8), 133.48 (C-Ar), 130.69 (C-3), 127.99 (C-5), 121.85 (C-9), 118.69 (C-4), 117.41 (C-6), 113.26 (C-7), 111.79 (C-2), 21.05 (C-15), 21.02(C-16), 20.85 (C-14).

Acc. ASAP-MS, *m/z*: 294.1481 $[M+H]^+$; Calc. for $[C_{19}H_{20}NO_2]^+$ = 294.1494.、

6.12 Synthesis of di(2,4,6-trimethylphenyl)-indigos

6.12.1 5,5'-di(2,4,6-trimethylphenyl)-indigo synthesis

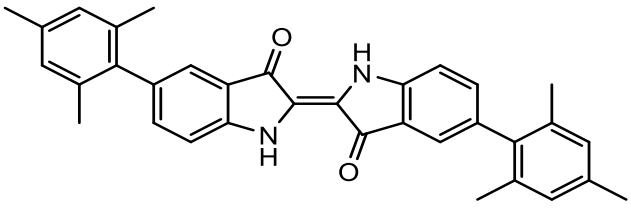

58

Formula:

$C_{34}H_{30}N_2O_2$

M_r = 498.61 g mol^{-1}

The generic method (Section 6.2.1) was used, employing 3-acetoxy-5-(2,4,6-trimethylphenyl)-indole (**56**, 0.351 g, 1.20 mmol) as the starting material. The product was purified as described to give the

final product as a dark blue solid(**58**), 5,5'-di(2,4,6-trimethylphenyl)-indigo (0.182 g, 0.365 mmol, 61 %)

Acc. ASAP-MS, *m/z*: 499.2392 $[M+H]^+$; Calc. for $[C_{34}H_{31}N_2O_2]^+$ = 499.2386.

6.12.1 6,6'-di(2,4,6-trimethylphenyl)-indigo synthesis

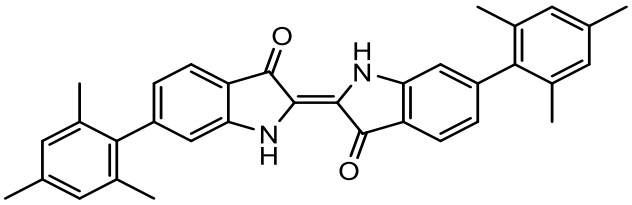

Formula:

$C_{34}H_{30}N_2O_2$

M_r = 498.61 g mol^{-1}

59

The generic method (Section 6.2.1) was used, employing 3-acetoxy-6-(2,4,6-trimethylphenyl)-indole (**57**, 0.486 g, 1.66 mmol) as the starting material. The product was purified as described to give the final product as a dark blue solid(**59**), 6,6'-di(2,4,6-trimethylphenyl)-indigo (0.233 g, 0.467 mmol, 56 %)

Acc. ASAP-MS, m/z: 499.2396 [M+H]+; Calc. for [C34H31N2O2]+ = 499.2386.

6.13 Synthesis of (p-nitrilephenyl)-indole

6.13.1 5-(p-nitrilephenyl)-indole synthesis

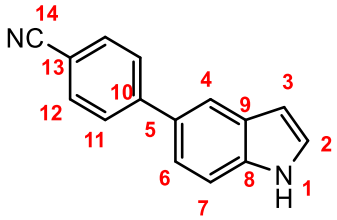

Formula:

$C_{15}H_{10}N_2$

M_r = 218.25 g mol^{-1}

60

The generic method (Section 6.2.3) was used, employing 5-bromo-indole (1.000 g, 5.101 mmol) as the starting material to react with p-tolyl boronic acid. The product was purified as described to give the final product (**60**), 5-(p-nitrilephenyl)-indole (0. 888 g, 4.07 mmol, 80 %)

^{1}H NMR (400 MHz, $CDCl_3$) δ 8.33 (s, 1H, N-H), 7.91 (t, J = 0.7 Hz, 1H, H-4), 7.79 – 7.72 (m, 4H, C-11&12), 7.53 (dt, *J* = 8.5, 0.8 Hz, 1H, H-2), 7.47 (dd, *J* = 8.5, 1.8 Hz, 1H, H-6), 7.32 (t, *J* = 2.8 Hz, 1H, H-7), 6.67 (ddd, *J* = 3.1, 2.0, 0.9 Hz, 1H, H-3).

^{13}C NMR (101 MHz, $CDCl_3$) δ 147.11 (C-14), 135.94 (C-Ar), 132.52 (C-Ar), 131.24 (C-Ar), 128.51 (C-Ar), 127.78 (C-8), 125.43 (C-9), 121.58 (C-2), 119.74 (C-4), 119.40 (C-6), 111.70 (C-5), 109.67 (C-7), 103.28 (C-3).

Acc. ASAP-MS, *m/z*: 219.0914 $[M+H]^+$; Calc. for $[C_{15}H_{11}N_2]^+$ = 219.0922.

The result is consistent with the literature.[65]

6.13.2 6-(p-nitrilephenyl)-indole synthesis

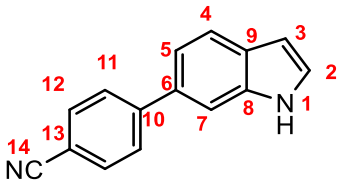

61

Formula:

$C_{15}H_{10}N_2$

M_r = 218.25 g mol^{-1}

The generic method (Section 6.2.3) was used, employing 6-bromo-indole (1.000 g, 5.101 mmol) as the starting material to react with p-tolyl boronic acid. The product was purified as described to give the final product (**61**), 6-(p-nitrilephenyl)-indole (0. 925 g, 4.24 mmol, 83 %)

^{1}H NMR (400 MHz, $CDCl_3$) δ 8.35 (s, 1H, N-H), 7.79 – 7.70 (m, 5H, H-4, 11&12), 7.65 (s, 1H, H-7), 7.40 (dd, *J* = 8.3, 1.7 Hz, 1H, H-5), 7.33 (t, *J* = 2.8 Hz, H-2), 6.63 (s, 1H, H-3).

^{13}C NMR (101 MHz, $CDCl_3$) δ 146.87, 136.27, 133.29, 132.55, 128.27, 127.82, 125.78, 121.39, 119.49, 119.28, 109.98, 109.87, 102.79.

Acc. ASAP-MS, *m/z*: 219.0917 $[M+H]^+$; Calc. for $[C_{15}H_{11}N_2]^+$ = 219.0922.

The result is consistent with the literature.[65]

6.14 Synthesis of (m-methoxyphenyl)-indole

6.14.1 5-(m-methoxyphenyl)-indole synthesis

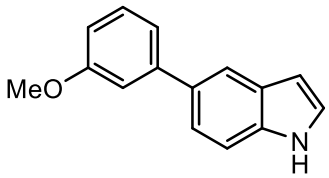

62

Formula:

$C_{15}H_{13}NO$

M_r = 223.27 g mol^{-1}

The generic method (Section 6.2.3) was used, employing 5-bromo-indole (1.000 g, 5.101 mmol) as the starting material to react with m-methoxyphenyl-boronic acid. The product was purified as described to give final product (**62**), 5-(m-methoxyphenyl)-indole (0.562 g, 2.52 mmol, 49 %)

^{1}H NMR (400 MHz, $CDCl_3$) δ 8.24 (s, 1H), 7.91 (t, *J* = 0.8 Hz, 1H), 7.53 – 7.38 (m, 3H), 7.33 – 7.29 (m, 1H), 7.27 – 7.24 (m, 2H), 7.24 – 7.21 (m, 0H), 6.93 (ddd, *J* = 8.2, 2.6, 1.0 Hz, 1H), 6.65 (ddd, *J* = 3.1, 2.0, 0.9 Hz, 1H), 3.93 (s, 3H).

^{13}C NMR (101 MHz, $CDCl_3$) δ 159.89, 144.17, 135.43, 133.24, 129.67, 128.36, 125.00, 121.92, 120.03, 119.30, 113.09, 111.88, 111.29, 103.00, 55.35.

Acc. ASAP-MS, *m/z*: 224.1065 $[M+H]^+$; Calc. for $[C_{15}H_{14}NO]^+$ = 224.1075.

6.14.2 6-(m-methoxyphenyl)-indole synthesis

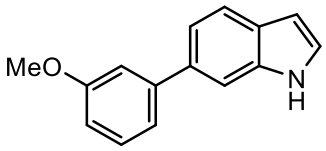

63

Formula:

$C_{15}H_{13}NO$

M_r = 223.27 g mol^{-1}

The generic method (Section 6.2.3) was used, employing 6-bromo-indole (1.000 g, 5.101 mmol) as the starting material to react with m-methoxyphenyl-boronic acid. The product was purified as described to give final product (**63**), 6-(m-methoxyphenyl)-indole (0.732 g, 3.28 mmol, 64 %)

Acc. ASAP-MS, *m/z*: 224.1066 $[M+H]^+$; Calc. for $[C_{15}H_{14}NO]^+$ = 224.1075.

6.15 Synthesis of 3-acetoxy-(m-methoxyphenyl)-indole

6.15.1 3-acetoxy-5-(m-methoxyphenyl)-indole synthesis

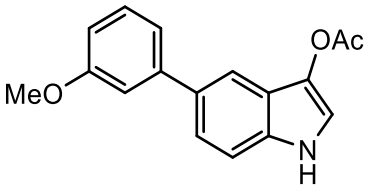

64

Formula:

$C_{17}H_{15}O_3N$

M_r = 281.30 g mol^{-1}

The generic method (Section 6.2.2) was used, employing 5-(m-methoxyphenyl)-indole (**62**, 0.562 g, 2.52 mmol) as the starting material. The product was purified as described to give the final product (**64**), 3-acetoxy-5-(m-methoxyphenyl)-indole (0.063 g, 0.224 mmol, 9 %).

Acc. ASAP-MS, *m/z*: 282.1132 $[M+H]^+$; Calc. for $[C_{17}H_{16}NO_3]^+$ = 282.1130.

6.15.2 3-acetoxy-6-(m-methoxyphenyl)-indole synthesis

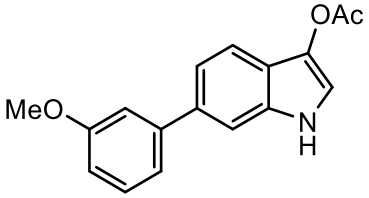

65

Formula:

$C_{17}H_{15}O_3N$

M_r = 281.30 g mol^{-1}

The generic method (Section 6.2.2) was used, employing 6-(m-methoxyphenyl)-indole (**63**, 0.732 g, 3.28 mmol) as the starting material. The product was purified as described to give the final product (**65**), 3-acetoxy-6-(m-methoxyphenyl)-indole (0.233 g, 0.828 mmol, 25 %).

Acc. ASAP-MS, *m/z*: 282.1130 $[M+H]^+$; Calc. for $[C_{17}H_{16}NO_3]^+$ = 282.1130.

6.16 Synthesis of (m-methoxyphenyl)-indigos

6.16.1 6,6'-di(m-methoxyphenyl)-indigo synthesis

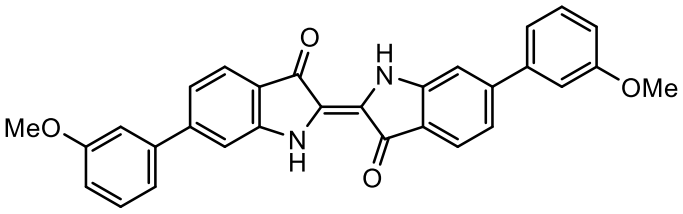

66

Formula:

$C_{30}H_{22}N_2O_4$

M_r = 474.52 g mol^{-1}

The generic method (Section 6.2.1) was used, employing 3-acetoxy-6-(m-methoxyphenyl)-indole(**65**, 0.233 g, 0.828 mmol) as the starting material. The product was purified as described to give the final product as a dark-green solid (**66**), 6,6'-di(m-methoxyphenyl)-indigo (0.168 g, 0.354 mmol, 86 %)

Acc. ASAP-MS, *m/z*: 575.2704 $[M+H]^+$; Calc. for $[C_{30}H_{23}N_2O_4]^+$ = 475.1658.

6.17 Synthesis of R-ethynyl-indoles

6.17.1 5-(3,3-dimethylbutyn-1yl)-indole synthesis

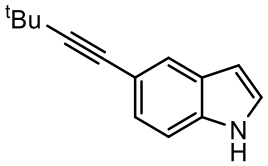

67

Formula:

$C_{14}H_{15}N$

M_r = 197.28 g mol^{-1}

The generic method (Section 6.2.4) was used, employing 5-bromo-indole (1.000 g, 5.101 mmol) as the starting material to react with 3,3-dimethylbut-1-yne. The product was purified as described to give the final product (**67**), 5-(3,3-dimethylbutyn-1yl)-indole (0. 825 g, 4.18 mmol, 82 %)

Acc. ASAP-MS, *m/z*: 198.1265 $[M+H]^+$; Calc. for $[C_{14}H_{16}N]^+$ = 198.1283.

6.17.2 5-(p-n-butyl-phenylethynyl)-indole synthesis

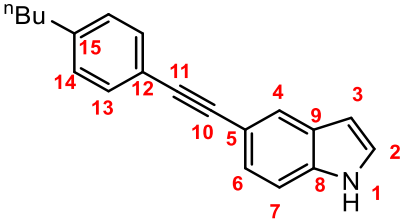

68

Formula:

$C_{20}H_{19}N$

M_r = 273.37 g mol^{-1}

The generic method (Section 6.2.4) was used, employing 5-bromo-indole (1.000 g, 5.101 mmol) as

the starting material to react with p-n-butyl-phenylacetylene. The product was purified as described to give the final product (**68**), 5-(p-n-butyl-phenylethynyl)-indole (0. 985 g, 3.60 mmol, 71 %)

^{1}H NMR (400 MHz, $CDCl_3$) δ 8.25 (s, 1H, NH), 7.88 (s, 1H, H-4), 7.49 (dt, J = 8.2, 1.7 Hz, 2H, H-14), 7.39 (s, 2H, H-6&7), 7.26 (dd, J = 3.2, 2.4 Hz, 1H, H-2), 7.19 (d, J = 8.2 Hz, 2H, H-13), 6.54 (dt, J = 3.1, 2.4 Hz, 1H, H-3), 2.65 (t, J = 7.6 Hz, 2H, Bu-H), 1.63 (quin, J = 7.6 Hz, 2H, Bu-H), 1.38 (six., J = 7.3 Hz, 2H, Bu-H), 0.96 (t, J = 7.3 Hz, 3H, Bu-H).

Acc. ASAP-MS, *m/z*: 274.1589 $[M+H]^+$; Calc. for $[C_{20}H_{20}N]^+$ = 274.1596.

6.17.1 4-(p-*tert*-butyl-phenylethynyl)-indole synthesis

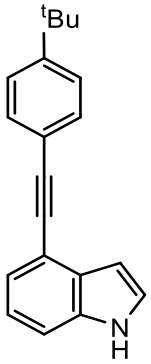

69

Formula:

$C_{20}H_{19}N$

M_r = 273.37 g mol^{-1}

The generic method (Section 6.2.4) was used, employing 4-bromo-indole (1.000 g, 5.101 mmol) as the starting material to react with p-*tert*-butyl-phenylacetylene. The product was purified as described to give the final product (**69**), 4-(p-*tert*-butyl-phenylethynyl)-indole (1.115 g, 4.079 mmol, 80 %)

Acc. ASAP-MS, *m/z*: 274.1601 $[M+H]^+$; Calc. for $[C_{20}H_{20}N]^+$ = 274.1596.

6.17.2 5-(p-*tert*-butyl-phenylethynyl)-indole synthesis

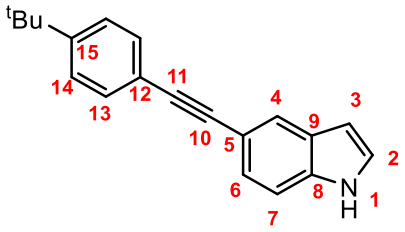

70

Formula:

$C_{20}H_{19}N$

M_r = 273.37 g mol^{-1}

The generic method (Section 6.2.4) was used, employing 5-bromo-indole (1.000 g, 5.101 mmol) as the starting material to react with p-*tert*-butyl-phenylacetylene. The product was purified as described to give the final product (**70**), 5-(p-*tert*-butyl-phenylethynyl)-indole (1.002 g, 3.67 mmol, 72 %)

^{1}H NMR (400 MHz, $CDCl_3$) δ 8.22 (s, 1H, NH), 7.89 (s, 1H, H-4), 7.52 (d, J = 8.6 Hz, 2H, H-14), 7.39 (s, 2H, H-6&7), 7.28 (d, *J* = 2.0, 1H, H-2), 7.25 (d, *J* = 8.6 Hz, 2H, H-13), 6.58 (ddd, *J* = 3.0, 2.0, 0.8 Hz, 1H, H-3), 1.36 (s, 9H, Bu-H).

Acc. ASAP-MS, *m/z*: 274.1589 $[M+H]^+$; Calc. for $[C_{20}H_{20}N]^+$ = 274.1596.

6.17.3 6-(p-*tert*-butyl-phenylethynyl)-indole synthesis

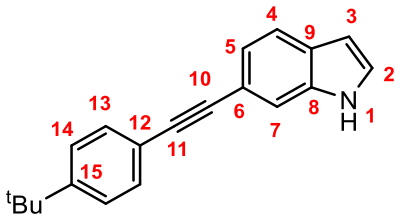

71

Formula:

$C_{20}H_{19}N$

M_r = 273.37 g mol^{-1}

The generic method (Section 6.2.4) was used, employing 6-bromo-indole (1.000 g, 5.101 mmol) as the starting material to react with p-*tert*-butyl-phenylacetylene. The product was purified as described to give the final product (**71**), 6-(p-*tert*-butyl-phenylethynyl)-indole (1.093 g, 4.00 mmol, 78 %)

^{1}H NMR (400 MHz, $CDCl_3$) δ 8.35 (s, 1H, N-H), 7.75 – 7.68 (m, 1H, H-7), 7.63 (dt, *J* = 8.1, 0.8 Hz, 1H, H-4), 7.52 (dt, *J* = 8.6, 2.1 Hz, 2H, H-14), 7.41 (dt, *J* = 8.6, 2.0 Hz, 2H, H-13), 7.33 (dd, *J* = 8.1, 1.4 Hz, 1H, H-5), 7.27 (dd, *J* = 3.2, 2.4 Hz, 1H, H-2), 6.56 (d, *J* = 3.2 Hz, 1H, H-3), 1.36 (s, 9H, Bu-H).

^{13}C NMR (101 MHz, $CDCl_3$) δ 151.11, 132.07, 131.24, 125.34, 123.60, 121.90, 120.79, 120.62, 116.55, 114.51, 112.02 (C-7), 102.93 (C-3), 90.34 (C-11), 88.03(C-10), 34.79 (Bu-C), 31.24 (Bu-C).

Acc. ASAP-MS, *m/z*: 274.1596 $[M+H]^+$; Calc. for $[C_{20}H_{20}N]^+$ = 274.1596.

6.17.4 7-(p-*tert*-butyl-phenylethynyl)-indole synthesis

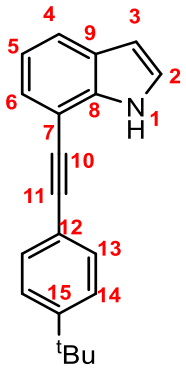

72

Formula:

$C_{20}H_{19}N$

M_r = 273.37 g mol^{-1}

The generic method (Section 6.2.4) was used, employing 7-bromo-indole (1.000 g, 5.101 mmol) as the starting material to react with p-*tert*-butyl-phenylacetylene. The product was purified as described to give the final product (**72**), 7-(p-*tert*-butyl-phenylethynyl)-indole (0.998 g, 3.65 mmol,

72 %)

Acc. ASAP-MS, *m/z*: 274.1595 $[M+H]^+$; Calc. for $[C_{20}H_{20}N]^+$ = 274.1596.

6.18 Synthesis of 3-acetoxy-R-ethynyl)-indoles

6.18.1 3-acetoxy-5-(3,3-dimethylbutyn-1yl)-indole synthesis

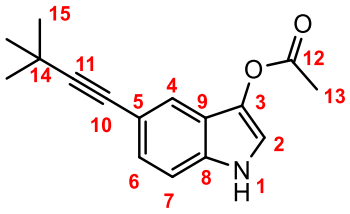

73

Formula:

$C_{16}H_{17}NO_2$

M_r = 255.32 g mol^{-1}

The generic method (Section 6.2.2) was used, employing 5-(3,3-dimethylbutyn-1yl)-indole (**67**, 0. 825 g, 4.18 mmol) as the starting material. The product was purified as described to give the final product (**73**), 3-acetoxy-5-(3,3-dimethylbutyn-1yl)-indole (0.332 g, 1.30 mmol, 31 %).

Acc. ASAP-MS, *m/z*: 256.1321 $[M+H]^+$; Calc. for $[C_{14}H_{16}N]^+$ = 256.1337.

6.18.2 3-acetoxy-5-(p-n-butyl-phenylethynyl)-indole synthesis

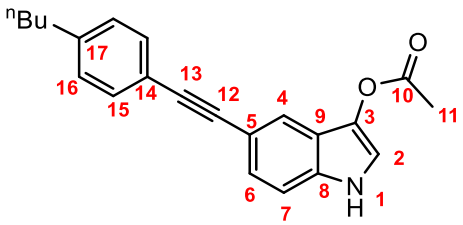

74

Formula:

$C_{22}H_{21}NO_2$

M_r = 331.41 g mol^{-1}

The generic method (Section 6.2.2) was used, employing 5-(p-n-butyl-phenylethynyl)-indole (**68**, 0. 985 g, 3.60 mmol) as the starting material. The product was purified as described to give the final product (**74**), 3-acetoxy-5-(p-n-butyl-phenylethynyl)-indole (0.462 g, 1.39 mmol, 39 %).

^{1}H NMR (400 MHz, $CDCl_3$) δ 7.94 (s, 1H, N-H), 7.80 (s, 1H), 7.48 (d, *J* = 7.6 Hz, 2H), 7.41 (d, *J* = 11.3 Hz, 2H), 7.33 (d, *J* = 8.4 Hz, 1H), 7.18 (d, *J* = 8.1 Hz, 2H), 2.64 (t, *J* = 7.7 Hz, 2H, Bu-H), 2.40 (s, 3H, Bu-H), 1.69 – 1.56 (m, 2H, Bu-H), 1.45 – 1.31 (m, 2H, Bu-H), 0.95 (t, *J* = 7.3 Hz, 3H).

^{13}C NMR (101 MHz, $CDCl_3$) δ 168.60, 142.94, 132.50, 131.39, 130.57, 128.45, 126.46, 121.37, 120.90, 120.03, 114.94, 114.15, 111.47, 89.88, 87.58, 35.61, 33.45, 22.35, 21.00, 13.98.

Acc. ASAP-MS, *m/z*: 332.1654 $[M+H]^+$; Calc. for $[C_{22}H_{22}NO_2]^+$ = 332.1651.

6.18.3 3-acetoxy-4-(p-*tert*-butyl-phenylethynyl)-indole synthesis

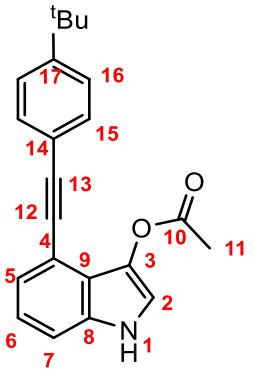

75

Formula:

$C_{22}H_{21}NO_2$

M_r = 331.41 g mol^{-1}

The generic method (Section 6.2.2) was used, employing 4-(p-*tert*-butyl-phenylethynyl)-indole (**69**, 0.128 g, 0.468 mmol) as the starting material. The product was purified as described to give the final product (**75**), 3-acetoxy-4-(p-*tert*-butyl-phenylethynyl)-indole (0.288, 0.091 mmol, 19 %).

Acc. ASAP-MS, *m/z*: 332.1644 $[M+H]^+$; Calc. for $[C_{22}H_{22}NO_2]^+$ = 332.1651.

6.18.4 3-acetoxy-5-(p-*tert*-butyl-phenylethynyl)-indole synthesis

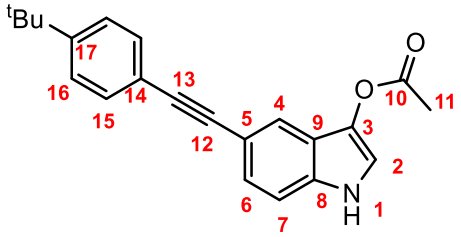

76

Formula:

$C_{22}H_{21}NO_2$

M_r = 331.41 g mol^{-1}

The generic method (Section 6.2.2) was used, employing 5-(p-*tert*-butyl-phenylethynyl)-indole (**70**, 1.002 g, 3.67 mmol) as the starting material. The product was purified as described to give the final product (**76**), 3-acetoxy-5-(p-*tert*-butyl-phenylethynyl)-indole (0.315 g, 0.950 mmol, 26 %).

^{1}H NMR (400 MHz, $CDCl_3$) δ 7.94 (s, 1H, N-H), 7.80 (s, 1H), 7.50 (d, *J* = 8.5 Hz, 2H), 7.43 – 7.37 (m, 4H), 7.31 (d, *J* = 8.5 Hz, 1H), 2.40 (s, 3H), 1.36 (s, 9H, Bu-H).

^{13}C NMR (101 MHz, $CDCl_3$) δ 168.63, 151.06, 132.50, 131.21, 130.56, 126.48, 125.33, 121.38, 120.76, 120.02, 114.93, 114.17, 111.48, 89.89, 87.52, 34.78, 31.23, 21.02.

Acc. ASAP-MS, *m/z*: 332.1647 $[M+H]^+$; Calc. for $[C_{22}H_{22}NO_2]^+$ = 332.1651.

6.18.5 3-acetoxy-6-(p-*tert*-butyl-phenylethynyl)-indole synthesis

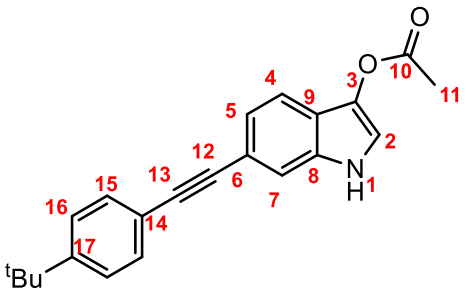

Formula:

$C_{22}H_{21}NO_2$

M_r = 331.41 g mol^{-1}

77

The generic method (Section 6.2.2) was used, employing 6-(p-*tert*-butyl-phenylethynyl)-indole (**71**, 1.093 g, 4.00 mmol) as the starting material. The product was purified as described to give the final product (**77**), 3-acetoxy-6-(p-*tert*-butyl-phenylethynyl)-indole (0.428 g, 1.29 mmol, 32 %).

^{1}H NMR (400 MHz, $CDCl_3$) δ 8.00 (s, 1H, N-H), 7.57 – 7.37 (m, 7H), 7.31 (dd, *J* = 4.8, 2.0 Hz, 1H), 2.13 (s, 3H), 1.36 (s, 9H, Bu-H).

^{13}C NMR (101 MHz, $CDCl_3$) δ 168.76, 151.27, 132.68, 131.26, 125.36, 123.67, 123.28, 120.58, 119.77, 118.79, 114.81, 114.32, 113.96, 89.92, 88.54, 34.79, 31.22, 21.01.

Acc. ASAP-MS, *m/z*: 332.1638 $[M+H]^+$; Calc. for $[C_{22}H_{22}NO_2]^+$ = 332.1651.

6.18.6 3-acetoxy-7-(p-*tert*-butyl-phenylethynyl)-indole synthesis

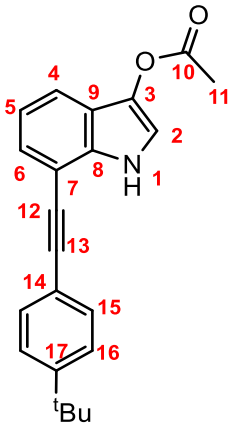

Formula:

$C_{22}H_{21}NO_2$

M_r = 331.41 g mol^{-1}

78

The generic method (Section 6.2.2) was used, employing 7-(p-*tert*-butyl-phenylethynyl)-indole (**72**, 0.998 g, 3.65 mmol) as the starting material. The product was purified as described to give the final product (**78**), 3-acetoxy-7-(p-*tert*-butyl-phenylethynyl)-indole (0.288, 0.869 mmol, 24 %).

Acc. ASAP-MS, *m/z*: 332.1642 $[M+H]^+$; Calc. for $[C_{22}H_{22}NO_2]^+$ = 332.1651.

6.19 Synthesis of di(R-ethynyl)-indigos

6.19.1 5,5'-di(*tert*-butyl-ethynyl)-indigo synthesis

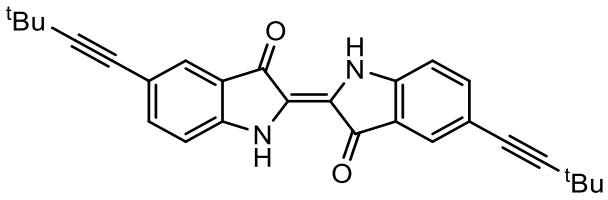

79

Formula:

$C_{28}H_{26}N_2O_2$

M_r = 422.53 g mol^{-1}

The generic method (Section 6.2.1) was used, employing 3-acetoxy-5-(3,3-dimethylbutyn-1yl)-indole (**73**, 0.332 g, 1.30 mmol) as the starting material. The product was purified as described to give the final product as a greenish black solid (**79**), 5,5'-di(3,3-dimethylbutyn-1yl)-indigo (0.180 g, 0.398 mmol, 61 %)

Acc. ASAP-MS, *m/z*: 423.3101 $[M+H]^+$; Calc. for $[C_{28}H_{27}N_2O_2]^+$ = 423.3092.

6.19.2 5,5'-di(p-n-butyl-phenylethynyl)-indigo synthesis

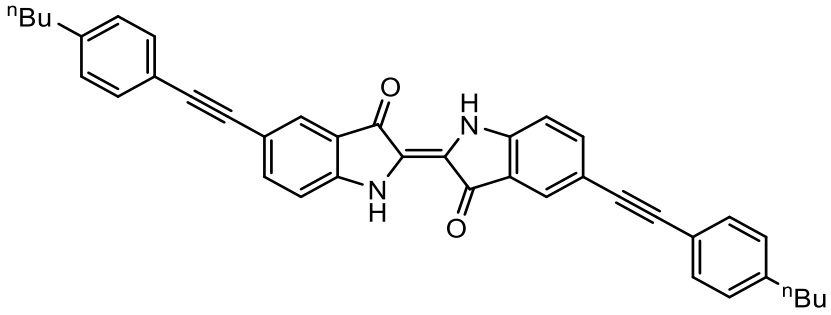

80

Formula: $C_{40}H_{34}N_2O_2$

M_r = 574.72 g mol^{-1}

The generic method (Section 6.2.1) was used, employing 3-acetoxy-5-(p-n-butyl-phenylethynyl)-indole (**74**, 0.462 g, 1.39 mmol) as the starting material. The product was purified as described to give the final product as a greenish black solid (**80**), 5,5'-di(p-n-butyl-phenylethynyl)-indigo (0.318 g, 0.553 mmol, 80 %)

Acc. ASAP-MS, *m/z*: 575.2704 $[M+H]^+$; Calc. for $[C_{40}H_{35}N_2O_2]^+$ = 575.2698.

6.19.1 5,5'-di(p-*tert*-butyl-phenylethynyl)-indigo synthesis

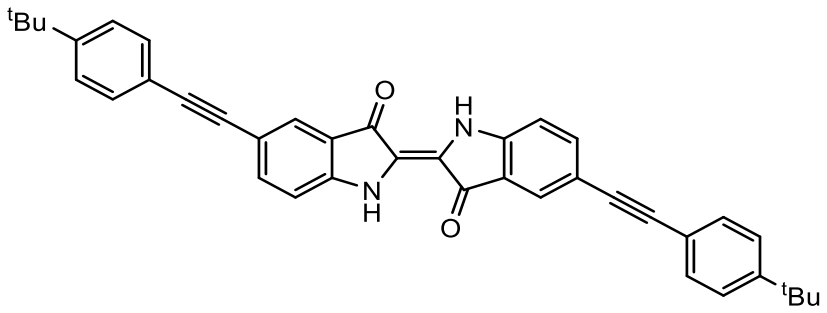

81

Formula: $C_{40}H_{34}N_2O_2$

M_r = 574.72 g mol^{-1}

The generic method (Section 6.2.1) was used, employing 3-acetoxy-5-(p-*tert*-butyl-phenylethynyl)-indole (**76**, 0.315 g, 0.950 mmol) as the starting material. The product was purified as described to give the final product as a dark greenish blue solid (**81**), 5,5'-di(p-*tert*-butyl-phenylethynyl)-indigo (0.217 g, 0.396 mmol, 83 %)

Acc. ASAP-MS, *m/z*: 575.2690 $[M+H]^+$; Calc. for $[C_{40}H_{35}N_2O_2]^+$ = 575.2698.

6.19.1 6,6'-di(p-*tert*-butyl-phenylethynyl)-indigo synthesis

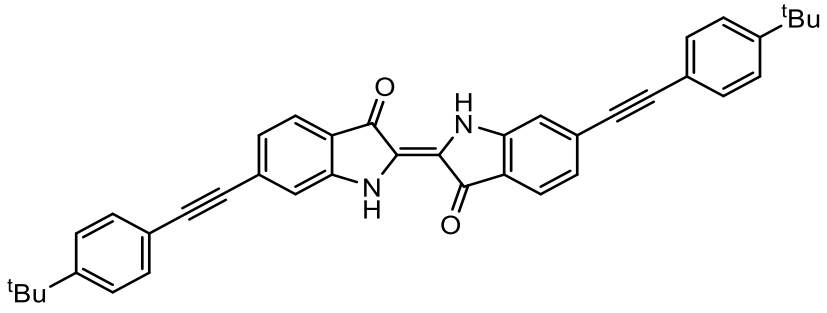

82

Formula: $C_{40}H_{34}N_2O_2$

M_r = 574.72 g mol^{-1}

The generic method (Section 6.2.1) was used, employing 3-acetoxy-6-(p-*tert*-butyl-phenylethynyl)-indole (**77**, 0.428 g, 1.29 mmol) as the starting material. The product was purified as described to give the final product as a greenish black solid (**82**), 6,6'-di(p-*tert*-butyl-phenylethynyl)-indigo (0.328 g, 0.571 mmol, 88 %)

Acc. ASAP-MS, *m/z*: 575.2696 $[M+H]^+$; Calc. for $[C_{40}H_{35}N_2O_2]^+$ = 575.2698.

6.19.1 7,7'-di(p-*tert*-butyl-phenylethynyl)-indigo synthesis

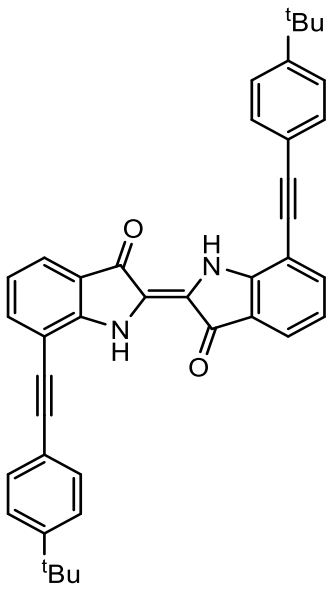

83

Formula:

$C_{40}H_{34}N_2O_2$

M_r = 574.72 g mol^{-1}

The generic method (Section 6.2.1) was used, employing 3-acetoxy-7-(p-*tert*-butyl-phenylethynyl)-indole (**78**, 0.288, 0.869 mmol) as the starting material. The product was purified as described to give the final product as a dark greenish blue solid (**83**), 5,5'-di(p-*tert*-butyl-phenylethynyl)-indigo (0.201 g, 0.367 mmol, 84 %)

Acc. ASAP-MS, *m/z*: 575.2690 $[M+H]^+$; Calc. for $[C_{40}H_{35}N_2O_2]^+$ = 575.2698.

6.20 Synthesis of *N,N'*-diBoc-indigos

6.20.1 *N,N'*-diBoc-indigo synthesis

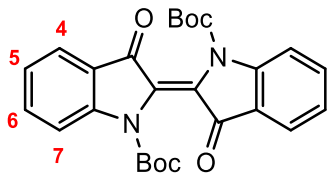

84

Formula:

$C_{26}H_{26}N_2O_6$

M_r = 462.49 g mol^{-1}

The generic method (Section 6.2.5) was used, employing indigo (0.800 g, 3.05 mmol) as the starting material. The product was purified as described to give the final product as a Rose-colour solid (**84**), *N,N'*-diBoc-6,6-dibromoindigo (0.570 g, 1.23 mmol, 40 %)

^{1}H NMR (400 MHz, $CDCl_3$) δ 8.04 (d, *J* = 8.4 Hz, 2H, H-7), 7.79 (d, *J* = 7.4 Hz, 2H, H-4), 7.63 (ddd, *J* = 8.4, 7.4, 1.4 Hz, 2H, H6), 7.23 (t, *J* = 7.4 Hz, 2H, H-5), 1.64 (s, 18H, Boc-H).

Acc. ASAP-MS, *m/z*: 463.1852 $[M+H]^+$; Calc. for $[C_{26}H_{25}N_2O_6Br_2]^+$ = 463.1869.

6.20.2 *N,N*'-diBoc-5,5-dibromoindigo synthesis

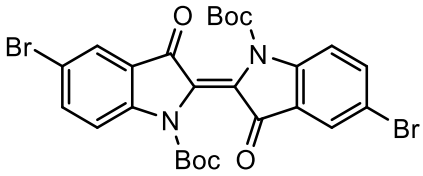

85

Formula:

$C_{26}H_{26}N_2O_6Br_2$

M_r = 620.28 g mol^{-1}

The generic method (Section 6.2.5) was used, employing 5,5'-dibromoindigo (0.510 g, 1.21 mmol) as the starting material. The product was purified as described to give the final product as a Rose-colour solid (**85**), *N,N*'-diBoc-6,6-dibromoindigo (0.301 g, 0.490 mmol, 40 %)

Acc. ASAP-MS, *m/z*: 619.0198 $[M+H]^+$; Calc. for $[C_{26}H_{25}N_2O_6Br_2]^+$ = 619.0079.

6.20.3 *N,N*'-diBoc-6,6-dibromoindigo synthesis

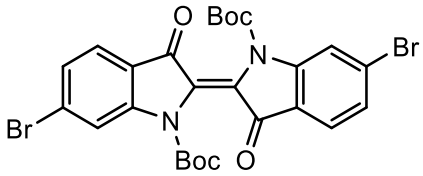

86

Formula:

$C_{26}H_{24}N_2O_6Br_2$

M_r = 620.28 g mol^{-1}

The generic method (Section 6.2.5) was used, employing 6,6'-dibromoindigo (0.389 g, 0.926 mmol) as the starting material. The product was purified as described to give the final product as a Rose-colour solid (**86**), *N,N*'-diBoc-6,6-dibromoindigo (0.245 g, 0.395 mmol, 43 %)

Acc. ASAP-MS, *m/z*: 619.0068 $[M+H]^+$; Calc. for $[C_{26}H_{25}N_2O_6Br_2]^+$ = 619.0079.

6.21 Synthesis of indirubins

6.21.1 5,5'-dibromoindirubin synthesis

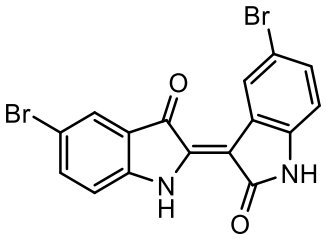

87

Formula:

$C_{16}H_8N_2O_2Br_2$

M_r = 420.06 g mol^{-1}

The generic method (Section 6.2.6) was used, employing 5-bromo-isatin (0.5 g, 2.21 mmol) as the starting material. The product was purified as described to give the final product as a purple solid (**87**), 5,5'-dibromoindirubin (0.135 g, 0.321 mmol, 29 %)

Acc. ASAP-MS, *m/z*: 418.8995 $[M+H]^+$; Calc. for $[C_{16}H_9N_2O_2Br_2]^+$ = 418.9031.

6.21.1 6,6'-dibromoindirubin synthesis

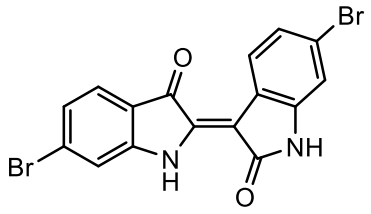

88

Formula:

$C_{16}H_8N_2O_2Br_2$

M_r = 420.06 g mol^{-1}

The generic method (Section 6.2.6) was used, employing 6-bromo-isatin (0.5 g, 2.21 mmol) as the starting material. The product was purified as described to give the final product as a reddish-purple solid (**88**), 6,6'-dibromoindirubin (0.119 g, 0.283 mmol, 26 %)

Acc. ASAP-MS, *m/z*: 418.9002 $[M+H]^+$; Calc. for $[C_{16}H_9N_2O_2Br_2]^+$ = 418.9031.

6.21.1 5,6'-dibromoindirubin synthesis

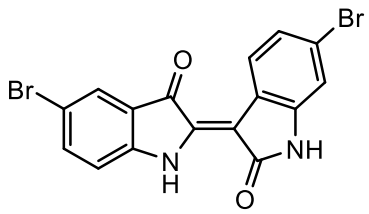

89

Formula:

$C_{16}H_8N_2O_2Br_2$

M_r = 420.06 g mol^{-1}

The generic method (Section 6.2.7) was used, employing 3-acetoxy-5-bromoindole (**32**, 0.250 g, 0.984 mmol) and 6-bromo-isatin (0.221 g, 0.984 mmol) as the starting material. The product was purified as described to give the final product as a purple solid (**89**), 5,6'-dibromoindirubin (0.239 g, 0.569 mmol, 58 %)

Acc. ASAP-MS, *m/z*: 418.9017 $[M+H]^+$; Calc. for $[C_{16}H_9N_2O_2Br_2]^+$ = 418.9031.

6.21.1 6,5'-dibromoindirubin synthesis

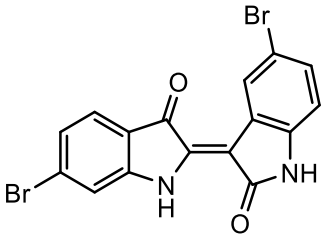

90

Formula:

$C_{16}H_8N_2O_2Br_2$

M_r = 420.06 g mol^{-1}

The generic method (Section 6.2.7) was used, employing 3-acetoxy-6-bromoindole (**33**, 0.250 g, 0.984 mmol) and 5-bromo-isatin (0.221 g, 0.984 mmol) as the starting material. The product was purified as described to give the final product as a purple solid(**90**), 6,5'-dibromoindirubin (0.198 g, 0.471 mmol, 48 %)

Acc. ASAP-MS, *m/z*: 418.9021 $[M+H]^+$; Calc. for $[C_{16}H_9N_2O_2Br_2]^+$ = 418.9031.

7. Acknowledgement

The time while I was researching in 2020-2021, was a sad year for the entire human race where the Covid-19 forced many of us to stop working to save lives. I feel extremely lucky to have the chance to stay in our lab to focus on research during such a hard time.

My sincerest appreciation to my supervisor, Professor Andrew Beeby. He took care of me from both perspectives of knowledge and spirit. To know Prof Beeby is my most enjoyable, most fortunate, and most honourable thing in Durham. Unfortunately, most of the time, I can only see him under his mask, even if he is such a lovely, funny, and spiritual inspiring man. I truly wish this year was not under the miserable pandemic so that in my memory I can have more moments and chances to remember him better so that I can clearly remember his smiling face for a few more decades when I get old. Honestly speaking, I often feel like he is my father, especially whenever I tell him about some tiny achievements because I hope by any chance, he can be glad and enjoy that I was once his student.

Many thanks to my research group colleague, Joseph Kershaw. We worked on very similar projects and shared a lot of ideas and experimental results. Although we just had two months to work together, his accompany made me feel less lonely.

Also many thanks to Professor Patrick Steel and his research team. They also helped me a lot to familiarise myself with the rules and provided me with a lot of essential chemicals and a centrifuge.

Thanks to Professor Mark Fox who helped to solve some of the quantum calculations of my indigos and helped me to with the relevant problems that I have.

Thanks to Professor Ian Baxendale who provided sufficient 5-bromoindole as a gift, which is the “pioneer” chemical for any newly attempted synthetic approach.

Additional thanks to the teams of NMR, Mass Spec, glass blowing team, store, and other services provided by the department and the university. Your work in such an awful year supported my research free of worry.

Thanks to the University of Durham and my college, Collingwood. I really appreciate my four years of study here and everything I learnt over here, especially the last year, 2020-2021 when the Covid-19 forced the entire human race to stop working to save lives. Under such a circumstance, I feel extremely lucky to be permitted to continue to stay in the lab to focus on my research.

Also, I am glad and find it funny that although it is not exactly the Tyrian purple, my institution, Durham University, changed its colour to purple in 2005 when we realized that purple is an affordable colour so we would look more royal and honourable.

Special thanks to the molecule “indigo and its family members”, your awful water-solubility made the colour of my jeans hard to be washed off. Rather than worrying about my legs getting blue, I can walk around in my jeans on rainy days (even in Britain).

Lastly, whoever you are, thank you so much for reading my thesis and hope you enjoyed it.

References

1 K. Aino, K. Hirota, T. Okamoto, Z. Tu, H. Matsuyama, I. Yumoto, *Front. Microbio.*, 2018, 9, 2196.

2 N. Tokuyasu, K. Shomori, K. Amano, S. Honjo, T. Sakamoto, J. Watanabe, M. Amisaki, M. Morimoto, E. Uchinaka, T. Yagyu, H. Saito, H. Ito, Y. Fujiwara, *Yonago Acta Medica*, 2018, **61**, 128-136.

3 *Redelec.ch*, 2021.

4 A. Baeyer, V. Drewsen, *Berichte der deutschen chemischen Gesellschaft*, 1882, **15**, 2856-2864.

5 R. Christie, *Colour chemistry,* RSC, Cambridge, 2nd edn., 2015, ch. 4.

6 H. Zollinger, *Color chemistry: Syntheses, Properties, Appl. Org. Dyes Pigm.*, VCH, Weinheim, 2nd edn., 1991, ch. 8, pp. 191-192.

7 R. Paul, *Denim,* Woodhead Publishing, Cambridge, 2015.

8 H. Kim, S. Jang, J. Kim, Y. Yang, Y. Kim, B. Kim, K. Choi, *Dyes Pigm.*, 2017, 140, 29-35.

9 A. Fabara, M. Fraaije, *Appl. Microbio. and Biotech.*, 2019, 104, 925-933.

10 A. Baeyer, V. Drewsen, *Chem. Ber., 1883, **16**, 2205.*

11 W. Beck, K. Sünkel, *Zeitschrift für anorganische und allgemeine Chemie*, 2020, **646**, 248-255.

12 G. Haucke, G. Graneß, *Angewandte Chemie*, 1995, 107, 116-117.

13 R. Christie, *Biotech. & Histochem.*, 2007, 82, 51-56.

14 H. Pandraud, *Acta Crystallographica*, 1961, **14**, 901-908.

15 M. Puchalska, K. Poe-Pawlak, I. Zadrona, H. Hryszko, M. Jarosz, *J. Mass Spec.*, 2004, **39**, 1441-1449.

16 M. Sytnyk, E. Głowacki, S. Yakunin, G. Voss, W. Schöfberger, D. Kriegner, J. Stangl, R. Trotta, C. Gollner, S. Tollabimazraehno, G. Romanazzi, Z. Bozkurt, M. Havlicek, N. Sariciftci, W. Heiss, *J. Am. Chem. Soc.*., 2014, 136, 16522-16532.

17 M. Kasha, H. Rawls, M. Ashraf El-Bayoumi, *Pure App. Chem.*, 1965, 11, 371-392.

18 P. Süsse, M. Steins, V. Kupcik, *Zeitschrift für Kristallographie - Crystalline Mat.*, 1988, 184, 269-274.

19 J. Porada, J. Neudörfl, D. Blunk, *New J. Chem.*, 2015, 39, 8291-8301.

20 G. Miehe, P. Su¨sse, V. Kupcik, E. Egert, M. Nieger, G. Kunz, R. Gerke, B. Knieriem, M. Niemeyer, W. Lu¨ttke, Angew. Chem., Int. Ed., 1991, 30, 964–967.

21 G. Grimme, P. Boldt, S. Grimme, P. Jones, *Chemische Berichte*, 1993, 126, 1015-1021.

22 B. Das, A. Guha, A. Wahab, *J. Phys. Org. Chem.*, 2020, 33.

23 Hyejin Hong, C.M.Conover, D.T.Hofsommer, C.A.Sanz, R.G.Hicks, *Org.Biomol.Chem.*2020, **18**, 5838

24 H. Pandraud, *Acta Crystallographica*, 1961, 14, 901-908.

25 *Simtrum.com*, 2022.

26 M. Watanabe, N. Uemura, S. Ida, H. Hagiwara, K. Goto, T. Ishihara, *Tetrahedron*, 2016, 72, 4280-4287.

27 J. Seixas de Melo, A. Moura, M. Melo, *J. Phys. Chem. A*, 2004, 108, 6975-6981.

28 J. Seixas de Melo, R. Ronda˜ o, H. D. Burrows, M. J. Melo, S. Navaratnam, R. Edge, G. Voss, *Chem. Phys. Chem.*, 2006, 7, 2303–2311.

29 Z. Ju, J. Sun, Y. Liu, *Molecules*, 2019, 24, 3831.

30 P. SADLER, *J. Org. Chem.*, 1956, 21, 316-318.

31 M. Cole, G. Eggleston, A. Triplett, Adv. Sugar Crop Proc. Conv. 2016, **1**.

32 H. Zollinger, *Color chemistry*, VCH, Weinheim, 2nd edn., 1991, ch. 8.3, pp. 191-199.

33 Fassler D, Gade, R, Kaden, *J. Mol. Struc. (1988) 174(C) 389-393*

34 O. Pitayatanakul, T. Higashino, T. Kadoya, M. Tanaka, H. Kojima, M. Ashizawa, T. Kawamoto, H. Matsumoto, K. Ishikawa, T. Mori, *J. Mater. Chem. C*, 2014, 2, 9311-9317.

35 H. Langhals, *New J. Chem.*, 2008, 32, 21-23.

36 I. Klimovich, A. Zhilenkov, L. Kuznetsova, L. Frolova, O. Yamilova, S. Troyanov, K. Lyssenko, P. Troshin, *Dyes Pigm.*, 2021, 186, 108966.

37 W.Beck, C.Schmidt, R.Wienold, M.Steimann, B.Wagner, *Angew.Chem.,Int.Ed.*, 1989, **28,** 1529

38 A. Lenz, C. Schmidt, A. Lehmann, B. Wagner, W. Beck, *Zeitschrift für Naturforschung B*, 1997, **52**, 474-484.

39 D. Konarev, S. Khasanov, A. Kuzmin, A. Shestakov, A. Otsuka, H. Yamochi, G. Saito, R. Lyubovskaya, *Dalt. Trans.*, 2016, 45, 17095-17099.

40 T. Maugard, E. Enaud, P. Choisy, M. D. Legoy, *Phytochem.*, 2001, **58**, 897-904.

41 N. Gandra, A. Frank, O. Le Gendre, N. Sawwan, D. Aebisher, J. Liebman, K. Houk, A. Greer, R. Gao, *Tetrahedron*, 2006, **62**, 10771-10776.

42 R. Gerke, L. Fitjer, P. Müller, I. Usón, K. Kowski, P. Rademacher, *Tetrahedron*, 1999, **55**, 14429-14434.

43 D. Farka, M. Scharber, E. Głowacki, N. Sariciftci, *J. Phys. Chem. A*, 2015, **119**, 3563-3568.

44 H. Güsten, *J. Chem. Soc. D*, 1969, **0**, 133b-134.

45 A. Katritzky, W. Fan, A. Koziol, G. Palenik, *J. Heterocyclic Chem.*, 1989, 26, 821-828.

46 J. Bergman, C. Stlhandske, *Tetrahedron Lett.*, 1994, 35, 5279-5282.

47 G. Huang, K. Liu, P. Wen, J. Liu, *Synthesis*, 2010, 2010, 3623-3626.

48 E. Owens, N. Bruschi, J. Tawney, M. Henary, *Dyes Pigm.*, 2015, 113, 27-37.

49 B. Robinson, *The Fischer indole synthesis*, UMI, Ann Arbor, 1993.

50 L. Ren, G. Nan, Y. Wang, Z. Xiao, *J. Org. Chem.*, 2018, **83**, 14472-14488.

51 P. Tisovský, R. Šandrik, M. Horváth, J. Donovalová, K. Jakusová, M. Cigáň, R. Sokolík, A. Gáplovský, M. Gáplovský, J. Filo, *Molecules*, 2017, **22**, 1961.

52 J. Setsune, T. Matsuura, T. Fujiwara, T. Kitao, *Chemistry Lett.*, 1984, 13, 1755-1758.

53 Y. Tanoue, A. Terada, K. Sakata, M. Hashimoto, S. Morishita, M. Hamada, N. Kai, *Fischeries Science*, 2001, **67**, 726-729.

54 C. Shao, G. Shi, Y. Zhang, S. Pan, X. Guan, *Org. Letters*, 2015, **17**, 2652-2655.

55 H. Hénon, F. Anizon, R. Golsteyn, S. Léonce, R. Hofmann, B. Pfeiffer, M. Prudhomme, *Bioorg. & Medicinal Chem.*, 2006, **14**, 3825-3834.

56 M. Sytnyk, E. Głowacki, S. Yakunin, G. Voss, W. Schöfberger, D. Kriegner, J. Stangl, R. Trotta, C. Gollner, S. Tollabimazraehno, G. Romanazzi, Z. Bozkurt, M. Havlicek, N. Sariciftci, W. Heiss, *J. Am. Chem. Soc.*, 2014, **136**, 16522-16532.

57 C. Wang, J. Yan, M. Du, J. Burlison, C. Li, Y. Sun, D. Zhao, J. Liu, *Tetrahedron*, 2017, 73, 2780-2785.

58 T. Maugard, E. Enaud, P. Choisy, M. Legoy, *Phytochem.*, 2001, 58, 897-904.

59 G. Huang, K. Liu, P. Wen, J. Liu, *Synthesis*, 2010, **2010**, 3623-3626.

60 A. Pennec, R. Daniellou, P. Loyer, C. Nugier-Chauvin, V. Ferrieres, *Carbohyd Res*, 2015, **402**, 50-55.

61 F. Petronijevic, C. Timmons, A. Cuzzupe, P. Wipf, *Chem. Commun.*, 2008, DOI: 10.1039/b816989f, 104-106.

62 P. Qiu, J. Y. Zhao, X. Shi, X. H. Duan, *New J. Chem.*, 2016, **40**, 6568-6572.

63 Y. Yang, R. Li, Y. Zhao, D. Zhao, Z. Shi, *J. Am. Chem. Soc.*, 2016, **138**, 8734-8737.

64 G. Huang, K. Liu, P. Wen, J. Liu, *Synthesis*, 2010, **2010**, 3623-3626.

65 G. A. Molander, B. Canturk, L. E. Kennedy, *J. Org. Chem.*, 2009, **74**, 973-980.